UNIVERSITY OF CALIFORNIA
RIVERSIDE

Uncovering the Genetic Basis of Local Adaptation With Long-Term Evolution Experiments in Barley

A Dissertation submitted in partial satisfaction
of the requirements for the degree of

Doctor of Philosophy

in

Plant Biology

by

Jill May Marzolino

March 2026

Dissertation Committee:
Dr. Daniel Koenig, Chairperson
Dr. Timothy Close
Dr. Zhenyu Jia

The Dissertation of Jill May Marzolino is approved:

_____

_____

_____

Committee Chairperson

University of California, Riverside

ACKNOWLEDGEMENTS

A dissertation is founded on, shaped by, and corrected by the work and effort of many people. I would like to thank and acknowledge the work of the co-authors that participated in the projects that form this dissertation. Ruth S. Perez-Alfaro, Matthew Kahler, and Juliana McGowan contributed to Chapter 1. Chapter 2 was possible with the assistance of Jacob Landis, Astrid Junker, and Thomas Altmann. Chapter 3 was created in collaboration with Keely Brown, Ruth S. Perez-Alfaro, Jacob Landis, and Angelica Guercio. Daniel Koenig led, organized, and advised for each of these projects.

My time in graduate school has been indelably shaped by interactions with and feedback from everyone I have had the privilege to know and work with. Copious thanks go to my colleagues in the Koenig & Seymour labs: Dr. Emmanuel Ávila De Dios, Dr. Taylor Beaulieu, Dr. Keely Brown, Burcu Çelikli, Dr. Isaac Dias, Dr. Chris Fiscus, Dr. Angelica Guercio, Robert Kettenstock, Matt Kuhler, Dr. Jacob Landis, Ryan Piscatella, Ruth Sarahi Perez Alfaro, Dr. Danelle Seymour, Dr. Aimee Uyehara, and Dr. Omar Zayed. Thank you all for the ideas, assistance, and camaraderie.

I would like to specially thank Dr. Chris Fiscus for teaching me how to be a graduate student; Dr. Jacob Landis for making sure I knew what I was doing and exemplifying professionalism; and Dr. Keely Brown for embodying kindness and scientific excellence. Thank you to Angelica, Robert, and Ruth for making work a delight.

Thanks go to my guidance, qualifying exam, and dissertation committee members: Dr. Timothy Close, Dr. Zhenyu (Arthur) Jia, Dr. Norman Ellstrand, Dr. Jaimie Van Norman, Dr. Dawn Nagel, and Dr. David Reznick for guiding my professional development and making suggestions that improved my work. I would also like to extend thanks to Dr. Cathleen Jones and Dr. Carolyn Rasmussen for providing support,

mentorship, and confidence. I am deeply grateful to Dr. Vince Buffalo for inspiring, guiding, and teaching me — in person at Davis and through your book in Riverside and beyond. Finally, thank you to my advisor Dr. Daniel Koenig. Dan, your knowledge, passion, and communication skills inspired me from the beginning to the very end. Thank you for taking a chance on me, making a safe space in your lab, and always expecting more.

Great thanks go to my family and friends for their love and support. Thank you to my father for showing me the breadth and depth of comfort and feeling in art and nature, and for paying for Spot***, without which I might not have been able to make this. Thank you to my mother for taking me to the library, making me participate, and promising to support me in the lifestyle to which I've become accustomed. Thank you to my sister for inspiring me to make art if I want to and to live fully and beautifully. I still think you are the coolest and admire you greatly. Thanks to my beloved aunts for spreading family widely and warmly, and for asking about how I was instead of how my dissertation was going. Thank you to Joy's cousin Maryann for being our closest family, welcoming us into your home, and incorporating us into your friends. Thank you to my loyal friends who were a highlight and balm in dark days; you are marvelous and I wish you all the greatest happiness. Thank you to my partner Joy, for taking risks with me, making prolonged sacrifices, and supporting me to my greatest potential. You vastly improve every day, and I am so lucky to enjoy life with you.

This work is dedicated to

Joy, who worked the field at my side during the worst year ever

Paw-fessor PCH, for showing me the value of my tears from that year onward

and Joanne, who provided sisterhood, especially against my will, over my whole life.

ABSTRACT OF THE DISSERTATION

Uncovering the Genetic Basis of Local Adaptation With
Long-Term Evolution Experiments in Barley

by

Jill May Marzolino

Doctor of Philosophy, Graduate Program in Botany and Plant Sciences
University of California, Riverside, March 2026
Dr. Daniel Koenig, Chairperson

Environmental adaptation is a critical component for the survival of plant species. Understanding how genetic diversity is purged and preserved during evolution and the types of traits which contribute to fitness increases over large time spans helps clarify the relationships between genotypic and phenotypic variance. Throughout this dissertation I use the Composite Cross II evolution experiment in barley to explore the process of evolution to novel environments over the course of nearly a century and connect genotype with phenotype. The seed bank of this population provides unprecedented access to the story of evolution in a valuable model crop species. In Chapter 1 I show how the connection between flowering time and fecundity depends upon environmental factors. In Chapter 2 I expand the scope to explore additional physical, developmental traits that contribute to competitive ability in the experiment. In Chapter 3 I explore how genetic diversity stored in the population helps preserve its fitness during radical environmental changes and that some of the genetic controls and pathways under selection in the original environment undergo a reversal in response to new selective pressures.

TABLE OF CONTENTS

LIST OF FIGURES

Chapter 1

Chapter 2

Chapter 3

LIST OF TABLES

Introduction

Plants can survive in many varied environments because they adapt through the accumulation of locally beneficial genetic changes (Leimu and Fischer 2008; Long et al. 2015; Schlötterer et al. 2015). However, climate change is advancing faster than plants can adapt (Jump and Penuelas 2005; Raza et al. 2019; Ahuja et al. 2010; Chakraborty and Newton 2011). Environmental stresses such as prolonged drought, intensifying storms, and increased UV exposure can all damage plant tissues and inhibit crop productivity. Flowering time, plant size, disease resistance, water use efficiency, and drought tolerance are frequently significant subjects for plant adaptation (Milano et al. 2016; Campitelli et al. 2016; Taylor et al. 2016). Furthermore, genotype-by-environment interactions are important during adaptation to new environments (Lasky et al. 2015). Annual mean temperature, annual precipitation, and precipitation in the wettest month have been identified as crucial factors for adaptation to new environments (Zhang et al. 2019). Allele fitness in a new environment depends strongly on the environmental origin of the population. For example, while a few quantitative trait loci (QTL) promote biomass across multiple environments in switchgrass, other morphological changes like leaf size, tissue density, and stomatal conductance associated with variable adaptation to drought (Hamilton et al. 2015; Lowry et al. 2019; Taylor et al. 2016). Providing further evidence of how cultivated plants adapt to environmental changes adds to our understanding of the pathways and process of evolution and can inform the breeding of crop varieties that can withstand the challenges of shifting climates and mitigate these environmental hazards.

Barley (*Hordeum vulgare*) is an excellent crop system for studying local adaptation because it is thought to be one of the first domesticated crops and underwent domestication in three to six independent sites in Eurasia (Stein and Muehlbauer 2018), Lister et al. 2018; Newton et al. 2011; Morrell and Clegg 2007). The species then spreads across the globe, adapting to diverse environments and accumulating extensive genetic diversity (Zhou 2010). That diversity has been captured in modern gene banks that collected over 400,000 barley accessions representing adaptation to almost every type of environment (Knüpffer 2009). Today it is the world's fourth most important grain crop and is a useful model species for wheat because it is easy to grow in large numbers, 99% selfing, easy to sterilize and cross, and has a high-quality reference genome (Stein and Muehlbauer 2018; Natural resources conservation servic...). Studying the process of evolution in this crop system allows insight into the factors that contribute to wide-scale and long-term environmental adaptation and provides information about varieties' use in different climate zones.

Studying adaptation is often limited to surveying available genetic and phenotypic diversity from naturally occurring systems and using genome wide association studies (GWAS) to identify associations between genetic and trait variance (Challa and Neelapu 2018; Bamba et al. 2019; Olatoye et al. 2018; Jabbari et al. 2018). These survey-style approaches limit research because of confounding factors like population structure, the frequency of adaptive variants, and the availability of genetic diversity. A modern approach to this problem is combining experimental evolution with modern sequencing technologies to monitor genetic changes in populations at the genome level in 'evolve & resequence' (E&R) experiments. The majority of these experiments use small laboratory

samples under specific selective regimes to understand evolutionary processes (Long et al. 2015; Turner and Miller 2012; Schlötterer et al. 2015). These laboratory experiments often exclude complexities of the natural environment and cannot be maintained for long. One counterexample is Lenski's long-term experimental evolution experiment of perpetuating progeny bacterial colonies and competing to compare fitness (Lenski 2017; Good et al. 2017). This experiment provides evidence for how beneficial mutations develop and compete in the *E. coli* system, but it is difficult to establish and maintain such large, long-term experimental populations. Overall, experiments that can encompass greater genetic diversity and longer time spans for genetic change allow deeper insights into long-term patterns of evolution.

Using intercross-derived populations recombines extant genetic diversity to expand phenotypic variance and remove population structure. The composite cross II (CC II) experiment combines these features with long-term evolution and allows us to dissect the genetic basis of adaptation to a novel environment in a multicellular organism and crop species. The Composite Cross II was founded by crossing 28 barley lines collected from the major barley growing regions of the world (Harlan and Martini 1929). The offspring of these crosses were then competed against one another in large populations at locations across the United States for nearly a century. Each year, seed was collected from the population and a random subset was used to plant the next generation (Harlan and Martini 1929; Suneson and Wiebe 1942). No conscious selection regime was exerted on progeny seeds and large population sizes (10,000 to 20,000 individuals grown each generation) minimize the effect of drift, so natural selection shapes the genetics of the population (Zhang et al. 2004). This experimental design

enables us to detect selection as a major factor of non-random, non-neutral, adaptive genetic change.

Initial studies of the CC II used allozyme markers and found that natural selection targeted flowering time, plant height, spike number, and total seed number (Allard 1996). Modern genomic investigations show that the CCII became increasingly genetically homogenous, with two primary genotypes dominating later stages of the experiment (Landis et al. 2024). They further uncovered genome regions associated with increasing fitness and changes in flowering time based on phenotypes collected from a greenhouse experiment. In this dissertation, I add to a comprehensive understanding of environmental adaptation in this population by documenting and mapping flowering time in a novel environment, describing additional traits associated with increased fitness during adaptation, and investigate the effect of prior adaptation and reductions in genetic diversity on the population's ability to evolve in a novel location.

Chapter 1 explores the relationship between fitness and flowering time over generations in the Composite Cross II with a field experiment based in Riverside, California.

Chapter 2 expands our knowledge of the changes that occurred and the types of traits under selection in the CC II over time by leveraging developmental phenotypes measured with a high-throughput phenotyping platform.

Chapter 3 examines the role of environment on the evolutionary process by mapping the genetic basis of adaptation to two different environments.

References

Ahuja I, de Vos RCH, Bones AM, Hall RD. 2010. Plant molecular stress responses face climate change. Trends Plant Sci. 15(12):664–674. http://dx.doi.org/10.1016/j.tplants.2010.08.002.

Allard RW. 1996. Genetic basis of the evolution of adaptedness in plants. Euphytica. 92(1):1–11. https://doi.org/10.1007/BF00022822.

Bamba M, Kawaguchi YW, Tsuchimatsu T. 2019. Plant adaptation and speciation studied by population genomic approaches. Dev Growth Differ. 61(1):12–24. http://dx.doi.org/10.1111/dgd.12578.

Campitelli BE, Des Marais DL, Juenger TE. 2016. Ecological interactions and the fitness effect of water-use efficiency: Competition and drought alter the impact of natural MPK12 alleles in Arabidopsis. Ecol Lett. 19(4):424–434. http://dx.doi.org/10.1111/ele.12575.

Chakraborty S, Newton AC. 2011. Climate change, plant diseases and food security: an overview. Plant Pathol. 60(1):2–14. https://onlinelibrary.wiley.com/doi/abs/10.1111/j.1365-3059.2010.02411.x.

Challa S, Neelapu NRR. 2018. Chapter 9 - Genome-Wide Association Studies (GWAS) for Abiotic Stress Tolerance in Plants. In: Wani SH, editor. Biochemical, Physiological and Molecular Avenues for Combating Abiotic Stress Tolerance in Plants. Academic Press. p. 135–150. http://www.sciencedirect.com/science/article/pii/B9780128130667000097.

Good BH, McDonald MJ, Barrick JE, Lenski RE, Desai MM. 2017. The dynamics of molecular evolution over 60,000 generations. Nature. 551(7678):45–50. http://dx.doi.org/10.1038/nature24287.

Hamilton JA, Okada M, Korves T, Schmitt J. 2015. The role of climate adaptation in colonization success in Arabidopsis thaliana. Mol Ecol. 24(9):2253–2263. http://dx.doi.org/10.1111/mec.13099.

Harlan HV, Martini ML. 1929. A Composite Hybrid Mixture1. Agron J. 21:487–490. http://dx.doi.org/10.2134/agronj1929.00021962002100040014x.

Jabbari M, Fakheri BA, Aghnoum R, Mahdi Nezhad N, Ataei R. 2018. GWAS analysis in spring barley (Hordeum vulgare L.) for morphological traits exposed to drought. PLoS One. 13(9):e0204952. http://dx.doi.org/10.1371/journal.pone.0204952.

Jump AS, Penuelas J. 2005. Running to stand still: adaptation and the response of plants to rapid climate change. Ecol Lett. 8(9):1010–1020. http://doi.wiley.com/10.1111/j.1461-0248.2005.00796.x.

Knüpffer H. 2009. Triticeae Genetic Resources in ex situ Genebank Collections. In: Muehlbauer GJ, Feuillet C, editors. Genetics and Genomics of the Triticeae. Vol. 413. New York, NY: Springer US. p. 31–79. [accessed 2019 Jul 25]. http://link.springer.com/10.1007/978-0-387-77489-3_2.

Landis JB, Guercio AM, Brown KE, Fiscus CJ, Morrell PL, Koenig D. 2024. Natural selection drives emergent genetic homogeneity in a century-scale experiment with barley. Science. 385(6705):eadl0038. http://dx.doi.org/10.1126/science.adl0038.

Lasky JR, Upadhyaya HD, Ramu P, Deshpande S, Hash CT, Bonnette J, Juenger TE, Hyma K, Acharya C, Mitchell SE, et al. 2015. Genome-environment associations in sorghum landraces predict adaptive traits. Sci Adv. 1(6):e1400218. http://dx.doi.org/10.1126/sciadv.1400218.

Leimu R, Fischer M. 2008. A meta-analysis of local adaptation in plants. PLoS One. 3(12):e4010. http://dx.doi.org/10.1371/journal.pone.0004010.

Lenski RE. 2017. Experimental evolution and the dynamics of adaptation and genome evolution in microbial populations. ISME J. 11(10):2181–2194. http://dx.doi.org/10.1038/ismej.2017.69.

Lister DL, Jones H, Oliveira HR, Petrie CA, Liu X, Cockram J, Kneale CJ, Kovaleva O, Jones MK. 2018. Barley heads east: Genetic analyses reveal routes of spread through diverse Eurasian landscapes. PLoS One. 13(7):e0196652. http://dx.doi.org/10.1371/journal.pone.0196652.

Long A, Liti G, Luptak A, Tenaillon O. 2015. Elucidating the molecular architecture of adaptation via evolve and resequence experiments. Nat Rev Genet. 16(10):567–582. http://dx.doi.org/10.1038/nrg3937.

Lowry DB, Lovell JT, Zhang L, Bonnette J, Fay PA, Mitchell RB, Lloyd-Reilley J, Boe AR, Wu Y, Rouquette FM Jr, et al. 2019. QTL × environment interactions underlie adaptive divergence in switchgrass across a large latitudinal gradient. Proc Natl Acad Sci U S A. 116(26):12933–12941. http://dx.doi.org/10.1073/pnas.1821543116.

Milano ER, Lowry DB, Juenger TE. 2016. The Genetic Basis of Upland/Lowland Ecotype Divergence in Switchgrass (Panicum virgatum). G3 . 6(11):3561–3570. http://dx.doi.org/10.1534/g3.116.032763.

Morrell PL, Clegg MT. 2007. Genetic evidence for a second domestication of barley (Hordeum vulgare) east of the Fertile Crescent. Proc Natl Acad Sci U S A. 104(9):3289–3294. http://dx.doi.org/10.1073/pnas.0611377104.

Natural resources conservation service plant guide: Barley. Natural Resources Conservation Service. https://plants.usda.gov/DocumentLibrary/plantguide/pdf/ccpg_horde.pdf.

Newton AC, Flavell AJ, George TS, Leat P, Mullholland B, Ramsay L, Revoredo-Giha C, Russell J, Steffenson BJ, Swanston JS, et al. 2011. Crops that feed the world 4. Barley: a resilient crop? Strengths and weaknesses in the context of food security. Food Security. 3(2):141. https://doi.org/10.1007/s12571-011-0126-3.

Olatoye MO, Hu Z, Maina F, Morris GP. 2018. Genomic Signatures of Adaptation to a Precipitation Gradient in Nigerian Sorghum. G3 . 8(10):3269–3281. http://dx.doi.org/10.1534/g3.118.200551.

Raza A, Razzaq A, Mehmood SS, Zou X, Zhang X, Lv Y, Xu J. 2019. Impact of Climate Change on Crops Adaptation and Strategies to Tackle Its Outcome: A Review. Plants. 8(2). http://dx.doi.org/10.3390/plants8020034.

Schlötterer C, Kofler R, Versace E, Tobler R, Franssen SU. 2015. Combining experimental evolution with next-generation sequencing: a powerful tool to study adaptation from standing genetic variation. Heredity . 114(5):431–440. http://dx.doi.org/10.1038/hdy.2014.86.

Stein N, Muehlbauer GJ, editors. 2018. The Barley Genome. Springer, Cham. https://link.springer.com/book/10.1007/978-3-319-92528-8.

Suneson CA, Wiebe GA. 1942. Survival of barley and wheat varities in mixtures. Journal of the American Society of Agronomy. http://agris.fao.org/agris-search/search.do?recordID=US201301498239.

Taylor SH, Lowry DB, Aspinwall MJ, Bonnette JE, Fay PA, Juenger TE. 2016. QTL and Drought Effects on Leaf Physiology in Lowland Panicum virgatum. Bioenergy Res. 9(4):1241–1259. https://doi.org/10.1007/s12155-016-9768-5.

Turner TL, Miller PM. 2012. Investigating natural variation in Drosophila courtship song by the evolve and resequence approach. Genetics. 191(2):633–642. http://dx.doi.org/10.1534/genetics.112.139337.

Zhang L, Juenger TE, Lowry DB, Behrman KD. 2019. Climatic impact, future biomass production, and local adaptation of four switchgrass cultivars. GCB Bioenergy. 210:81. https://onlinelibrary.wiley.com/doi/abs/10.1111/gcbb.12609.

Zhang Q, Jana S, Maroof MAS. 2004. A Diagnostic Analysis of Genetic Differentiation Among Subpopulations of a Barley Composite Cross Using Isozyme Markers. Hereditas. 118(1):63–70. http://doi.wiley.com/10.1111/j.1601-5223.1993.t01-3-00063.x.

Zhou MX. 2010. Barley Production and Consumption. In: Zhang G, Li C, editors. Genetics and Improvement of Barley Malt Quality. Berlin, Heidelberg: Springer Berlin Heidelberg. p. 1–17. https://doi.org/10.1007/978-3-642-01279-2_1.

Chapter 1 - The importance of flowering time for fitness measurements in a century-long evolution experiment in barley

Abstract

Flowering time is a critical component of plant fitness, especially for agricultural species like cultivated barley. Using a historic evolution experiment founded from global genetic diversity, we investigate the process of environmental adaptation with modern genomic technology. We grew 225 genotyped lines from generations throughout the population's evolutionary history in the field and phenotyped flowering time, fecundity, and seed mass. Early research conducted with this population found increases in height, flowering time, and yield. Our experiment confirms significant increases in flowering time, fecundity, and seed mass over time. We also confirm major diversity loss in the earliest stage of the experiment when the most drastic trait changes occurred. The following 40 generations exhibit smaller losses and fine-tuning of population changes. Specifically, we find evidence for stabilizing selection acting on flowering time and strong directional selection for higher seed weight acting consistently over time. Flowering time and seed production appear to have a quadratic relationship, which supports the idea of moderate flowering times having the highest fitness in the population's adapted environment. Finally, we uncovered evidence for the genetic controls of flowering time and fecundity in this population. This research furthers our understanding of the genetic components and processes of crop adaptation to a novel environment.

Introduction

Because of its intrinsic link with reproductive capacity, the timing of a plant's transition from vegetative to flowering development is critical for plant fitness. This transition is an important life history event for plants and flowering time, the duration from germination to flowering, has an inextricable link with an individual's fitness in the local environment (Gaudinier and Blackman 2020). Incorrect flowering time can result in physical barriers to outcrossing or negative environmental effects from intolerable temperatures that can damage reproductive tissues. Plant species often show variance in flowering time that concurs with an environmental gradient (Fournier-Level et al. 2011; Savolainen et al. 2013). Reciprocal transplant experiments can then prove populations exhibit higher fitness in their native environment, connecting the phenology of flowering time with fitness measurements (Hall and Willis 2006; Takou et al. 2019; Fournier-Level et al. 2022). Research in *Arabidopsis* documented directional selection acting on the start and end times of flowering (Toomajian et al. 2006; Sandring and Agren 2009). Abiotic stress and climate change research provide further evidence for the importance of flowering time as a crucial aspect of plant fitness. Documenting the concurrence of changing local temperature with flowering time and other measurements of ‘spring onset’ shows that plant species repeatedly adapt with earlier flowering times and faster life cycles (Bradley et al. 1999; Menzel and Fabian 1999; Sparks et al. 2000; Fitter and Fitter 2002; Primack et al. 2004; Ferguson et al. 2019; Collins et al. 2025).

Breeding efforts during domestication, expansion, and improvement have increased biotic resistance, abiotic stress tolerance, and regional fitness in small grains like wheat and barley. Expanding a crop’s range while maintaining high yield requires

aligning plant life cycles with local seasonality through identifying allelic variance in flowering time (Cockram et al. 2007). When planted in a temperate zone, plants can capitalize upon an extended growing season, but they need an appropriate vernalization response to initiate flowering in the spring after a cold winter. On the other hand, in Mediterranean climates, shorter vegetative phases, faster life cycles, and earlier flowering dates are beneficial for avoiding drought during sensitive periods of flower development and grain filling (Shavrukov et al. 2017). Although bread wheat is one of the most important crops for food production and has undergone extensive breeding, barley can outperform wheat yield partially through optimal flowering times across diverse environments (Fjellheim et al. 2014; Abu-Elenein et al. 2021; Harris et al. 2025). Barley exhibits extensive variance in flowering time that has allowed its spread through temperate zones (Cockram et al. 2011). Understanding the genetic mechanisms controlling flowering time in annual grasses facilitates effective manipulation of flowering-time genes to rapidly breed plant lines tailored for specific environments.

Since plant reproductive structures are vulnerable to temperature extremes and improper seasonal timing can radically reduce fitness, plants need to coordinate flowering time with reliable internal and external signals. Decades of research have documented heritable variance in flowering response and tracked the biological mechanisms controlling all aspects of plant flowering (Levy and Dean 1998; Piñeiro and Coupland 1998; Maple et al. 2024). Often studied in the model plant species *Arabidopsis thaliana*, a small European annual, flower initiation is coordinated by several pathways, responding to both internal and external cues. Internal controls consist of three pathways relating to plant age (endogenous), hormone levels (gibberellic acid), and plant

development fully independent from external cues (autonomous) (Srikanth and Schmid 2011). Two external pathways integrate environmental signals from temperature (thermosensitive and vernalization) and light (photoperiod). The thermosensitive pathway coordinates flowering response based on the ambient temperature, while the vernalization pathway induces flowering after a prolonged exposure to cold temperatures and is not present in all plant species (Jin and Ahn 2021). Finally, the photoperiod pathway involves signals from photoreceptors indicating the length of light and dark periods to indicate season, integrated with the day/night cycle regulated by the circadian clock (Lin 2000). Although the central mechanisms controlling flowering time are conserved across plant species, each species exhibits a unique genetic architecture.

Flowering time regulation in barley is controlled by the same pathways conserved across plant life, and the environmentally sensitive vernalization and photoperiod pathways play an important role in fine-tuning flowering time for success in local environments. Diverse allelic variants in these pathways have allowed for broad barley cultivation (Fernández-Calleja et al. 2021 May 9). In barley, the *VRN-H3* gene is the conserved ortholog of the *FLOWERING LOCUS T* (*FT*) gene identified in *Arabidopsis* that centrally promotes flowering (Yan et al. 2006). The central gene of the vernalization pathway in barley, *VRN-H1*, promotes flowering only after prolonged cold exposure. Non-responsive mutations in *VRN-H1* are a critical component of barley's post-domestication expansion into colder European climates where over-winter survival is not possible (Cockram et al. 2011). This northward movement was also facilitated by allelic variants in photoperiod genes *PPD-H1* and *PPD-H2* that allow for delayed flowering response (Fernández-Calleja et al. 2021 May 9). The wild, dominant allele of

PPD-H1 increases expression of *VRN-H3* under long-day light exposure to induce flowering, and is common in lower latitudes like southern Asia and Europe and the Mediterranean where plants can over-winter and flower in the spring. The recessive, less-functional, photoperiod insensitive allele, *ppd-h1*, is common in central and northern Europe where spring-planted barley needs an extended vegetative period for desirable yields during an autumn harvest. The clear geographic distribution of these two long-day-pathway alleles supports the association between this locus and the critical climate-related flowering response. The other central photoperiod locus, *PPD-H2*, is responsive to short days and also has two known allelic variants with distributions associated with climate geography. The dominant, functional allele is common in both winter and spring barley lines in southern Europe where it promotes flowering in short-day conditions, while the nonfunctional, recessive allele is common in central and northern European ranges' winter barley lines where the allele extends the vegetative stage. Although PPD-H2 has a large effect on flowering time and a clear environmental association as shown through signatures of divergent selection, the gene's exact effect is modulated by interactions with other genes in the vernalization and photoperiod pathways. Finally, *HvCEN* is perhaps the most important genetic variant for adaptation in barley. This centromeric ortholog of the CENTRORADIALIS gene identified in *Antirrhinum*, is a central flowering repressor with 3 common haplotype variants out of 13 global variations. These haplotypes are associated with either early or late flowering and vary geographically. Again, the later flowering haplotypes predominate in European spring lines to extend the growing season while early flowering haplotypes are common in the Mediterranean and winter lines where accelerated development is beneficial.

Barley's extensive range and adaptation to diverse local environments provide a rich genetic stock for studying evolution in novel environments.

Capitalizing on the abundant genetic diversity of barley, breeders have founded many "composite cross" populations of interbred barley landrace lines. Here we use the Composite Cross II (CC II): a population made by intercrossing 28 landrace lines collected from across the globe (Harlan and Martini 1929). The progeny of these crosses were then set into a long-running evolution experiment by being cultivated in Davis, California for more than 58 generations over the span of a century without conscious selection (Allard and Jain 1962; Saghai Maroof et al. 1983). Due to large population sizes, with upwards of 10,000 individuals per year and near complete inbreeding (98-99%) rates, we can observe the effect of natural selection on this population over time (Suneson 1956; Jain and Allard 1960).

Early work with the CC II population was based on phenotyping after about 30 generations of evolution and genotyping with allozyme markers (Allard et al. 1972; Weir et al. 1972). This and later research uncovered directional shifts in the average flowering time, yield, and plant height in the population (Bal et al. 1959; Allard and Jain 1962). Here we expand on this work using modern genome-sequencing techniques to understand the genetic basis of these observations over a longer period of time. Work published in Landis et al. 2024 found support for increased flowering time, yield, and height and connected these phenotypic shifts with the key genes undergoing evolution in the population. Furthermore, it documented the loss of large amounts of genetic diversity from the population in the first 18 generations of the experiment followed by slower decreases over the following 40 generations. Over time in the evolution experiment, one

lineage descended from a line pre-adapted to the California environment came to dominate the population. One of the key phenotypic advantages of this line is an early flowering time, and the population shows evidence of purifying selection on flowering time as the population converged around this pre-adapted parent's flowering date.

Phenotyping for this experiment, however, was assessed in a greenhouse environment with consistent, controlled 14:10 long days, abundant automatic watering, and limited growing space in 1-liter pots. Here we leverage the same population and sequencing data to better elucidate the genetic basis of phenotypic change in this population by assessing the flowering time of genetically diverse plant lineages in the less-controlled field environment. This field site in Riverside, California is subject to the natural day/night cycle from fall to spring, local soil conditions, less targeted but plentiful watering, and exposure to biotic stress. We measured flowering time, 100-seed weight, and fecundity (the estimated total number of seeds produced per plot) for a genetically diverse selection of 225 individuals from across 58 generations of the CC II, including all 28 CCII parents alongside 82 F_{18}, and 59 F_{58} progeny. This *plein air* experiment draws out measurable genotypic differences that help clarify the evolutionary path of natural selection, the relationships between traits in this evolution experiment, and the genetic basis of our fitness measurements. We uncovered evidence for stabilizing selection acting on flowering time to remove extremely early and late flowering lines. There is also evidence of strong directional selection for higher 100-seed weight which acted consistently over all generations. Plant fecundity significantly increases over time, but selective pressure for both flowering time and fecundity reversed over the course of the experiment.

Methods

Plant material

A total of 255 previously genotyped lines of barley (*Hordeum vulgare*) were used in this experiment. These include the 28 parental lines of the Composite Cross II population (Harlan and Martini 1929) and 227 progeny lines from 4 generations of the evolution experiment. Specifically, 82 genotypes from generation 18, 68 from generation 28, 18 from generation 50, and 59 lines from generation 58 were chosen to represent the widest available selection of genetic diversity in the population (based on haplotypes identified in Landis et al. 2024). To create a data set representative of each genotype's frequency in the population for a given generation, we classified each line according to its haplotype. We know the frequencies of our haplotypes from population-level sequencing (covered in Landis et al. 2024) and sampled the lines to represent as many as possible. To recover a population-level representative distribution of trait values, we sampled each haplotype's phenotypic value to match the haplotype's frequency in each tested generation. This data set provides an approximation of the occurrence of both rare and common haplotypes at their true representation within a given generation during the population's evolution.

Growth Conditions

Plants were grown in quarter acre fields within Riverside, California with a fall (November) planting and spring (May/June) harvest in 2021-2022 and 2022-2023. The field season lasted 131 days for the trial ending in 2022 and for 139 days for the trial ending in 2023. Fields were previously used for growing cowpeas and had basic

fertilizers applied at a low level before planting. The Composite Cross II experiment was rain-fed, so the population is theoretically adapted to low water requirements, but we avoided water stress during germination and establishment as well as seed set and seed filling by watering weekly for about 3 hours to supplement rainfall. Watering was lowered leading up to maturation and drying.

Each plot was approximately 1 square foot and was separated from its neighbors by about 4 feet of open space to allow easy differentiation between neighboring plants at their mature size. Genotype planting order was randomized within one block and duplicated without separate randomizations within the replicate block. We checked for discernable differences due to planting location and observed no clear effect of field position (see Supplemental Figure 1).

Plot Phenotyping

To scale seed production per plot by the number of producing individuals, we counted the number of germinated and surviving seedlings for each plot one to three weeks after planting when most seeds had sprouted and established to the 2-leaf stage.

Plants were checked for flowering every other day. Flowering time is defined as the number of days between planting and when at least 50% of the plot showed awn emergence beyond the flag leaf sheath. A few lines exhibited flowering well outside the time frame for the bulk of the field. Early-flowering plots were marked as close as possible to their estimated emergence date, and extremely late-flowering plots were

revisited at weekly intervals to distinguish late flowering from plots with no flowering within the recording time.

We harvested one sheaf of barley from each plot, threshed the heads to collect clean seeds, and weighed the total seed mass produced by each plot. A small random subset of seed was counted, weighed, and scaled to quantify 100-seed weight.
Specific phenotyping definitions and equations include:

yield

total weight of seed produced for a plot

100-seed weight

seed weight scaled to the number of seeds in a small sample, multiplied by 100

$$100\text{–}seed\ weight\ =\ \frac{sample\ seed\ mass}{sample\ seed\ count}\ \times\ 100$$

Trait measurements derived based on the previously defined traits follow:

seed count

estimated number of seeds making up the plots yield

$$seed\ count\ =\ \frac{total\ mass}{(\frac{100-seed\ mass}{100})}$$

fecundity

estimated number of seeds produced per surviving individual

$$fecundity\ =\ \frac{seed\ count}{surviving\ plants}$$

Estimating Genetic Variance and Traits Heritability

To extract reliable phenotypes, we extracted BLUPs (best linear unbiased predictors) for each genotype using the H2cal function from the inti package (Lozano-Isla 2025 Feb 26). The H2cal function is specifically designed for modeling the genetically attributable phenotype out of multi-environment field trials, including across replicate years. We used the same random model for the three traits used for analysis (flowering time, 100-seed weight, and fecundity):

$$y \sim Experiment\ year + Genotype + (Genotype \times Experiment\ year)$$

$$y = X\beta + Z\mu + W(\beta \cdot \mu) + \epsilon$$

where y denotes a vector of plant-replicate trait values; X is an incidence matrix associating observations with fixed effects coefficients of the year of the experimental replicate in vector β; Z is an incidence matrix associating observations with random effects of biological replicate in vector μ; W is the incidence matrix associating observations with the interaction of the random and fixed effect of genotype by year; and ϵ is the vector of random residuals. From this model we extracted a BLUP for each genotype and broad-sense heritability for each trait.

The average phenotypic change over generations in the population, “R” or “response” in Breeders equation was calculated for each trait by scaling with the scale function in R, finding the average trait value for each generation, taking the difference between pairs of

generations, and then dividing that phenotypic change between generations by the number of generations between the two time points:

$$R = \frac{\bar{x}_{later} - \bar{x}_{earlier}}{number\ of\ generations\ between\ earlier\ \&\ later}$$

With the broad-sense heritability and response, we can use the Breeder's equation

$(R = H^2 \cdot s)$, rearranged to

$$s = \frac{R}{H^2},$$

to estimate selection pressure for each trait over different generational time spans.

Association Mapping

Genome sequencing for individuals used in this experiment were taken from Landis et al. 2024. See population sampling, sequencing, and genome sequencing alignment and filtering methods there. Before performing genome-wide association studies (GWAS), we used vcftools (Danecek et al. 2011) (version 0.1.16-18) to remove indels and filter out variants that were fixed in progeny lines. These filters left us with 425070 genome sites and 225 sequenced progeny individuals. We then used Plink version 1.90 (Purcell et al. 2007) to generate .bed, .bim, and .fam files based on the vcf containing our filtered SNP list and further filtered out sites with minor allele frequency below 0.01 which filtered out 74245 sites, leaving 350825 sites and 225 fully genotyped individuals. Phenotypes were added to .fam files afterward with a custom R script. Relatedness among individuals was also accounted for by incorporating a kinship matrix in the models. The kinship matrix was created with GEMMA version 0.98.5 (Zhou and Stephens 2012) and used as a covariate in the model. Remaining population structure was corrected by including 10 principal components calculated with the plink command pca as another covariate for the

model. We conducted univariate GWAS for 350825 variants with a linear mixed model across the 225 progeny lines for each trait using GEMMA for flowering time, 100-seed weight, and fecundity.

Population Allele Frequency

To understand the evolutionary path taken in our population, we calculated the allele frequencies for each generation at all genome sites by extracting allele counts from the vcf file for all 899 previously sequenced individuals with the script extractsite_counts.py. The allele counts were used when testing for significant change in allele frequency over generations with a Chi square test using the ‘chisq.test’ function from the ‘stats’ package version 3.6.2 in R.

To compare the change in allele frequencies of our significant sites with a neutral expectation, we separated SNPS into 2 groups: sites identified by GWAS as significantly or suggestively associated with a trait and a randomly selected subset of sites not associated with any traits. For a more accurate comparison, we sorted neutral genome sites into bins based on their allele frequency in the parents based on frequency bins at intervals of 0.05 and then randomly sampled the number of sites matching those observed for the trait-associated sites in the same interval. At these sampled sites, progeny allele frequencies were recorded, the differences between generations were found and averaged, and this cycle was repeated 1000 times to provide a distribution of allele frequency changes at neutral sites.

Results

Evidence for selection on fitness related traits in CCII in the field

We conducted a multi-year field experiment to understand how flowering time and fitness co-evolved in CCII. Over two years we grew the CCII parents alongside 82 F_{18} and 59 F_{58} progeny under field conditions similar to those to which the CCII was adapted. We then evaluated flowering time and two fitness associated traits: 100-seed weight, and fecundity (estimated total number of seeds per plot) for each genotype. We then fit mixed effects linear models accounting for both year and genotype to estimate best linear unbiased predictors (BLUP) that served as trait values for each genotype in subsequent analyses (Dataset_2_BLUPs.tsv). By combining estimated trait values with the frequency of each multi-locus genotype at F_{18} and F_{58} we could impute changes in trait distributions over evolutionary time in CCII (Figure 1A).

We began by exploring trait variation amongst the 28 parents of the CCII. The 28 parents contain lines with both winter and spring growth habits, two- and six-row floret architecture, and varieties collected from all the major barley growing regions of the world. These major barley growing regions span the breadth of global environments, so the parental lines also represent a width of environmental adaptations. This includes lines adapted to an environmental spectrum from cold and temperate to Mediterranean. The progeny produced from crossing such genetic backgrounds provide ample genetic and phenotypic variation for exploring environmental adaptation. Previous studies of evolution of CCII can be divided into an early phase (here F_1 to F_{18}) where early flowering was favored, seed size increased, and yields substantially improved, and a late phase (here F_{18} to F_{58}) where seed size continued to increase, but later flowering was

favored and inconsistent changes in yield were observed ((Bal et al. 1959; Allard and Jain 1962b)). We sought to confirm these observations with our genotyped data.

Significant variability across generations was found for all three traits (Table 1, Kruskal-Wallis $p < 0.05$). Average flowering time decreased by 3.6 days during the early phase (109.4 days in parents to 105.8 days in F_{18}, Dunn $p = 0.099$, Figure 1A, Table 2). The later mean flowering time of the parents was largely due to 6 late flowering parents (Wisconsin Winter, Sandrel, Han River, Algerian, Trebi, and Orel). The latest flowering lines (Wisconsin Winter, Sandrel, Trebi, and Orel) are classified as winter habit and the Mediterranean climate of California is often insufficient to fully vernalize and induce flowering. Late flowering progeny of these parents did not appear to survive to generation F_{18} (Figure 1A). In the late phase, flowering time significantly increased by 3.78 days, from 105.8 to 109.5 days (Kruskal $p = 3.65 \times 10^{-24}$, Dunn post hoc $p = 1.75 \times 10^{-14}$).

In contrast to flowering time, average seed weight increased consistently across the early and late phases of the experiment from the parents (4.6 g/100 seed) to F_{58} (5.2 g/100 seed) (Dunn post hoc $p = 0.012$ and 3.96×10^{-24}). The rate of change in seed mass was more rapid in the early phase (per seed increase of 176 µg/generation) than in the late phase (seed increase of 75 µg/generation) which is consistent with depletion of genetic variation in this trait over time.The most direct indicator of fitness in the experiment, fecundity, increased significantly from 0.977 to 1.01 (relative fecundity; 171.7 seeds/plant to 177.8 seeds/plant) (Dunn post hoc $p = 0.04$). The initial increase in fecundity was followed by a more modest reduction to 0.99 (174.3 seeds/plant) in F_{58} (Dunn post hoc $p = 7.22 \times 10^{-04}$).

Stabilizing selection, where phenotypic extremes are less fit than intermediate values, has been invoked to explain the complex evolution of flowering time over the course of CCII (Jain and Allard 1960; Jain 1961; Allard 1988). Consistent with this hypothesis, CCII showed strong reductions in variance in flowering time across generations (Levene test, $p_{early} = 3.92x10^{-12}$, $p_{late} = 1.13x10^{-27}$, Table 3). The other two traits also show a significant reduction in variance over time (Levene test 100 seed weight $p_{early} = 0.007$, $p_{late} = 1.13x10^{-23}$; Levene test fecundity $p_{early} = 0.0013$, $p_{late} = 7.13x10^{-15}$) suggesting that the removal of genetic variance by drift and directional selection may also contribute to this shift. Changes in population distributions between the parents and progeny are not necessarily even or consistent. For flowering time, we see the removal of both early and late flowering lines, but the strength of removal is asymmetrical. Late-flowering lines are relatively common in the parents, but are almost completely removed in the progeny (Figure 1B). This shift is brought about through a strong convergence in the progeny around flowering at 110 days. Changes for seed mass and fecundity are more unidirectional and occur through the removal of low-value lines and an increase in higher seed weight and larger seed number individuals.

In summary, our field experiments reveal that CCII evolved overall later flowering time, higher seed weight, and increased seed production. Only seed weight increased consistently over time, while flowering time and fecundity evolved in opposite directions in the early and late stages of the experiment. All traits showed a reduction in variance over time in the population, with the most conspicuous changes in variance being observed for flowering time. While seed weight and fecundity appear to undergo directional changes, flowering time seems to evolve toward less extreme values.

The relationship between seed weight, flowering time, and fitness in CCII

We next explored the scale of selection acting on our focal traits over the course of the experiment. First, we used our fecundity measurements as a proxy for plant fitness to estimate the relationship between plant fitness and seed weight and flowering time. Only flowering time had a significant correlation with fitness (Spearman's correlation; flowering time $\rho = -0.217$, $p = 0.00047$; seed weight $\rho = -0.019$, $p = 0.7551$). We also tested the fit of quadratic trait relationships and found that the relationship between flowering time and fecundity is somewhat better explained by a quadratic equation ($AIC_{linear} = 323$, $AIC_{quadratic} = 321$; Supplementary Table 1). This data does not show a clear linear relationship between flowering time and 100-seed weight ($\rho = 0.099$, $p = 0.1132$) (Figure 1D). These results also hold true when looking at only progeny lines and when a linear model is fit to each generation's trait relationship (Supplementary Figure 2).

We also estimated selection coefficients (S) for each trait based on the rate of change in trait values over evolutionary time and the heritable fraction of trait variance. Broad sense heritabilities in the three traits estimated from our initial mixed effects model ranged from strong to moderate for flowering time, seed weight, and fecundity respectively ($H^2_{overall}=0.91$, $H^2_{overall}=0.68$, $H^2_{overall}=0.27$, Dataset 3). Our use of broad-sense heritability is appropriate in this calculation because barley is overwhelmingly self-fertilizing (Brown et al. 1978). Specific heritability estimates for our time periods of interest reflect the decreasing variance over time. Flowering time and seed weight maintain similar heritability estimates over time (flowering time $H^2_{early}=0.93$, $H^2_{late}=0.87$; seed weight $H^2_{early}=0.72$, $H^2_{late}=0.65$) while fecundity shows a large reduction that may reflect the removal of useful genetic variance ($H^2_{early}=0.46$, $H^2_{late}=0.15$). For all three traits

the absolute value of S is larger during the early phase than in the second phase (flowering time, S_{early} = -0.048, S_{late} = 0.024; seed weight, S_{early} = 0.08, S_{late} = 0.036; fecundity S_{early} = 0.077, S_{late} =-0.06) (Figure 1C, Table 4). The direction of selection shifts between the early and late phases of the experiment for both flowering time and fecundity, however S is an order of magnitude smaller for fecundity in the late phase. This provides evidence for the strength of selection during the early part of the experiment and the extent to which trait and genetic variance are removed over time in the population.

VRN-H1 is the major locus controlling CCII flowering time in the field

To understand the genetic components controlling trait variance, we conducted genome-wide association studies (GWAS) for each trait. We tested 350825 sites for 225 progeny lines and found 41 sites passed the Bonferroni correction significance threshold (Figure 2A). Almost all of these sites (40 out of 41) are significantly associated with flowering time and all of which are located on chromosome 5H. The other significant site is associated with fecundity and is located on chromosome 1H. We will refer to these two Bonferroni-threshold passed sites as “significant” candidate sites.

The significant site identified on chromosome 1H overlaps a gene encoding a chloroplastic-like photosynthetic NDH subunit (NCBI). Allele differences at this site are associated with a difference of 10.8 seeds/plant (Figure 2B). The significant association on chromosome 5H is coincident with a genome region identified as under strong selection (Landis et al. 2024). This region may contain the major flowering locus VRN-H1 which controls vernalization response in barley and would have a strong impact on flowering time in vernalization-requiring lines (Trevaskis et al. 2003; Yan et al. 2003).

Homozygotes with alternate alleles have an average difference in flowering time of 5 days (Figure 2B).

A non-significant peak on chromosome 4H coincides (within 25 Mb) with a previously detected association in greenhouse experiments overlying VRN-H2 (Landis et al. 2024) (Figure 3A). Deletions in this gene region can remove vernalization requirements and promote earlier flowering (Yan et al. 2004). Changing alleles at this site is associated with a 3.7 day difference in flowering time and a 3 seed difference in fecundity (Figure 3B).

Genome Targets of Natural Selection

To expand our list of sites for subsequent analysis we also included the lead SNP associated with 46 additional, non-significant but potentially 'suggestive' peaks based on the 'clump' command in plink (see Methods). These additions include 12 sites for 100-seed weight, 25 sites for fecundity, and 9 sites for flowering time. This less stringent list allows us to explore directional changes in allele frequency that may be associated with population trait changes. We will refer to the full list of 48 suggestive and significant SNPs as our 'top' candidates. For the 48 identified sites, we plotted their allele frequencies over time in the population, polarized toward the allele associated with increased trait values (Figure 4A). The 10 sites associated with flowering time include sites that reach fixation after starting at a range of frequencies. While many of these sites start near fixation and may be moved by drift, several sites show large shifts in frequency over the generations and provide distinct candidates for investigating natural selection.

The allele frequencies for the two significant sites associated with flowering time and fecundity are plotted in Figure 4B. The significant flowering time associated site

shows a frequency change of 0.43 (from 0.52 in parents to 0.95 in F_{58}). Allele change at this site is associated with a 2 day increase in flowering time, and the large change in allele frequency makes this locus an interesting candidate for adaptation.

The fecundity associated site shows smaller frequency change from 0.15 in the parents to fixation at 0 in the F_{58} progeny generation. A change in allele at this site is associated with a 13 seed yield difference (Figure 3B). Because this allele started at low frequency, we cannot distinguish whether the allele is likely removed from the population due to selection or drift. These identified genome regions help identify the genetic elements controlling traits in this population, and help expand our understanding of important evolutionary components beyond this experiment.

To identify alleles that significantly changed over generations, we extracted progeny generations' allele counts and tested for significant differences with a Chi squared test comparing allele counts between parents and F_{18} and between F_{18} and F_{58}. Although we tested the 425070 sequenced sites that segregate in the progeny and found 293118 sites with significant changes in at least one of the time periods tested, we are mostly interested in the allele frequency changes for our top sites of interest. Landis et al. contains a more thorough analysis of genome evolution in this population. Sites examined were filtered to genome sites used in our GWAS analysis, but allele counts for these sites were taken from population-level sampling progeny of 899 lines with 460 lines retained for the frequencies from relevant generation (28 parents, 218 lines from F_{18}, 215 lines from F_{58}). To understand whether the observed change in allele frequencies for our top sites are indicative of selective evolutionary pressure, we made a comparison between the allele frequency distributions of our trait-associated sites and

randomly sampled neutral genome sites. We randomly sampled 48 neutral (i.e. not trait-related) genome sites which have the same allele frequency as our trait-associated sites in the parental generation to use as our comparative baseline. Then, we recorded the allele frequency of that site in the F_{18} and F_{58} generations and took the median value of these frequencies to represent the average path of allele frequency change in neutral genome sites in our population, and this process was repeated 1000 times. That sampling provides us with a random-genome-site frequency spectrum. Figure 4C compares the site frequency spectrum for these two sets of genome sites - those 48 sites suggestively associated with a trait, and 1000 replicates of the randomly sampled sites with starting allele frequency matched to that of the trait-sites, as a proportion of the total sites. This panel explores two diverging evolutionary paths and shows the difference in allele frequency trajectory for trait-associated, putatively naturally selected sites and neutral, non-selected genome sites. The neutral distributions set our expectation. Comparing the distributions of associated and neutral sites at F_{18}, we can see a greater proportion of GWAS-identified sites at intermediate frequencies. This may indicate that alleles are being driven though the population from high frequency to low and vice versa. When comparing the allele frequency distributions in F_{58} we see a complex configuration. More GWAS-associated sites are fixed at 0 and are not present at other frequencies below 0.5, but above that threshold the neutral sites are closer to fixation. This suggests that deleterious trait-associated alleles are being fully removed from the population over 58 generations while beneficial trait-associated alleles are not completely driven to fixation or are maintained at a high frequency in the population.

However, since many of our GWAS sites are only suggestive of trait association, we cannot rule out these sites may not be under selection.

Discussion

We know that this population changed genetically over time based on the research in Landis 2024, and have evidence for large phenotypic shifts in the population on average over the course of 58 generations of evolution in the population. Previous work with the CC II has also documented increases in plant height, later flowering times, and higher yields. Furthermore, most of these changes occurred during the early phase of the experiment (from parents to F_{18}). Here we find support for stabilizing selection acting on flowering time and directional selection acting on 100-seed weight and fecundity. We found further support for strong reductions in phenotypic variance within the first 18 generations in the population as highly unfit individuals are removed from the population. For flowering time, we see a stronger initial removal of late-flowering lines in the early generations followed by a reduction in early-flowering lines during the subsequent 40 generations. This significant shift toward a later flowering date during the progeny generations indicates a fitness benefit in the Davis, CA environment. On the other hand, 100-seed weight shows evidence of consistent selection for larger seeds. The consistent increase in seed weight confirms a positive relationship between seed weight and fitness in this population. These two contrasting traits provide insight into the strength and timing of trait selection in this large and diverse population. Investigating the genetic basis of our three measured traits, we found one significant GWAS peak and two suggestive peaks which account for large-effect changes in flowering time. Overall, this experiment

provides further evidence for the evolutionary pathways of complex phenotypes in this population as it evolved toward a local fitness maxima in the Davis environment.

Decades of research have established flowering time as a critical component of fitness which drives local adaptation in plants. Phenotypic variance in flowering time is especially important in crop species like barley because it allows expansion into diverse environments. The genetic network controlling flowering time has been well studied in Arabidopsis thaliana while a full understanding of the control mechanisms is still unfolding in wheat and barley. Wild and landrace barley varieties harbor abundant natural variation which could provide a clearer picture of the genetic basis of flowering time control, including novel alleles and mutations. The Composite Cross II is a unique experiment that has been ongoing over nearly a century wherein a genetically diverse population was allowed to adapt to the environment with minimal agricultural disturbance and no conscious selection. This germplasm allows us to investigate the path of evolution over time as a genetically diverse population adapts to its environment. Since flowering time naturally varies across environmental gradients and is a critical life-history trait, we focus this experiment on clarifying the relationship between flowering time and fitness in this evolution experiment to understand the process of adaptation in a large and diverse crop population.

Modern phenotyping efforts in the CC II were conducted on a large number of plants, the assessments were carried out on many genetically redundant plant lineages which were grown and phenotyped in a controlled greenhouse environment. In this experiment we can expand our understanding of evolution in this population by phenotyping unique genetic backgrounds in an agricultural field environment in

Riverside, California. Results from both experiments illustrate how strong selection acts to remove unfit individuals from the population in the first 18 generations.

While modern research into the Composite Cross II has uncovered some of the genetic basis of evolutionary pressure in the population, efforts to characterize the phenotypic shifts and understand how selective pressure acts on the population and various traits are ongoing. Further research into this population may include more extensive comparisons of phenotyping outcomes based on growth environment and the underlying environmentally responsive mechanisms. The original experiment allowed the population to adapt to the environment of Davis, California, and growing plants and conducting observations in Riverside, California may introduce conflict around environmentally impacted traits like flowering time which affect yield and fitness measurements. Following research can clarify how daily growth and life cycle traits lead to our end-point observations or the traits leading to potential trade-offs between flowering time, seed weight, and fecundity in this population. Finally, because of the unique growth history of this population, future research could investigate the evolution of inter-plant “competitiveness” to clarify how specific plant lines came to dominate the population in an unstructured agricultural environment and the traits and genetic variance associated with these dominant lines.

Our study leverages a highly diverse, long-running evolution experiment population, the Composite Cross II to show how a multicellular plant species adapts to the local environment. We show how the population reaches a local fitness maximum for flowering time by purging first very late and then very early flowering lines. This evolutionary change in average flowering time is also associated with small increases in

seed production (fecundity). This finding provides support for the importance of flowering time as an aspect of environmental adaptation in plants, and for the importance of environmental responsiveness for appropriate flowering times. This experiment furthers our understanding of the process of evolution by returning to assess the CC II material with modern genomics after further decades of evolution. We provide insight into the initially strong action of selection removing trait variance and evidence for consistent selective pressure for larger seed weight over 58 generations in this population. Our findings contribute to the global understanding of the selective mechanisms that drive evolution and how consistently diversity is maintained and expunged during evolution.

References

Abu-Elenein J et al. 2021. Agronomic performance and flowering behavior in response to photoperiod and vernalization in barley (Hordeum vulgare L.) Genotypes with contrasting drought tolerance behavior. Environ Exp Bot. 192(104661):104661. https://doi.org/10.1016/j.envexpbot.2021.104661

Allard RW, Jain SK. 1962a. Population studies in predominantly self-pollinated species. II. Analysis of quantitative genetic changes in a bulk-hybrid population of barley. Evolution. 16(1):90–101. https://doi.org/10.1111/j.1558-5646.1962.tb03201.x

Allard RW, Jain SK. 1962b. Population studies in predominantly self-pollinated species. II. Analysis of quantitative genetic changes in a bulk-hybrid population of barley. Evolution. 16(1):90–101. https://doi.org/10.2307/2406269

Allard RW, Kahler AL, Weir BS. 1972. The effect of selection on esterase allozymes in a barley population. Genetics. 72(3):489–503

Allard RW. 1988. The Wilhelmine E. Key 1987 invitational lecture. Genetic changes associated with the evolution of adaptedness in cultivated plants and their wild progenitors. J Hered. 79(4):225–238. https://doi.org/10.1093/oxfordjournals.jhered.a110503

Bal BS, Suneson CA, Ramage RT. 1959. Genetic shift during 30 generations of natural selection in barley. Agron J. 51(9):555–557. https://doi.org/10.2134/agronj1959.00021962005100090014x

Bradley NL, Leopold AC, Ross J, Huffaker W. 1999. Phenological changes reflect climate change in Wisconsin. Proc Natl Acad Sci U S A. 96(17):9701–9704. https://doi.org/10.1073/pnas.96.17.9701

Brown AHD, Zohary D, Nevo E. 1978. Outcrossing rates and heterozygosity in natural populations of Hordeum spontaneum Koch in Israel. Heredity. 41(1):49–62. https://doi.org/10.1038/hdy.1978.63

Cockram J et al. 2007. Control of flowering time in temperate cereals: genes, domestication, and sustainable productivity. J Exp Bot. 58(6):1231–1244. https://doi.org/10.1093/jxb/erm042

Cockram J, Hones H, O'Sullivan DM. 2011. Genetic variation at flowering time loci in wild and cultivated barley. Plant Genet Resour. 9(2):264–267. https://doi.org/10.1017/s1479262111000505

Collins CG et al. 2025. Flowering time responses to warming drive reproductive fitness in a changing Arctic. Ann Bot. 135(1-2):255–268. https://doi.org/10.1093/aob/mcae007

Danecek P et al. 2011. The variant call format and VCFtools. Bioinformatics. 27(15):2156–2158. https://doi.org/10.1093/bioinformatics/btr330

Felicity Harris et al. 2025. Phenology FUNdamentals: Redefining flowering times in wheat and barley for future climates - Grains Research and Development Corporation. Grains Research and Development Corporation. [accessed 2025 Sept 11]. https://grdc.com.au/resources-and-publications/grdc-update-papers/tab-content/grdc-update-papers/2025/02/phenology-fundamentals-redefining-flowering-times-in-wheat-and-barley-for-future-climates

Ferguson JN et al. 2019. Accelerated flowering time reduces lifetime water use without penalizing reproductive performance in Arabidopsis. Plant Cell Environ. 42(6):1847–1867. https://doi.org/10.1111/pce.13527

Fernández-Calleja M, Casas AM, Igartua E. 2021. Major flowering time genes of barley: allelic diversity, effects, and comparison with wheat. Theor Appl Genet.. https://doi.org/10.1007/s00122-021-03824-z

Fitter AH, Fitter RSR. 2002. Rapid changes in flowering time in British plants. Science. 296(5573):1689–1691. https://doi.org/10.1126/science.1071617

Fjellheim S, Boden S, Trevaskis B. 2014. The role of seasonal flowering responses in adaptation of grasses to temperate climates. Front Plant Sci. 5:431. https://doi.org/10.3389/fpls.2014.00431

Fournier-Level A et al. 2011. A map of local adaptation in Arabidopsis thaliana. Science. 334(6052):86–89. https://doi.org/10.1126/science.1209271

Fournier-Level A et al. 2022. Adaptive significance of flowering time variation across natural seasonal environments in Arabidopsis thaliana. New Phytol. 234(2):719–734. https://doi.org/10.1111/nph.17999

Gaudinier A, Blackman BK. 2020. Evolutionary processes from the perspective of flowering time diversity. New Phytol. 225(5):1883–1898. https://doi.org/10.1111/nph.16205

Hall MC, Willis JH. 2006. Divergent selection on flowering time contributes to local adaptation in Mimulus guttatus populations. Evolution. 60(12):2466–2477. https://www.ncbi.nlm.nih.gov/pubmed/17263109

Harlan HV, Martini ML. 1929. A Composite Hybrid Mixture1. Agronomy Journal. 21(4):487–490. https://doi.org/10.2134/agronj1929.00021962002100040014x

Jain SK, Allard RW. 1960. POPULATION STUDIES IN PREDOMINANTLY SELF-POLLINATED SPECIES, I. EVIDENCE FOR HETEROZYGOTE ADVANTAGE IN A CLOSED POPULATION OF BARLEY. Proc Natl Acad Sci U S A. 46(10):1371–1377 https://www.ncbi.nlm.nih.gov/pubmed/16590760

Jain SK. 1961. Stabilizing Selection for Heading Time in a Bulk-Hybrid Population of Barley. Nature. 191(4793):1123–1124. https://doi.org/10.1038/1911123b0

Jin S, Ahn JH. 2021. Regulation of flowering time by ambient temperature: repressing the repressors and activating the activators. New Phytol. 230(3):938–942. https://doi.org/10.1111/nph.17217

Landis JB et al. 2024. Natural selection drives emergent genetic homogeneity in a century-scale experiment with barley. Science. 385(6705):eadl0038. https://doi.org/10.1126/science.adl0038

Levy YY, Dean C. 1998. The transition to flowering. Plant Cell. 10(12):1973–1990. https://doi.org/10.1105/tpc.10.12.1973

Lin C. 2000. Photoreceptors and regulation of flowering time. Plant Physiol. 123(1):39–50. https://doi.org/10.1104/pp.123.1.39

LOC123397780 photosynthetic NDH subunit of lumenal location 5, chloroplastic-like [Hordeum vulgare subsp. vulgare (domesticated barley)] - Gene - NCBI. [accessed 2025 Nov 25]. https://www.ncbi.nlm.nih.gov/gene?cmd=search&term=123397780

Lozano-Isla F. 2025. Tools and Statistical Procedures in Plant Science [R package inti version 0.6.7]. [accessed 2025 July 10]. https://CRAN.R-project.org/package=inti

Maple R et al. 2024. Flowering time: From physiology, through genetics to mechanism. Plant Physiol. 195(1):190–212. https://doi.org/10.1093/plphys/kiae109

Menzel A, Fabian P. 1999. Growing season extended in Europe. Nature. 397(6721):659–659. https://doi.org/10.1038/17709

Piñeiro M, Coupland G. 1998. The control of flowering time and floral identity in Arabidopsis. Plant Physiol. 117(1):1–8.pdf. https://doi.org/10.1104/pp.117.1.1

Primack D et al. 2004. Herbarium specimens demonstrate earlier flowering times in response to warming in Boston. Am J Bot. 91(8):1260–1264. https://doi.org/10.3732/ajb.91.8.1260

Purcell S et al. 2007. PLINK: a tool set for whole-genome association and population-based linkage analyses. Am J Hum Genet. 81(3):559–575. https://doi.org/10.1086/519795

Saghai Maroof MA, Webster RK, Allard RW. 1983. Evolution of resistance to scald, powdery mildew, and net blotch in barley composite cross II populations. Theor Appl Genet. 66(3-4):279–283 [accessed 2018 Feb 22]. https://doi.org/10.1007/BF00251159

Sandring S, Agren J. 2009. Pollinator-mediated selection on floral display and flowering time in the perennial herb Arabidopsis lyrata. Evolution. 63(5):1292–1300. https://doi.org/10.1111/j.1558-5646.2009.00624.x

Savolainen O, Lascoux M, Merilä J. 2013. Ecological genomics of local adaptation. Nat Rev Genet. 14(11):807–820. https://doi.org/10.1038/nrg3522

Shavrukov Y et al. 2017. Early flowering as a drought escape mechanism in plants: How can it aid wheat production? Front Plant Sci. 8:1950. https://doi.org/10.3389/fpls.2017.01950

Sparks TH, Jeffree EP, Jeffree CE. 2000. An examination of the relationship between flowering times and temperature at the national scale using long-term phenological records from the UK. Int J Biometeorol. 44(2):82–87. https://doi.org/10.1007/s004840000049

Srikanth A, Schmid M. 2011. Regulation of flowering time: all roads lead to Rome. Cell Mol Life Sci. 68(12):2013–2037. https://doi.org/10.1007/s00018-011-0673-y

Suneson CA. 1956. An evolutionary plant breeding method. Agron J. 48(4):188–191 https://dl.sciencesocieties.org/publications/aj/abstracts/48/4/AJ0480040188

Takou M et al. 2019. Linking genes with ecological strategies in Arabidopsis thaliana. J Exp Bot. 70(4):1141–1151. https://doi.org/10.1093/jxb/ery447

Toomajian C et al. 2006. A nonparametric test reveals selection for rapid flowering in the Arabidopsis genome. PLoS Biol. 4(5):e137. https://doi.org/10.1371/journal.pbio.0040137

Trevaskis B et al. 2003. MADS box genes control vernalization-induced flowering in cereals. Proc Natl Acad Sci U S A. 100(22):13099–13104. https://doi.org/10.1073/pnas.1635053100

Weir BS, Allard RW, Kahler AL. 1972. Analysis of complex allozyme polymorphisms in a barley population. Genetics. 72(3):505–523

Yan L et al. 2003. Positional cloning of the wheat vernalization gene VRN1. Proc Natl Acad Sci U S A. 100(10):6263–6268. https://doi.org/10.1073/pnas.0937399100

Yan L et al. 2004. The wheat VRN2 gene is a flowering repressor down-regulated by vernalization. Science. 303(5664):1640–1644. https://doi.org/10.1126/science.1094305

Yan L et al. 2006. The wheat and barley vernalization gene VRN3 is an orthologue of FT. Proc Natl Acad Sci U S A. 103(51):19581–19586. https://doi.org/10.1073/pnas.0607142103

Zhou X, Stephens M. 2012. Genome-wide efficient mixed-model analysis for association studies. Nat Genet. 44(7):821–824. https://doi.org/10.1038/ng.2310

Figures & Tables

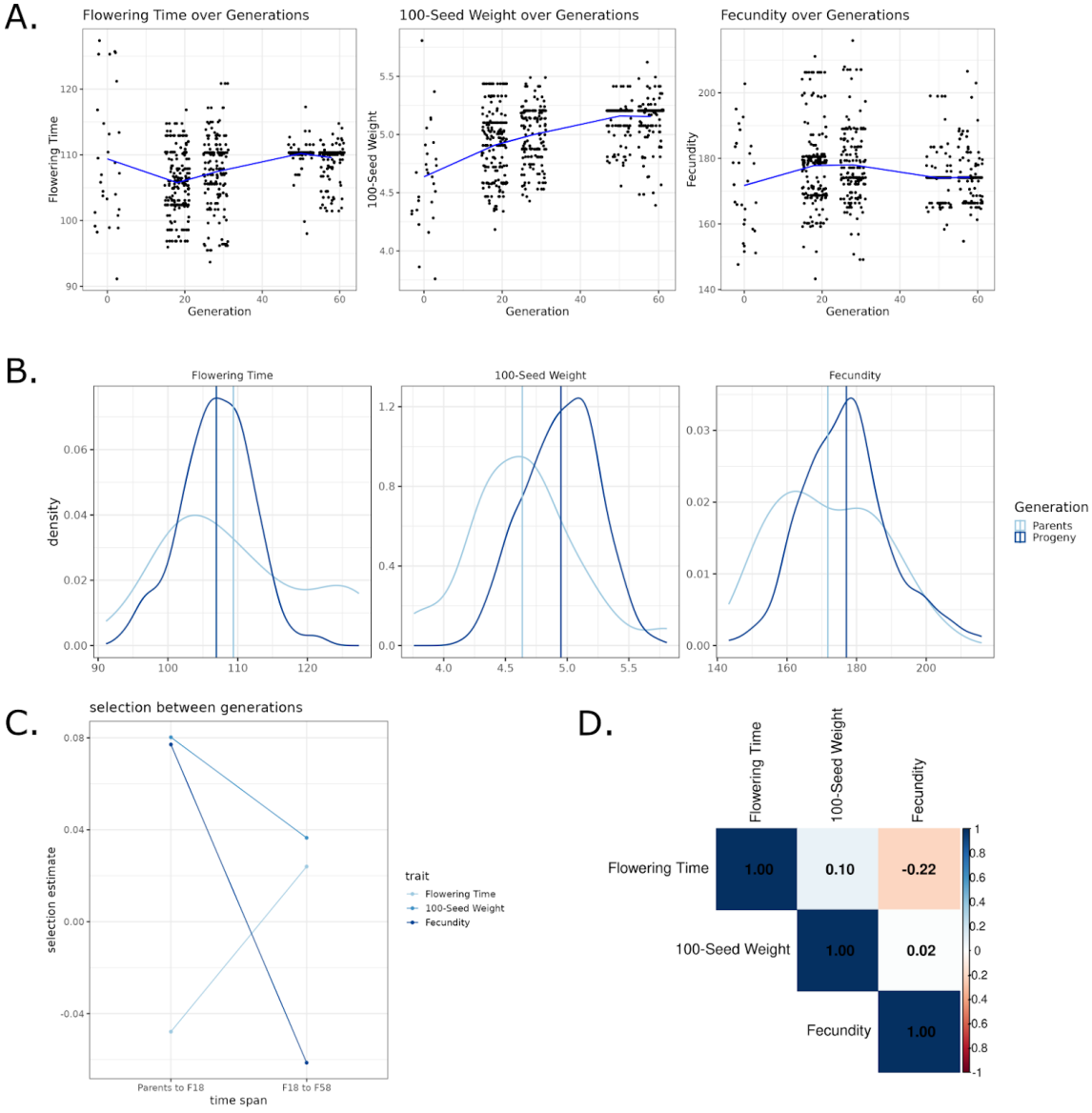

Figure 1.1 - Consistent selection drives increases in seed mass while changing flowering time does not appear to lead to increases in fecundity

A. Strip plots of trait values over generations with phenotype frequency imputed based on the frequency of the corresponding genotype in the original population. The blue line indicates trait average. **B.** Density plots of trait distributions for two generation-groups: the light blue represents the parental phenotypes while the darker blue inclusively encompasses that of all the progeny generations (F_{18}, F_{28}, F_{50}, and F_{58}). Vertical lines in the corresponding color indicate the mean value for that group. Each genetic background is represented once in this dataset as opposed to panel As haplotype-frequency imputed data which reflects the population's trait value with highly redundant genotypes in the later generations. **C.** Strip plots showing the selection estimate as defined in the breeder's equation ($S = R \cdot H^2$) for two time periods: between the parents and F_{18} generation and from F_{18} to F_{58}. Points are colored by trait and a line connects the two time period's values to emphasize the direction and magnitude of trait change in different evolutionary time periods in the experiment. **D.** Heatmap of the Spearman's correlation value calculated for each trait pair. More saturated blue color squares indicate higher positive correlation and red a stronger negative correlation.

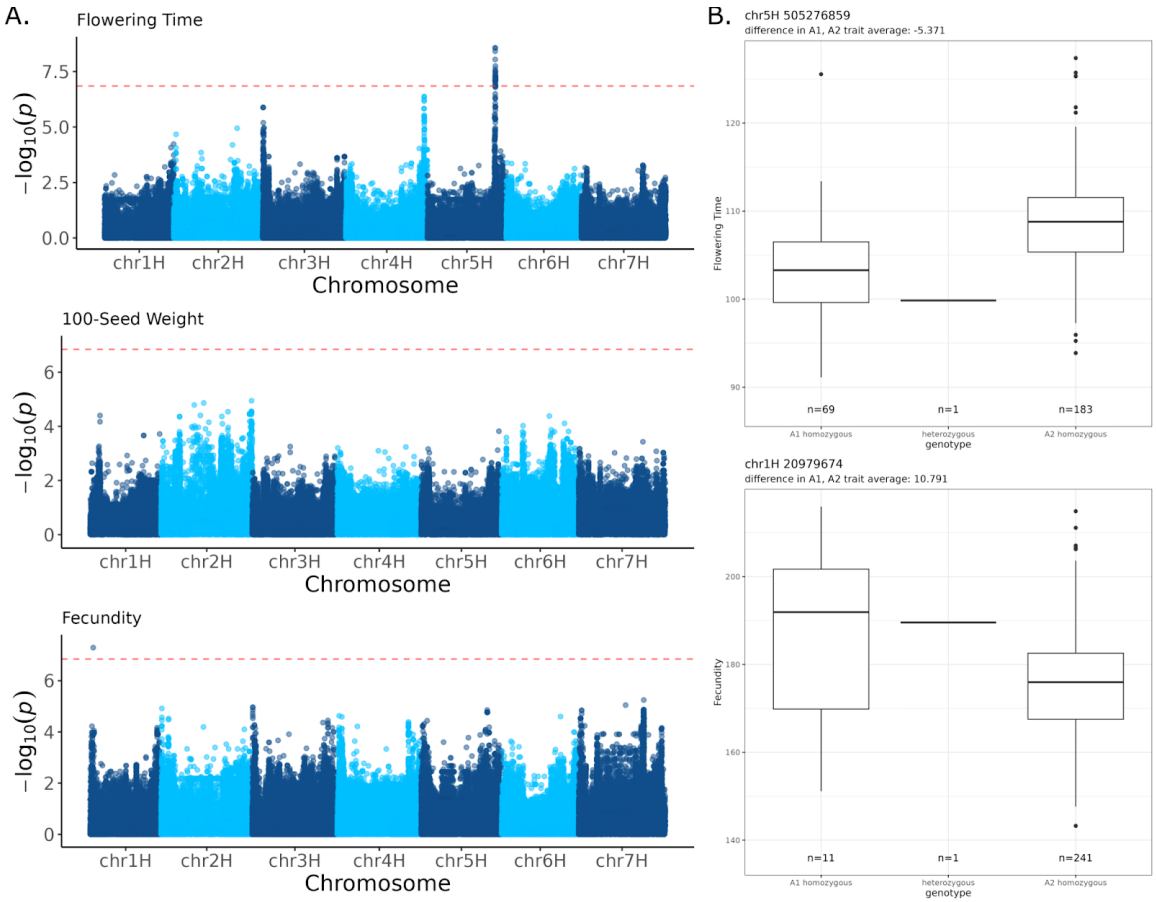

Figure 1.2 - Genetic variants connected to differences in flowering time and fecundity

A. Manhattan plots showing the -log10 p value indicating the likelihood that a given genomic region is associated with the given trait indicated in the top-left corner. Chromosomes are differentiated with alternating colors. The dashed line represents the Bonferroni threshold, above which points indicate statistical significance corrected for multiple comparisons. **B.** Allele effect plots from significant sites.

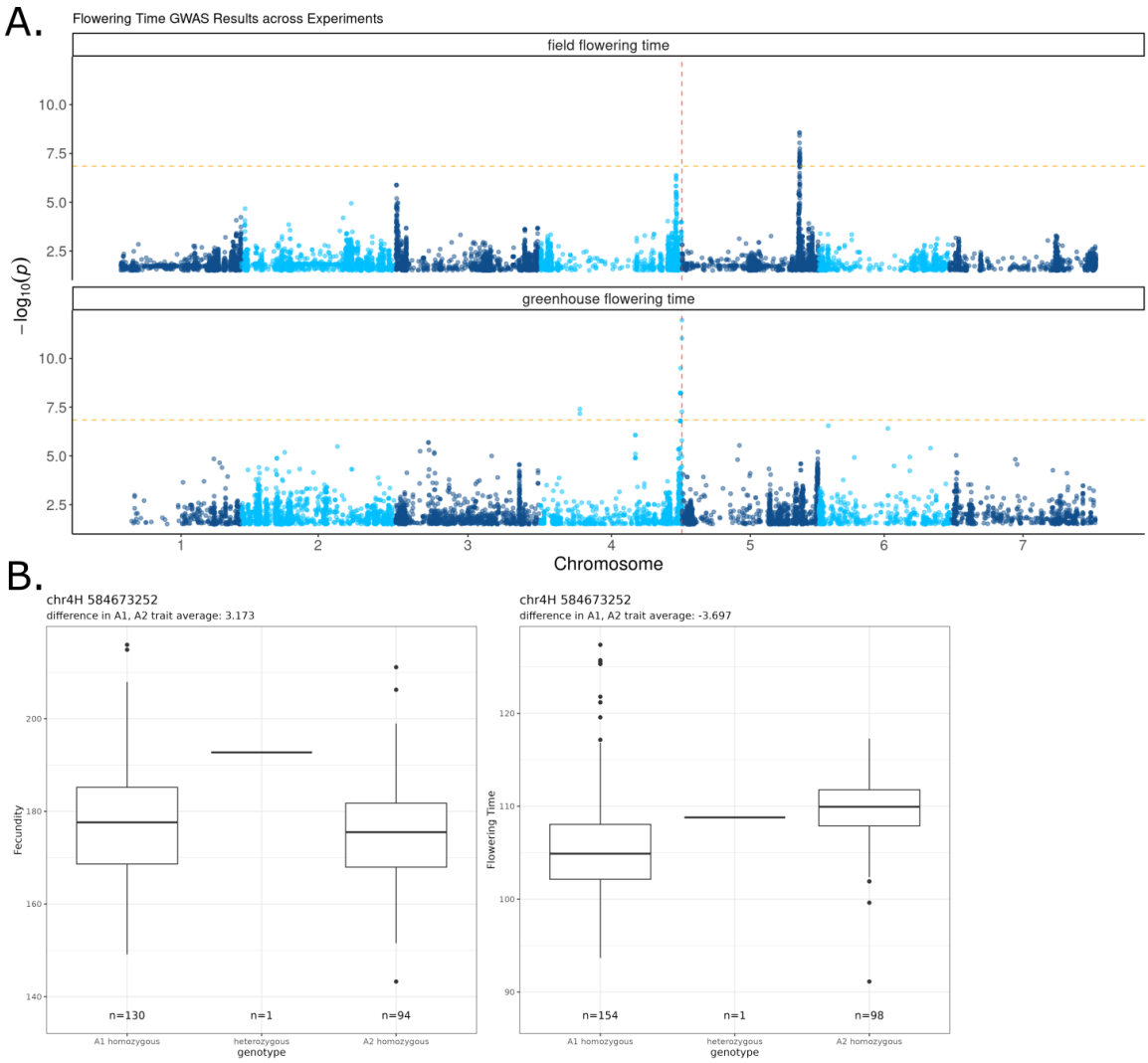

Figure 1.3 - Greenhouse candidate region associated with change in flowering time and small difference in fecundity in field phenotypes

A. Manhattan plots for flowering time with phenotypes collected from the field (this experiment, top) and the greenhouse (Landis et al. 2024). Each point represents the likelihood that the site is associated with the trait. Chromosomes are differentiated with alternating colors. The dashed orange line represents the Bonferroni threshold, above which points indicate statistical significance corrected for multiple comparisons. The red dashed line overlaps the site with the strongest association with flowering time in the greenhouse. **B.** Allele effect plots for flowering time and fecundity for the 'suggestive' central site of the chromosome 4 peak identified with flowering time data collected in the field.

A. Allele Frequency over Generation

site frequency polarized to trait increase

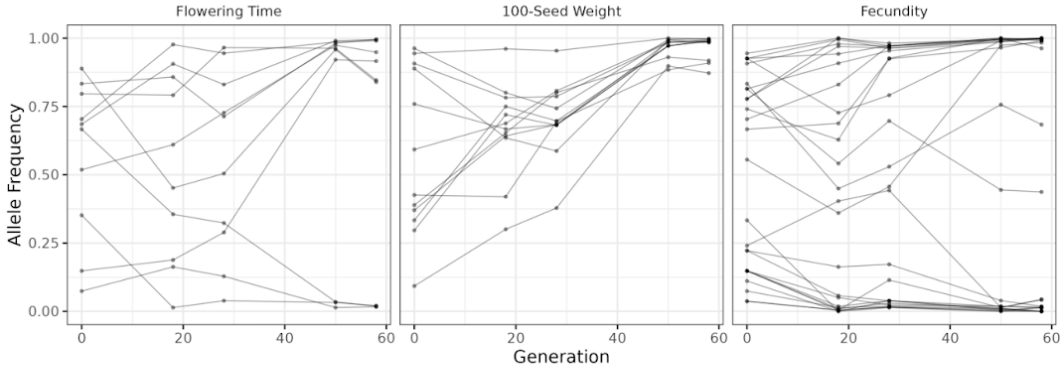

B. Allele Frequency over Generation

site frequency polarized to trait increase

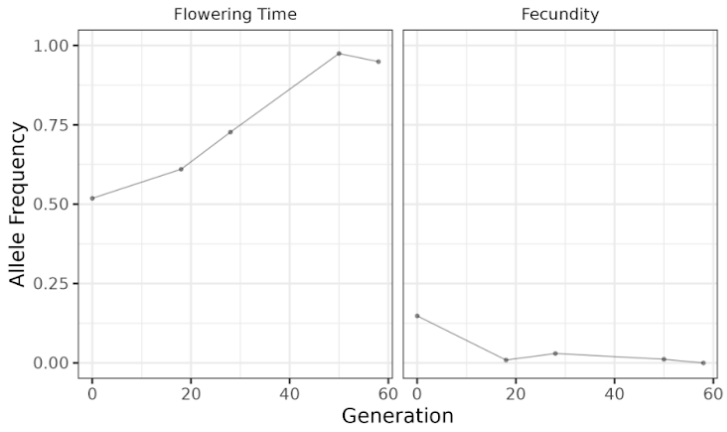

C. Site Frequency Spectrum

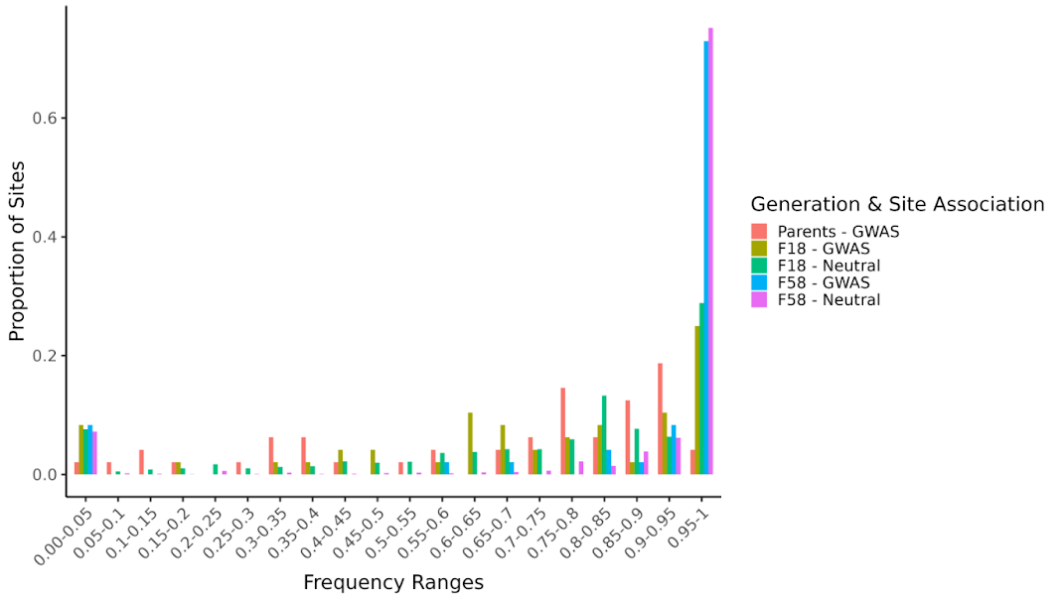

Figure 1.4 - Trait associated genomic sites show variable signs of selection over span of experiment

A-B. Allele frequencies across generations for “suggestive” (**A**) and significant (**B**) GWAS sites for each trait. Allele frequencies are polarized to trait increases, so a decrease in the allele frequency suggests a phenotypic shift toward lower trait values or selection against high trait values. **C.** A site frequency spectrum where each bar represents the number of genomic sites with allele frequencies belonging to that frequency bin, as a proportion of the total sites. Frequencies are binned in 0.05 spans. Allele frequencies sourced from sites identified with GWAS and a neutral sampling of genome sites which are colored according to group and generation, see Methods.

Table 1.1 - ANOVA test for significant trait changes during early and late phases

ANOVA p-value	trait	equal variances	Parents to F_{18} post hoc p-value	F_{18} to F_{58} post hoc p-value
3.65E-24	Flowering Time	FALSE	0.0993	1.75E-14
2.59E-42	100-seed weight	FALSE	0.0123	3.96E-24
1.53E-06	FECUNDITY	FALSE	0.0403	7.22E-04

Table 1.2 - Trait averages over generations

Generation	Flowering Time	Flowering Time Scaled	Fecundity	Fecundity Scaled	Relative Fecundity	100-seed weight	100-seed weight scaled
0	109	0.238	171	-0.424	0.977	4.64	-1.55
18	105	-0.564	177	0.212	1.01	4.91	-0.52
28	107	-0.2	178	0.232	1.01	5	-0.168
50	110	0.417	174	-0.187	0.99	5.16	0.44
58	109	0.275	174	-0.161	0.999	5.16	0.427

Table 1.3 - Trait variance and Levene test results

traits	Generation 0	Generation 18	Generation 58	P to F_{18} p-value	F_{18} to F_{58} p-value
Flowering Time	998	23	5.25	3.92E-12	1.13E-27
100-seed weight	0.187	0.088	0.027	0.007149	1.13E-23
FECUNDITY	223	148	37	0.001313	7.13E-15

Table 1.4 - Breeders Equation results

Generation	trait	response	H2	selection
Parents to F_{18}	Flowering Time	-0.201	0.93	-0.216
Parents to F_{18}	100-seed weight	0.015	0.716	0.021
Parents to F_{18}	Fecundity	0.338	0.458	0.738
Parents to F_{18} (standard deviation)	Flowering Time	-0.045	0.93	-0.048
Parents to F_{18} (standard deviation)	100-seed weight	0.057	0.716	0.08
Parents to F_{18} (standard deviation)	Fecundity	0.035	0.458	0.077
F_{18} to F_{58}	Flowering Time	0.095	0.874	0.108
F_{18} to F_{58}	100-seed weight	0.0062	0.648	0.0096
F_{18} to F_{58}	Fecundity	-0.089	0.152	-0.587
F_{18} to F_{58} (standard deviation)	Flowering Time	0.0209	0.874	0.024
F_{18} to F_{58} (standard deviation)	100-seed weight	0.024	0.648	0.0365
F_{18} to F_{58} (standard deviation)	Fecundity	-0.009	0.152	-0.0613

Chapter 2 - Identifying specific traits contributing to success in a competitive field experiment in *Hordeum vulgare* based on high-throughput automated phenotyping

Abstract

Over nearly a century of cultivation, the barley composite cross II (CC II) population evolved higher fitness in the environment of Davis, California. Previous study of this population found increases in the average height and earlier flowering time, but all research was based on single time-point measurement. Now we are using trait measurements from a modern high-throughput phenotyping platform to better understand the changes that take place during adaptation to a novel environment. We collected data for novel traits at daily resolution to clarify the developmental phenotypes that set apart highly fit individuals in this population's evolutionary history. The raw trait measurements were condensed with modeling to describe the growth rate of each genetic background. We recapitulate earlier findings of strong contractions in trait variance during the first 18 generations of the population, and add observations of significant changes in the growth rates of plant width, leaf width, and leaf length. These changes take place during both early and later periods of adaptation in the population's history. We identify candidate genome regions associated with 9 trait components and uncover a common genetic basis for leaf width, plant height, and flowering time. Variance at the identified genome sites are associated with large phenotypic differences and exhibit larger allele frequency shifts over time than neutral genome sites. This study

helps clarify relevant traits for adaptation to a specific environment and provides evidence for potential developmental pathways associated with such evolutionary paths.

Introduction

Crop species' adaptation to novel environments has allowed global human spread. Understanding the evolutionary process of adaptation advances basic knowledge of biological systems and informs breeding. Research into agriculturally relevant species frequently focuses on yield. However, many aspects like field and plant fitness, harvest and processing ability, and product quality contribute to better productivity for the same inputs. Plant architecture and growth pattern are important components of agricultural production for small grain row crops. Seedling growth rate, plant height, leaf number, leaf angle, and pigmentation can all confer fitness advantages especially in high density plantings (Tungland et al. 1987; Kuczyńska et al. 2013; Gauley and Boden 2019; Zheng et al. 2022). The Green Revolution increased yield per acre with fertilizer use and higher planting density of dwarf and semi-dwarf varieties with upright growth habits (Sinclair and Sheehy 1999; Evenson and Gollin 2003; Hedden 2003). Upright posture reduces inter-plant competition and increases harvestability while dwarfed growth channels more photosynthetic product into fruit and prevents lodging which reduces grain harvest and quality (Sinclair and Sheehy 1999; Caierao 2006; Rajkumara 2008). Loss-of-function alleles in the *semidwarf1* (Sdw1) or *denso* gene were originally popular for producing dwarf wheat and barley varieties but have negative pleiotropic effects (Dockter and Hansson 2015; Skov Kristensen et al. 2016). The deleterious effects drove a search for alternatives, including control over specific aspects of plant architecture (Shaaf et al. 2019). Mutations in the *Erectoides-k* (Ert-k) gene produce semi-dwarf barley lines without affecting flowering time, plant development, or climate tolerance (Skov Kristensen et al. 2016). Ert-k alleles vary in culm length and spike architecture. Grain

spike density, determined by rachis and internode lengths (nodes per rachis length), confer yield increases in rice and wheat (Huang et al. 2009; Tanaka et al. 2013). This yield benefit may be due, in part, to increased capture of a larger number of grains spread across fewer spikes. Houston et al. (2013) uncovered the molecular interaction controlling grain density in barley. Mutations associated with tiller angle, leaf angle, and leaf size in barley have been associated with yield and quality differences between varieties (Shaaf et al. 2019). Disentangling the genetic basis of such traits requires detailed phenotyping of adequate trait diversity.

The difficulty of phenotyping minute or detailed traits reliably, in field environments, and at large scales has prevented broad understanding of many traits that may provide useful control over plant behavior, response, and performance. Practicality has often limited researchers to collecting single data points per measured trait for each tested individual. In plant sciences, measurements are often taken for seedlings to shorten time spans or at the end of life (for annuals) or after an extended maturation period (for perennials). However these single time points represent only a small fraction of a plant's life. Advancing experimental systems have allowed researchers to begin rectifying this gap with automated phenotyping systems. These phenotyping platforms can capture nearly limitless data points by photographing many times during a lifespan and provide a more complete description of biological development (Pieruschka and Schurr 2019). Image analysis software then allows the calculation and extraction of hundreds of small and specific trait measurements for as many individuals as the phenotyping system can hold and process (Junker et al. 2015). This technology is a vast improvement over the limited manual phenotyping possible for individuals, and these

systems have successfully been used to identify quantitative trait loci (QTL) underlying a plethora of phenotypes (Tisné et al. 2013; Junker et al. 2015; Parent et al. 2015; Yang et al. 2015; Dodig et al. 2021). Researchers have used this technology to quantify biomass (Busemeyer et al. 2013; Neumann et al. 2017), floret length and width (Youssef et al. 2017), seedling root and shoot architecture (Abdel-Ghani et al. 2019), and many traits simultaneously (Badr et al. 2000; Gyenis et al. 2007; Crowell et al. 2016; Genievskaya et al. 2024). The rich data produced by phenotyping platforms can be used to rapidly advance our understanding of trait relationships and help identify traits with a common genetic basis. Studying sets of phenotypes and their development holistically also allows researchers to more fully understand the genetic systems that control trait complexes and may help uncover overlooked trait variance, fitness trade-offs, or cryptic genes.

This experiment uses measurements extracted from an automated phenotyping platform at the Leibniz Institute of Plant Genetics and Crop Plant Research (IPK) to quantify the growth and development of 192 genetically diverse individuals from time points over 58 generations of a long-running evolution experiment in barley. This population, the Composite Cross II (CC II), was founded in 1929 by intercrossing 28 landrace lines collected from the major barley-growing regions of the world (Harlan and Martini 1929). The progeny of these crosses were then grown without conscious selection in rain-fed fields in Davis, California for more than 58 generations over the span of nearly a century (Allard 1988; Allard et al. 1992; Landis et al. 2024). A fraction of the seeds produced were saved from each generation and provide a snapshot of the evolutionary process of this population's adaptation to a novel environment. Due to large population sizes, with upwards of 10,000 individuals per year and near complete

inbreeding (98-99%) rates, this population allows unique observation of the process and effects of natural selection over time (Allard 1988). Earlier research into this resource found the population evolved an earlier flowering time as well as increased plant height and yield (Allard et al. 1992). However, modern genomic investigation found that genetic changes were observed throughout the entire evolutionary history (58 generations) but physical changes in yield were greater in the first 18 generations (Hockett et al. 1983; Landis et al. 2024). This study aims to identify specific traits contributing to increased fitness without improved yield that occurred during the population's environmental adaptation.

We seek to uncover evidence of additional beneficial physical changes in the population during its adaptive path. For this experiment, we focus on identifying developmental differences associated with fitness benefits in the population. By quantifying the growth rate of each genetic lineage in our population, we can clarify how, when, and if plants diverge during development. Looking beyond end-point measurements like height and yield, we quantified the development of differences over the plants' lifespan as growth rates based on daily measurements from a high-throughput phenotyping platform as intercept-slope pairs or BLUPs to represent genetically meaningful trait values. Pairing these developmental phenotypes with whole-genome sequencing in this population allows us to investigate the genetic basis of changes in phenotype growth-rates that lead to the previously observed shifts in the population's terminal height, flowering time, and yield. The daily documentation of growing barley across a wide variety of traits allows us to impartially investigate the traits most important for distinguishing individuals during development, the timelines of trait

development, and the traits most beneficial for increased fitness in this population. Finding specific traits beyond height and yield that were under selection in this population over time may help clarify the types of traits, developmental strategies, and specific parameters of successful individuals and genetic backgrounds in this population. The scope of our automatic phenotyping data also allows us to connect many specific plant architecture traits with identifiable genetic diversity in this population and identify potential trade offs in barley growth as well as characteristics that may hinder or benefit agricultural plantings. To better understand the developmental sequences leading to reproductive success, we modeled the daily collected phenotypes as growth rates using a combination of linear and nonlinear mixed-effects model fits depending on the trait.

Methods

Plant material

This experiment uses barley (*Hordeum vulgare*) lines with unique genetic backgrounds that come from the Composite Cross II (CC II) population. The CC II population was made by intercrossing 28 landrace lines collected from across the globe (Harlan and Martini 1929; Suneson 1956). The progeny from these crosses were then planted and cultivated in rain-fed fields with minimal human inputs in Davis, California for more than 58 generations over the span of nearly a century without conscious selection (Allard 1988). Seed from each generation was saved to encapsulate the state of the population at points throughout the history of the evolution experiment. Due to large population sizes, with upwards of 10,000 individuals per year and near complete inbreeding

(98-99%) rates, we can observe the effect of natural selection on this population over time (Suneson 1956; Jain and Allard 1960).

A total of 192 previously genotyped barley lines were used in this experiment. These included the 28 parental lines of the Composite Cross II population and representative sampling from four of the progeny generations (18, 28, 50, and 58) throughout the population's history. We selected 57 lines from generation 18, 56 lines from generation 28, 16 lines from generation 50, and 35 lines from generation 58. Lines were selected to maximize the examined genetic diversity, so more genotypes are used for earlier generations of the experiment when diversity had not been removed from the population.

Plant growth and experimental design

Seeds produced from a previous experiment published in Landis et al. 2024 at the University of California, Riverside were shipped to the Leibniz Institute of Plant Genetics and Crop Plant Research (IPK; Gatersleben, Germany) for imaging on the LemnaTec automated phenotyping platforms on the IPK campus (Junker et al. 2015). Seeds were germinated in a small phytochamber with 14 hour days and a temperature of 17°C day and 15°C night. Each of the 192 lines were planted in a randomized order with one genotype per carrier on both the left side and the right side of the phytochamber, so each genotype was grown in duplicate, with each set of 192 having a unique randomization order. Carriers were filled with soil consisting of a mix of 85% (v) Substrate 1 and 15% (v) sand. Prior to planting, 50 mLs of water was added to each carrier and the mass of the carrier was recorded. Six seeds were sown in each carrier in 1 cm deep holes and lightly covered. Each day, every carrier was weighed and the appropriate amount of

water was added to return to the starting mass. Starting three days after sowing, images were acquired daily on the LemnaTec Scanalyzer system from both a top view and side view in the visible light and fluorescence spectrum as previously described (Arend et al. 2016). Side images were acquired at angles of 0, 90, and 225 degrees. Visible light images were acquired in the visible light spectrum (~390–750 nm) using a Basler (Basler AG, Ahrensburg, Germany) Pilot piA2400-17gc (RGB) camera with a resolution of 2056 × 2454 (side) and 2454 × 2056 (top) pixels. Fluorescence images (excitation: 400-500 nm, emission: 520–750 nm) were captured using a Basler Scout scA1400-17gc (RGB) camera with a resolution of 1234 × 1624 (side) and 1624 × 1234 (top) pixels, allowing for the quantification of static fluorescence signals. Photosynthetic operating efficiency of photosystem was measured once a week as a proxy for overall photosynthetic efficiency as previously described by (Tschiersch et al. 2017).

Once imaging at nine days after sowing was complete, plants were transplanted to the large imaging platform in the glass house with growth conditions of a 14 hour day length and a temperature of 20°C day and 18°C night. The adult high-throughput system consisted of 12 lanes each with 33 carriers, so we took four plants for each genotype from the same seedling carrier and planted two plants each into two carriers following the randomization order from the first 192 samples in the seedlings, with some parental lines used in triplicate to fill remaining carriers. The adult carriers were imaged in the visible light and fluorescence wavelengths from the top down and side views at 0, 45, and 135 degrees daily followed by weighing and watering. After week 6, watering was increased from 50 mL/plant to 125 mL/plant to obtain a higher target weight and avoid dessication. Photosynthetic kinetic measurements occurred once a week for four lanes

representing a subset of the samples, while 10 second light-adapted photosynthetic measurements occurred once a week for all samples. Manual counting of tillers occurred twice on weeks two and eight in the adults. Flowering time was checked manually twice a week and recorded when at least one of the two plants in a carrier had started flowering. Fresh mass was measured at time of harvest (day 65 of the experiment) and dry mass was measured after harvested plants had been dried at 80°C for two weeks.

Multi-Camera Images Phenotypeing

The high-throughput images were processed with the Integrated Analysis Platform (IAP) pipeline to calculate phenotypes (Klukas et al. 2014). Although other researchers using high-throughput phenotyping platform (HTPP) systems often reduce their multi-camera phenotyping values to the average value (Hartmann et al. 2011; Muscolo et al. 2015; Pommerrenig et al. 2018), we found that this method led to lower-than-expected correlations between genotype replicates. Inspecting the original photos revealed that the automatic phenotyping software occasionally produced over-estimates based on straight-on (0 degrees) images. These erroneously large values are excluded by simply summarizing the repeated automatic measurements using the median instead of the mean value which produces higher correlations between replicates.

Trait Selection

Image processing with the IAP pipeline yielded measurements for 428 and 401 traits, for seedlings and adult plants respectively. Many of these measurements are redundant (ie. measuring in pixels vs. millimeters or visual vs. fluorescent light). We selected 8 meaningful and non-overlapping traits measured on both the LTA (seedlings) and LTC

(mature plants) systems. Three of these traits are color measurements which describe plant color and the consistency of that color. The other 5 traits are related to plant size and architecture: plant height and width, leaf length and width (measured from the top and side), and leaf count. Supplemental Table 1 contains all measured traits and any exclusion rationale and Supplemental Table 2 contains names and descriptions of the traits included for analysis.

Quality Filtering

Quality image-derived measurements are not available for all 65 days of the experiment (12 days for seedlings, 53 days for adult plants). During germination and early seedling growth, plants are frequently too small to be detected or accurately measured, so we excluded data for days 1 through 4. We further discarded the day plants were transferred from the seedling to adult plant growth systems (day 13) and any days missing more than 60% of values (days 14, 15, and 17). No data is available from days 25, 31, 39, 45, 53, and 60; this leaves measurements across 51 days.

To ensure trait measurements were not affected by the number of plants grown in the carriers, we retained only data from carriers where exactly six seeds germinated. This filter removed 49 carriers across 42 genotypes, representing about 13% of the raw data (2148 rows removed out of 16896, 12.7%). This removes 7 genotypes entirely from the seedling data set: 2 from F18, 4 from F28, and 1 from F58. Furthermore, one carrier (037) with more than 40% missing data over all days is excluded from downstream analysis. Since individual plants were transplanted into the adult growth system and none are missing a large portion of daily measurements, no individuals or genotypes are excluded from that part of the data.

Modeling Plant Growth

We manually selected a list of traits that could potentially be meaningfully fit with a linear model (the 5 plant size and architecture traits) and designed a model describing growth rate based on each replicate carrier's daily trait measurements. The singular phenotype extracted from the model can then be used to compare accessions. The physical traits were categorized as 'linear' or 'nonlinear' based on the goodness of fit ($r^2 > 0.5$) of a simple linear model of the form

$$y \sim \text{Days after sowing}$$

$$y = X\beta + \epsilon$$

where y denotes a vector of individual plant replicate observations of a given trait; X is an incidence matrix associating observations with the fixed effect of days after sowing in vector β; and ϵ is the vector of random residuals. Out of the 10 traits (each trait for both seedling and mature data sets), 7 traits were distinguished as 'linear' traits based on this criteria. This goodness of fit determines the descriptive value(s) we can extract from the model and is explained in more detail in the following sections. Modeling was done with the lme4 package (v1.1-35.3) in R (v4.3.0, (R Core Team 2023)).

Linear Model Slopes

For the 7 traits well fit by the simple linear model, we developed a mixed linear model to describe the growth rate for each biological replicate with the form:

$$y \sim \text{Days after Sowing} + \text{Genotype replicate}$$

$$y = X\beta + Z\mu + \epsilon$$

where y denotes a vector of individual plant replicate observations of a given trait; X is an incidence matrix associating observations with the fixed effect of days after sowing in vector β; Z is an incidence matrix associating observations with random effects of biological replicate in vector μ; and ϵ is the vector of random residuals. We extracted the slope and intercept to describe the individuals' growth, and these derived traits (referred to as intercepts and slopes or growth rate) were used for downstream analysis.

Non-Linear Model BLUPs

Color traits and traits that did not meet the minimum threshold of model fit $r^2 > 0.5$ were categorized as 'non-linear' traits. For these traits, we applied the same mixed model described for linear model slopes above, but in this case we extracted the best linear unbiased predictor (BLUP) for each replicate using the ranef command from the lme4 package. Like the linear traits' slopes, we use the biological replicates' BLUP as a derived phenotype for these nonlinear traits in all downstream analyses unless otherwise stated.

Intergenerational Differences

The Levene test was used to identify significantly different variance between generations (leveneTest from car v.3.1-2 package) for all derived traits. Traits with equal variance were tested for significant differences in trait average over generations with an ANOVA (aov from stats v.3.6.2 package), and traits with unequal variance between generation samples were tested with a nonparametric test for mean differences, the Kruskal-Wallis test (kruskal.test also from the stats package). For both tests, traits were modeled in the form of trait ~ generation. For traits with significantly different mean values between

generations, we applied either the post-hoc Tukey test (TukeyHSD from rstatix v0.7.2) or the Dunn test (dunnTest from FSA v0.9.4) for pairwise comparisons.

Trait Heritability Estimates & Selection

We used the H2cal function from the inti package (v 0.6.9) (Lozano-Isla 2025 Feb 26), to extract broad sense heritability based on the derived phenotypes described above for each pair of biological replicates from the random model

$$y \sim 1 + (1 \mid genotype)$$

$$y = Z\mu + \epsilon$$

where y denotes a vector of plant replicate derived trait values; Z is an incidence matrix associating observations with random effects of biological replicate in vector μ; and ϵ is the vector of random residuals. The broad sense heritability was calculated based on the available genetic variance in the parents and in the generation 18 progeny. The corresponding heritability was used when estimating selection based on responses between the parents and F_{18} and between F_{18} and F_{58} progeny, respectively.

The average phenotypic change over generations in the population, response in the Breeders' equation was calculated for each trait by scaling with the scale function in R, finding the average trait value for each generation, taking the difference between pairs of generations, and then dividing that phenotypic change between generations by the number of generations between the two time points:

$$R = \frac{\bar{x}_{later} - \bar{x}_{earlier}}{number\ of\ generations\ between\ earlier\ \&\ later}$$

With the broad-sense heritability and response, we can use the Breeders' equation ($R = H^2 \cdot s$), rearranged to

$$s = \frac{R}{H^2},$$

to estimate selection pressure for each trait over different generational time spans.

Principal Component Analysis

We performed principal component analysis (PCA) on the complete and combined derived-traits data set. Before performing principal component analysis, data was scaled and mean centered. PCA values were calculated with the prcomp command from the pcaMethods library v1.92.0 in R. PCA results were visualized with functions from the factoextra library v1.0.6 also in R.

Sequencing & Haplotype Sampling

Genome sequences for individuals are taken from Landis et al. 2024. See population sampling, library preparation, sequencing, and genome alignment and filtering methods described there; however, the reference genome assembly for sequence alignment and GWAS was updated to version 3 (Morex v3) (Navrátilová et al. 2022). To create a data set representative of each genotype's frequency in the population for a given generation, we classified each line according to its haplotype. We know the frequencies of haplotypes from the population-level sequencing covered in Landis et al. 2024 and sampled the lines to represent as many as possible. To recover a population-level representative distribution of trait values, we sampled each haplotype's phenotypic value to match the haplotype's frequency in each tested generation. This data set provides an approximation of the occurrence of both rare and common haplotypes at their true representation within a given generation during the population's evolution. This

haplotype-frequency based data set was used for analysis involving population averages and distributions.

Association Mapping

We used vcftools (Danecek et al. 2011) (v 0.1.16-18) to remove indels and filter sites to those with variance in the progeny lines. These filters left 358,634 genome sites and 162 sequenced progeny individuals. We used Plink version 1.90 (Purcell et al. 2007) to generate .bed, .bim, and .fam files based on the vcf containing our filtered single nucleotide polymorphism (SNP) list. Phenotypes were added to .fam files afterward with a custom R script. We conducted univariate genome wide association studies (GWAS) across the 164 progeny lines for each derived trait using GEMMA version 0.98.5 (Zhou and Stephens 2012). Relatedness among individuals was accounted for by incorporating a kinship matrix created with GEMMA as a covariate in the model. Remaining population structure was corrected by including 10 principal components calculated with the plink command pca a covariate for the model.

Population Allele Frequency

We calculated allele frequencies for each progeny generation at the sites tested in GWAS by extracting allele counts from 899 sequenced individuals with a custom python script (extractsite_counts.py). Allele frequencies were calculated based on the reference allele count.

To compare the change in allele frequencies of our significantly-changed and trait-associated sites with a neutral expectation, we separated SNPs into 3 groups:

1. sites identified by GWAS as significantly associated with a trait that also exhibited significant phenotypic changes in our experiment,
2. sites significantly associated with traits without any observed significant phenotypic difference, and
3. sites not associated with any traits.

We randomly sampled neutral sites (group 3) matching the number of sites in groups 1 and 2 and with the same starting allele frequencies (based on frequency bins at intervals of 0.05). We found the frequency difference between generations for each site and took the average value. This cycle was repeated 1000 times to provide a distribution of allele frequency changes at neutral sites matched to groups 1 and 2.

Results

Trait development patterns contributing to individual fitness differences

Individual lines sampled from progeny generations of the Composite Cross II (CC II) were grown on an automated phenotyping platform that documented their growth with photographs and computationally extracted phenotype measurements. Plants were evaluated on a smaller instrument during their seedling phase, from planting to 12 days after sowing, and a larger platform during their mature phase, from 12 days to 65 days after sowing. We focused on 5 physical traits and plant color over 65 days of development. The physical traits include plant height, plant width, leaf count, leaf length, and leaf width. Plant color is measured with hue in the hsv color system, and for this analysis we are including plant hue from the side and top-down as well as the standard deviation of the daily measurement of plant hue. Supplemental Table 1 is a complete list

of measured and analyzed traits, and Supplemental Table 2 has descriptions of all the traits included in downstream analysis.

There is abundant genetic and phenotypic diversity in the founding parents of the Composite Cross II (Landis et al. 2024). The pictures in Figure 1A were selected to illustrate the morphological differences within the population by showing the adult development of two individuals from lines named “Maison Carree” and “Wisconsin Winter.” Although the plants begin life similarly, they develop notably different mature morphologies. These differences include leaf number and flowering time. Maison Carree is a Mediterranean spring type barley from Algeria while Wisconsin Winter a winter type barley from Minnesota, USA. The observed differences are likely environmental adaptations, including the earlier flower initiation of Maison Carree (Landis et al. 2024).

Previous studies of evolution of CCII can be divided into an early phase (F_1 to F_{18}) where early flowering was favored, seed size increased, and yields substantially improved, and a late phase where seed size continued to increase, but later flowering was favored and inconsistent changes in yield were observed (Bal et al. 1959; Allard and Jain 1962; Allard 1988; Landis et al. 2024). The following analyses are considered in this context of an ‘early’ and ‘late’ phase of the population’s evolution. Since previous research identifies plant height as one of the traits that changed over generations in the population, we want to investigate when in the plants’ lifespan different genotypes may become distinguishable from one another based on physical measurements and plant architecture. The daily resolution of a variety of phenotypic measurements in this experiment allows direct investigation of whether growth rates increase suddenly or if growth differences accumulate based on smaller differences that build up over time.

Furthermore, documenting the trait trends for a wide variety of genetic backgrounds may provide evidence for selecting lines with specific desirable traits.

The growth trends for the five physical traits measured in seedlings are generally consistent across individuals (Figure 1B). Height, leaf width, and the number of leaves increase fairly consistently over the 6 days while average leaf length and plant width reach a plateau. In adult plants, plant height increases linearly over time, but there is greater variance in the growth rate after 20-30 days (Figure 1C). While all of these traits values increase over days of the experiment, the leaf length has a somewhat flat trend more similar to that seen in the seedlings. Leaf width on the other hand shows a diverging growth pattern for average leaf width appearing around days 30 to 40. Some genotypes appear to have consistent leaf width beyond this point while another group of lines show consistent increases over time. Similar to leaf width, some genotypes have a steady number of leaves throughout the experiment while most others continue to increase leaf number past days 35 to 40. Overall plant height and width are of particular interest in this experiment. We see broad consistency in plant width except for a few lines with lower growth rates which may come from varieties with especially upright plant architecture. A variety of growth patterns appear for plant height: a few lines have exceptional height as of day 30 while several tall lines appear only after day 40. Across these trait measurements, genetic backgrounds with unique morphology mostly differentiate themselves starting at 30 days of growth.

To understand how individual plants' growth patterns differ, the physical trait measurements are modeled as a slope and intercept, where appropriate, to describe the rate of growth. Color traits and the physical traits poorly fit by a simple linear regression

are modeled over individual lifespans as best linear unbiased predictors (BLUPs) to describe the genotype's daily phenotype (see Methods). Beyond distinguishing varieties by these single traits, we can identify influential and co-varying trait groups by applying principal component analysis (PCA) to the derived trait measurements.

PCs 1 and 2 show the wide spread of phenotypes for individuals in the parents and generation 18 (Figure 2B). Much of the trait variance is lost in the later progeny generations, however. PC 1 explains 27% of the variance in this data set and is largely structured by adult leaf width slope, leaf count slope, and width slope in one direction and adult hue standard deviation BLUP, leaf count intercept, top-down hue, and leaf width intercept in the opposite direction. Only adult measurements contribute more than 5% to the explained variance of PC 1, and it appears to capture an inverse relationship between trait slope and intercepts along with an opposition between plant color and color consistency with plant width, leaf number, and leaf width. PC 2 explains an additional 15% of trait variance and is structured by adult height intercept and seeding leaf width slope in one direction and by adult height slope, leaf length BLUP, seedling width BLUP, and seedling leaf count slope in the other direction. Once again a trait slope and intercept are anticorrelated, but no color traits strongly impact this component. PC 3 explains another 14% of trait variance and has major contributions from the seedling width BLUP, adult width intercept, seedling leaf count slope, seedling height slope, and adult height intercept in one direction and adult width slope and seedling side and top-down hue in the opposite direction. These results emphasize the importance of adult trait measurements for distinguishing individuals, show an inverse relationship between

trait intercept and slope, and indicate a potential relationship between leaf size and plant color.

Population-level morphology changes

We observed significant differences across generations for 14 trait components (slopes, intercepts, or BLUPs) (Table 1, ANOVA or Kruskal-Wallis $p < 0.05$). However, 7 of these did not have significant post hoc results when comparing trait averages between the parents and F_{18} generation or between F_{18} and F_{58} generations (Figure 2A). This indicates that any significant mean changes in these traits were transient. Only one seedling trait shows significant change over generations during our period of interest. Seedling average hue BLUP changed over the progeny generations (Tukey test $p_{late} = 0.0081$). The seedling hue BLUP decreases from 4.4×10^{-5} to -0.00014 (fraction of 1, see Methods) over those progeny generations. In adult plants, the hue standard deviation BLUP also significantly changed in the progeny generations (Tukey test $p_{late} = 4.71 \times 10^{-4}$). This generational difference also crosses zero ($F_{18} = 0.0000380$, $F_{58} = -0.0000345$). No other color traits have significant post hoc results for our periods of interest.

Several adult plant architecture traits show considerable variance over time. The overall plant width slope and intercept show significant changes when comparing progeny generations (Dunn test $p_{late} = 3.75 \times 10^{-5}$ and $p_{late} = 1.22 \times 10^{-5}$, respectively). The growth rate (slope) increases from 7.1 mm/day in generation 18 to 8.1 mm/day in generation 58 while the intercept decreases from 9 mm to -24 mm over the same time span (Table 2). Both of these trait components also show significant reductions in variance over generations as well (Levene test: intercept $p_{late} = 0.01$ and slope $p_{late} = 0.012$) (Table 3). In addition to the overall plant width, the average leaf width slope and

intercept also show significant differences between generations. In this case, though, the intercept changed during the early period of the experiment (Tukey test $p_{early} = 0.0017$) while the slope changed during the later period (Dunn test $p_{late} = 0.0017$). The leaf width intercept increased from the parents to progeny generation 18 from 11.8 mm to 12.9 mm. The leaf width slope also increased from 0.227 mm/day in F_{18} to 0.264 mm/day in F_{58}.

The average leaf width slope and intercept show inconsistent changes over generations. Leaf width intercept decreases early in the experiment before increasing between progeny generations (11.8 mm in parents, 12.9 mm in F_{18}, 12.4 mm in F_{58}). Average leaf width slope follows the opposite trend, as it decreases (from 0.248 mm/day in parents to 0.227 mm/day in F_{18}) and then increases (to 0.263 mm/day in F_{58}). These inconsistencies in the direction of change may result from the modeling method used, as each trait component may shift and be affected by changes in its counterpart. Taken together, however, we see significant increases in first the intercept of leaf width and then the slope, suggesting selection for wider leaves in the population over time. Finally, adult plants show a significant decrease in the average leaf length BLUP during the early phase of the experiment (Dunn test $p_{early} = 0.021$). These changes coincide with the increases in overall adult plant width, which provides evidence for selection on a spreading plant architecture alongside larger but shorter leaf surfaces.

The relationships between plant color, size, and flowering time

To understand the relationships between the measured traits, we calculated Spearman's correlation coefficient between derived trait measures (slopes, intercepts, and BLUPs) and flowering time over all genotypes. Plant growth rate phenotypes were modeled without a fixed intercept to allow for differences in plant size after transitioning from the

seedling to the adult phenotyping platform. As a result, many trait slope-intercept pairs have strong negative correlations (Figure 3A). Seedlings' trait measurements do not show many strong correlations, but we can confirm some expected relationships from the immature plants. From germination to the few-leaf stage (reached in about 9 days), the growth rates for number of leaves and plant width are positively correlated ($\rho = 0.57$). Seedling height growth is only weakly correlated with the growth rate for number of leaves and width ($\rho = 0.24$ & 0.27, respectively). We see a similar positive relationship between seedling height slope and adult height intercept ($\rho = 0.34$) which supports our modeling method. The number of leaves does not follow the same pattern. Seedling leaf number slope is not correlated with adult leaf number slope or intercept ($\rho = 0.06$ & 0.00, respectively). Finally, seedling leaf number slope & (plant) width BLUP is moderately correlated with adult leaf length BLUP ($\rho = 0.31, 0.27$). None of the seedling traits were strongly related to flowering time.

Physical trait measurements in adult plants mostly show moderate correlations. Adult plant width slope is positively correlated with leaf number slope ($\rho = 0.46$) and negatively with leaf number intercept ($\rho = -0.59$). Leaf width slope is somewhat correlated with leaf number slope ($\rho = 0.38$) and leaf length BLUP ($\rho = 0.28$). The lack of strong correlation between adult plant size measurements may suggest this population contains a variety of growth strategies. The positive relationships observed between plant height and leaf length and between plant width, leaf number, and leaf width bolster confidence in the measurement systems to a point.

Flowering time is a critical aspect of plant reproduction, so we are especially interested in strong correlations between flowering time and our automatically measured

traits. There are only 2 traits that correlate strongly ($|\rho| \geq 0.7$) with flowering time. Flowering time is strongly correlated with adult leaf width slope ($\rho = 0.8$) and intercept ($\rho = -0.62$). The other trait with a strong relationship with flowering time is the hue standard deviation BLUP ($\rho = -0.77$). Several other traits have moderate correlations with flowering time: top-down hue BLUP ($\rho = -0.52$), number of leaves slope ($\rho = 0.46$) and intercept ($\rho = -0.53$), and plant width slope ($\rho = 0.44$).

The standardization and automation of this experimental setup allowed us to investigate relationships between plant size and color. To understand the relationship between color traits around a plant and over its lifespan, we can look at plant hue from the side and from the top in seedlings and adult plants. Hue is strongly correlated in seedlings ($\rho = 0.72$), likely because there is little difference between the side and top of a plant in the seedling stage. Hue is moderately correlated across lifespan. Adult top-down hue correlated to seedling hue ($\rho_{side} = 0.4$, $\rho_{top} = 0.43$), while adult side hue has low correlation values with the same trait ($\rho_{side} = 0.17$, $\rho_{top} = 0.14$). Hue standard deviation, indicating the range of color values measured from a plant on a given day, has some relationship with seedling hues ($\rho_{side} = 0.26$, $\rho_{top} = 0.31$). Within adult plants, the hue standard deviation BLUP is more strongly associated with top-down hue ($\rho = 0.74$) than side hue ($\rho = -0.05$). Finally, adult leaf width slope is negatively associated with top-down hue ($\rho = -0.52$) and hue standard deviation BLUP ($\rho = -0.76$). The connection between flowering time, leaf number, leaf width, and plant color may indicate an important relationship between plant size, photosynthetic pigments, and maturation speed in this population.

Flowering time

Flowering time was manually scored periodically after 40 days and continued to the end of the experiment (see Methods). The bulk of flowering times were recorded on the final day (65 days, Dataset 1). On average, spring barley lines grown outside take 90 to 120 days to flower (Hickey et al. 2017; Crothers 2021; Gopinathan et al. 2025). In previous experiments with these and other barley lines, the population's average time between sowing and flowering was around 110 to 125 days, varying with local conditions (Marzolino unpublished). In speed breeding, warm temperatures (20°C days/18°C nights) and high-light conditions (22 hour day length) can induce flowering in around 60 days (Hickey et al. 2017; Gopinathan et al. 2025). Plants in this experiment grew under warm temperatures (20°C days/18°C nights) and long-day light conditions (14 hour day length) which accelerated flowering times. Flowering was observed as early as 41 days after sowing and the number of plants flowering increased until the end of the experimental observations at 65 days. Despite the growth conditions, not all plants reached maturity and flowered. Out of 396 plant carriers, 199 had at least one flowering individual (50.3%). These individuals represent 108 unique genotypes out of 192 (56%), with 86 (44.8%) genotypes with multiple replicates flowering. The percent of genotypes that did flower is roughly equal across generations: 44% of the parents, 62% in generation F_{18}, 53% in generation F_{28}, 47% in generation F_{50}, and 34% in generation F_{58} (Figure 3B). Because of the truncated time frame of the experiment and amount of missing data it is not appropriate to statistically test for significant differences in flowering time between generations.

Total and genetic variance, heritability, and selection on growth rates

Earlier experiments indicate large variance redactions in the early period of the experiment followed by smaller reductions in the late period (see Landis et al. 2024). To see if our developmental trait measurements recapitulate these findings, we measured total trait variance and tested for significant differences over generations. Few traits show significant decreases in total variance during the initial phase of the experiment (from the parents to F_{18}). Only seedling top-down hue, adult plant height slope, and adult plant width intercept have large reductions in trait variance early in the experiment (Table 3 & Table 4). Adult width intercept is also the only trait with significant variance reduction over both the early and late stages of the experiment. A variety of traits have a significant reduction in variance in the progeny generations: seedling leaf width slope and height slope, adult width slope, leaf width slope, leaf count slope and intercept, and side and top-down hue.

We calculated broad sense heritability for all trait components to understand the amount of genetic variation distinguishable across a variety of traits (Table 4). Seedling-based traits generally have lower broad-sense heritability than adult trait measurements ($mean_{seedlings} = 0.54$, $mean_{adults} = 0.83$). This could result from seedlings' smaller size being difficult to measure or biological constraints which limit size differences during early growth. Heritability scores are high for adult trait measurements across a variety of traits, supporting the consistency of our measurement method and the strong genetic basis of many traits. Plant height slope, leaf number slope and intercept, top-down average hue, hue standard deviation, and flowering time all show strong heritability estimates ($H^2 \geq 0.9$). The height intercept and leaf width slopes also

show higher than average heritability ($H^2 \geq 0.85$). This shows that the population contains abundant heritable trait variance for these traits.

We estimated selection coefficients based on scaled data and using heritability calculated for the genetic variance available in the starting generation when comparing trait changes between parents and F_{18} and between F_{18} and F_{58} (Table 5). The average selection coefficients were larger in the early phase of the experiment (avg. $S_{P\text{-}F18}$ = 0.0028, avg. $|S_{P\text{-}F18}|$ = 0.028 & avg. $S_{F18\text{-}F58}$ = -0.00074, avg. $|S_{F18\text{-}F58}|$ = 0.012). This is also true when comparing selection coefficient for seedlings (avg. $|S_{P\text{-}F18}|$ = 0.034, avg. $|S_{F18\text{-}F58}|$ = 0.011) and adult plants (avg. $|S_{P\text{-}F18}|$ = 0.025, avg. $|S_{F18\text{-}F58}|$ = 0.013). This confirms previous findings of strong selection pressure in the early generations of this experiment. Unlike broad-sense heritability, there is no clear difference between the average estimated selection values for seedling and adult measurements.

Traits that show significant changes in mean alongside a high selection coefficient suggest directional selection may have acted on these traits as the population adapted to the Davis environment. The 7 traits with significant post hoc results have larger selection estimates during the earlier phase of the experiment (avg. $|S_{P\text{-}18}|$ = 0.032, avg. $|S_{18\text{-}58}|$ = 0.021). For the early phase we found the largest selection estimates for adult leaf length BLUP, leaf width intercept, plant width slope, and leaf width slope (in descending order). The later phase has high selection for plant width slope, width intercept, and hue standard deviation BLUP. This suggests that leaf width was under selective pressure during the early phase of the experiment while plant width slope was under more continuous pressure.

Genetic Control of Development & Selection

We ran genome-wide association studies (GWAS) to identify any genomic sites associated with our measured traits. Results from running univariate GWAS on each trait identified 15 significant sites across 9 of the 19 tested trait components (slope, intercepts, and BLUPs) (Figure 4A). Significant sites were identified on chromosomes 1H, 2H, 3H, 4H, 6H, and 7H. The majority of sites are found on chromosome 4H (8 sites) compared to the second most on chromosomes 2H and 7H (2 sites each). Of the significant sites identified, 8 are unique positions. Five traits are associated with one significant position on chromosome 4H: adult leaf width slope, leaf count intercept, leaf count slope, hue standard deviation BLUP, and flowering time (Figure 4C). This suggests there may be pleiotropic action from an underlying variant near this site or many variants in this genomic region contributing to trait variation. Because of the association of this site with leaf number, leaf width, and flowering time, variation in this region may contribute to rapid growth rates that support early flowering. Only homozygotes were found at this site, and the allele difference between the two groups is associated with an average difference of 11.5 days (flowering time), 0.094 mm/day (average leaf width slope), 3 leaves (leaf number intercept), and 0.13 leaves/day (leaf number slope) (Figure 4B).

Another site on chromosome 4H is associated with three traits in adult plants: height slope, leaf width intercept, and top-down hue BLUP. The two identified sites on chromosome 4H are 5.5 Mb apart, but there may be some commonality between these regions as they are both associated with plant growth rates that can support rapid flowering. At this more distal genome site, alternate alleles in homozygotes are

associated with a 141 mm difference in height intercept, a 5.56 mm/day difference in height slope, and a 1.4 mm difference in leaf width intercept. Alternate alleles in an adjacent region (within 1 kb) also show an 8 day difference in flowering time. Even with the limited number of lines that flowered in this experiment, genetic variance in the tail of chromosome 4H provides strong evidence for genetic features contributing to differences in the timing of flower initiation. Finally, both leaf count intercept and slope are identified as significantly associated with a site on chromosome 7H. This region is a valuable target for further investigation into the control of adult leaf number in barley.

To expand our list of sites for subsequent analysis we also included the lead SNP associated with 212 additional, non-significant but potentially 'suggestive' association peaks based on the clump command in plink (see Methods). The combined peaks cover 180 unique sites across all 19 tested traits. We can compare the allele frequency changes for trait-associated and neutral genome sites to determine how trait selection drove evolutionary trends in the population over time. Trait-associated genome sites were divided based on whether the trait showed significant phenotypic shifts over generations and each group was matched to randomly sampled genome sites (see Methods). The distribution of allele frequency changes spans a larger range for sites associated with traits than for non-associated sites (Figure 4D). Comparing parent frequencies to those of F_{18}, trait-associated sites show frequency changes from +0.56 to -0.47 while neutral sites show changes from -0.01 to +0.11. The magnitude of changes are similar between trait-associated sites regardless of whether the traits exhibit significant differences over generations (significant trait sites' changes span -0.46 to +0.5 vs. trait-associated sites' change spanning -0.47 to +0.56). The average allele frequency

changes in the early generations are all close to 0 ($avg_{signif\ traits'\ sites}$ = 0.055, $avg_{trait\ sites}$ = 0.03, $avg_{neutral\ sites}$ = 0.06).

Progeny allele frequencies are polarized to the allele with increased frequency, so all $\Delta AF_{progney}$ are positive. This explains why the average ΔAF is larger for the later phase of the experiment (significant-trait-associated sites avg. ΔAF_{early} = 0.06 vs. avg. ΔAF_{late} = 0.16). However, there is little difference in the average ΔAF between site groups within the later phase of the experiment (progeny generations' average $\Delta AF_{sig\text{-}trait\ sites}$ = 0.16, $\Delta AF_{sig\text{-}trait\ neutral}$ = 0.12, ΔAF_{trait} = 0.18, $\Delta AF_{trait\ neutral}$ = 0.14). We still observe large differences in the maximum allele frequency changes between trait-associated sites and their neutral counterparts (maximum $\Delta AF_{sig\text{-}trait}$ = 0.56, $\Delta AF_{sig\text{-}trait\ neutral}$ = 0.17, ΔAF_{trait} = 0.72, $\Delta AF_{trait\ neutral}$ = 0.2). The minimum ΔAF is also lower for trait-associated sites than their neutral expectations (minimum $\Delta AF_{sig\text{-}trait}$ = 0.0002, $\Delta AF_{sig\text{-}trait\ neutral}$ = 0.03, ΔAF_{trait} = 0.0001, $\Delta AF_{trait\ neutral}$ = 0.06). So overall, we see that trait-associated genome sites exhibit a larger range of allele frequency changes than a site not associated with any traits.

Discussion

This paper seeks to build on earlier studies of the evolutionary process of the Composite Cross II population during its adaptation to the environment of Davis, California over the course of nearly a century. Research reported in Landis et al. 2024 showed the population's genetic changes and coinciding large phenotypic shifts over 58 generations in the population including increased plant height, later flowering time, and higher yields. In this work, we expand our understanding of the specific developmental patterns and physical traits that became more common in the population during this same time period.

We grew a diverse selection of CC II genotyped plants in a controlled greenhouse environment at the IPK in Germany where plant growth was documented over 65 days with daily photographs. Then automatic phenotyping software was used to extract measurements across a wide range of physical and color traits from the photos. In this experiment we analyze 5 major physical traits: plant height, plant width, leaf count, leaf length, and leaf width. Plant color measures include hue (measured from the side and top-down) and the standard deviation of the daily measurement of plant hue. We used these measurements as the basis for a linear model describing the growth rate for each unique genotype in the population. Traits that were not well fit by a linear model were used to derive BLUPs which convey an average trait value representing the genetic contribution (predicted breeding value) of the genotype. We use this data set to explore specific physical shifts in the composite cross population during adaptation to the Davis environment.

This experiment confirms previous findings in this population of large reductions in trait variance during the first 18 generations of adaptation. Trait variance continues to reduce in each subsequently tested generation, but the strongest selection acts early in the experiment to remove highly unfit individuals. These early generations also see significant changes in the population mean for increased leaf width intercept and decreased leaf length, though these traits do not show significant decreases in variance in that time period. During progeny generations, there are decreases in hue standard deviation, decreased width intercept, and increased plant width growth rate. Those plant width measurements also show significantly decreased trait variance and high selection values. No traits significantly differ over both early and late periods which may indicate

different selection strengths acting on certain traits over time. This is supported by the larger selection values calculated for trait changes during the first 18 generations than for those in the following 40 generations. Seedling measurements with significant mean changes include decreased hue and increased leaf width. The seedling measures have high selection values but not significant variance reductions. Adult and seedling measurements have similar selection estimates, though adult traits generally have higher broad-sense heritability. This suggests parity between seedling heritability and response. Overall, we find evidence supporting the importance of strong selection for wider seedling leaves, shorter adult leaves, and a faster growth rate for plant width during development.

Looking for differentiation between individuals, we found that seedlings largely conform to a single archetypal expression. Only seedling width has individuals with obvious growth differences. Other experiments may still find studying seedlings useful for identifying specific physical differences of interest, but seedling measurements were largely uninformative in this population and experiment. It remains unclear whether seedling form is constrained by selection or physiology. Adult plants on the other hand generally differentiated from one another at advancing ages near and after 30 days of this long-day greenhouse experiment. Looking for relationships between traits, seedling traits were not meaningfully correlated with other traits. Notably, plant width is correlated with leaf number, but not other traits which describe plant architecture. This may indicate that these barley plants maintain a variety of morphological trait combinations and are not restricted to one specific arrangement of plant and leaf height, width, length, and angle. Looking at our data set collectively with principal component analysis (PCA), we

found that PC1 explains a large amount (27%) of trait variance. The component is structured by leaf width, leaf count, and plant width slopes in opposition to leaf count intercept, leaf width intercept, hue standard deviation, and top-down hue. This suggests an anticorrelation between adult plants' general and width growth rate and the size of seedlings and adult plant color. The following components, 2 and 3, explain 15 and 14% of trait variance, respectively. They implicate a trade-off between seedling leaf width and adult height intercept with adult height, average leaf length BLUP, seedling leaf count slope, and seedling width BLUP. PC3 is powered by seedling hue BLUPs vs. seedling width BLUP, width intercept, seedling leaf count, seedling height, and adult height intercept. These component loadings suggest plant groups and generations are differentiated based on plant size, leaf width, and leaf number in early development where seedling measurements become adult intercepts. It is difficult to draw conclusions about plant color based on these derived hue measurements, but their importance in the PCA results note the potential for research into pigmentation in this population.

Because of the importance of flowering time for plant fitness as well as ultimate plant height in a bolting plant like barley, the population changes and trait relationships related to plant height should be tempered by the lack of reliable flowering time data in this experiment. Since only about half the plants flowered, we cannot draw meaningful conclusions on the variance of flowering phenotypes from this data set. Based on this general importance of flowering time and the limited results for trait measurements in seedlings, it is recommended that similar experiments prioritize documenting mature plant growth by planting seeds several weeks before transferring to a large-scale phenotyping platform. Because of their smaller size, seedling research may not require

cumbersome large-scale experimental setups. Still, systems such as the automated phenotyping platform at the IPK may be helpful if researchers want to explore specific motivated investigations in seedlings.

A major motivator of this research is understanding the adaptive path of the CC II population for a wider range of traits than previously undertaken. We explore the genetic basis of the study traits by conducting GWAS for 19 traits. We found 15 significant sites connected to trait variance across the traits, representing 8 unique sites. We identified common sites controlling variance for leaf width slope, leaf count intercept and slope, and hue standard deviation. This provides evidence to motivate further research into the underlying mechanisms contributing to leaf number, width, and color in this evolution experiment. We further sought to clarify the role of selection by tracking changes in allele frequency for trait-associated and neutral genome sites. We found that trait-associated sites exhibit a larger range of allele frequency changes than non-associated sites. Similar average frequency changes may indicate that directional selection at these sites drives larger shifts in allele frequency during adaptation in the population. This study leverages the phenotypic and genotypic diversity of a long-running evolution experiment to explore the adaptive pathways and genetic controls of a broad range of agronomically significant traits. We find evidence of strong directional selection early in the experiment affecting leaf length and broad support for negative correlations between leaf width and count and plant color. The results indicate a need for follow-up research into leaf pigmentation in this population and potential for directed study into optimized plant architecture in the Davis environment.

References

Abdel-Ghani AH et al. 2019. Genome-wide association mapping in a diverse spring barley collection reveals the presence of QTL hotspots and candidate genes for root and shoot architecture traits at seedling stage. BMC Plant Biol. 19(1):216. doi:10.1186/s12870-019-1828-5

Allard RW. 1988. Genetic Changes Associated with the Evolution of Adaptedness in Cultivated Plants and Their Wild Progenitors. J Hered. 79(4):225–238. doi:10.1093/oxfordjournals.jhered.a110503

Allard RW, Jain SK. 1962. POPULATION STUDIES IN PREDOMINANTLY SELF-POLLINATED SPECIES. II. ANALYSIS OF QUANTITATIVE GENETIC CHANGES IN A BULK-HYBRID POPULATION OF BARLEY. Evol. 16(1):90–101. doi:10.1111/j.1558-5646.1962.tb03201.x.

Allard RW, Zhang Q, Maroof M, Muona OM. 1992. Evolution of Multilocus Genetic Structure in an Experimental Barley Population. Genetics. 131(4):957. https://www.ncbi.nlm.nih.gov/pmc/articles/PMC1205105/.

Arend D et al. 2016. Quantitative monitoring of Arabidopsis thaliana growth and development using high-throughput plant phenotyping. Sci Data. 3(1):160055. http://dx.doi.org/10.1038/sdata.2016.55.

Badr A, Müller K, Schäfer-Pregl R, El Rabey H, Effgen S, Ibrahim HH, Pozzi C, Rohde W, Salamini F. 2000. On the origin and domestication history of Barley (*Hordeum vulgare*). Mol Biol Evol. 17(4):499–510. http://dx.doi.org/10.1093/oxfordjournals.molbev.a026330.

Bal BS, Suneson CA, Ramage RT. 1959. Genetic Shift During 30 Generations of Natural Selection in Barley1. Agronomy Journal. 51(9):555–557. https://onlinelibrary.wiley.com/doi/abs/10.2134/agronj1959.00021962005100090014x.

Busemeyer L, Ruckelshausen A, Möller K, Melchinger AE, Alheit KV, Maurer HP, Hahn V, Weissmann EA, Reif JC, Würschum T. 2013. Precision phenotyping of biomass accumulation in triticale reveals temporal genetic patterns of regulation. Sci Rep. 3:2442. http://dx.doi.org/10.1038/srep02442.

Caierao E. 2006. Effect of induced lodging on grain yield and quality of brewing barley. Crop Breed Appl Biotechnol. 6:215–221. [accessed 2026 Feb 18]. https://www.researchgate.net/publication/38101163_Effect_of_induced_lodging_on_grain_yield_and_quality_of_brewing_barley.

Crothers L. 2021 Feb 3. Barley. Sustainable Agriculture Research & Education Program. [accessed 2026 Jan 6]. https://sarep.ucdavis.edu/covercrop/barley.

Crowell S, Korniliev P, Falcão A, Ismail A, Gregorio G, Mezey J, McCouch S. 2016. Genome-wide association and high-resolution phenotyping link Oryza sativa panicle traits to numerous trait-specific QTL clusters. Nat Commun. 7:10527. http://dx.doi.org/10.1038/ncomms10527.

Danecek P, Auton A, Abecasis G, Albers CA, Banks E, DePristo MA, Handsaker RE, Lunter G, Marth GT, Sherry ST, et al. 2011. The variant call format and VCFtools. Bioinformatics. 27(15):2156–2158. http://dx.doi.org/10.1093/bioinformatics/btr330.

Dockter C, Hansson M. 2015. Improving barley culm robustness for secured crop yield in a changing climate. J Exp Bot. 66(12):3499–3509. https://dx.doi.org/10.1093/jxb/eru521.

Dodig D, Božinović S, Nikolić A, Zorić M, Vančetović J, Ignjatović-Micić D, Delić N, Weigelt-Fischer K, Altmann T, Junker A. 2021. Dynamics of Maize Vegetative Growth and Drought Adaptability Using Image-Based Phenotyping Under Controlled Conditions. Front Plant Sci. 12:652116. http://dx.doi.org/10.3389/fpls.2021.652116.

Evenson RE, Gollin D. 2003. Assessing the impact of the green revolution, 1960 to 2000. Science. 300(5620):758–762. http://dx.doi.org/10.1126/science.1078710.

Gauley A, Boden SA. 2019. Genetic pathways controlling inflorescence architecture and development in wheat and barley: Genes of wheat and barley inflorescence development. J Integr Plant Biol. 61(3):296–309. http://dx.doi.org/10.1111/jipb.12732.

Genievskaya Y, Chudinov V, Abugalieva S, Turuspekov Y. 2024. Novel QTL hotspots for barley flowering time, plant architecture, and grain yield. Agronomy (Basel). 14(7):1478. https://www.mdpi.com/2073-4395/14/7/1478.

Gopinathan G, Meints B, Sandro P, Gutiérrez L. 2025. Speed breeding with early harvest shortens the growth cycle of barley. Agronomy (Basel). 15(10):2275. http://dx.doi.org/10.3390/agronomy15102275.

Gyenis L, Yun SJ, Smith KP, Steffenson BJ, Bossolini E, Sanguineti MC, Muehlbauer GJ. 2007. Genetic architecture of quantitative trait loci associated with morphological and agronomic trait differences in a wild by cultivated barley cross. Genome. 50(8):714–723. http://dx.doi.org/10.1139/G07-054.

Harlan HV, Martini ML. 1929. A Composite Hybrid Mixture1. Agronomy Journal. 21(4):487–490. https://onlinelibrary.wiley.com/doi/abs/10.2134/agronj1929.00021962002100040014x.

Hartmann A, Czauderna T, Hoffmann R, Stein N, Schreiber F. 2011. HTPheno: An image analysis pipeline for high-throughput plant phenotyping. BMC Bioinformatics. 12(1):1–9. https://bmcbioinformatics.biomedcentral.com/articles/10.1186/1471-2105-12-148.

Hedden P. 2003. The genes of the Green Revolution. Trends Genet. 19(1):5–9. http://dx.doi.org/10.1016/S0168-9525(02)00009-4.

Hickey LT, Germán SE, Pereyra SA, Diaz JE, Ziems LA, Fowler RA, Platz GJ, Franckowiak JD, Dieters MJ. 2017. Speed breeding for multiple disease resistance in barley. Euphytica. 213(3):64. http://dx.doi.org/10.1007/s10681-016-1803-2.

Hockett EA, Eslick RF, Qualset CO, Dubbs AL, Stewart VR. 1983. Effects of Natural Selection in Advanced Generations of Barley Composite Cross II1. Crop Sci. 23(4). https://www.researchgate.net/publication/250113113_Effects_of_Natural_Selection_in_Advanced_Generations_of_Barley_Composite_Cross_II1.

Houston K, McKim SM, Comadran J, Bonar N, Druka I, Uzrek N, Cirillo E, Guzy-Wrobelska J, Collins NC, Halpin C, et al. 2013. Variation in the interaction between alleles of HvAPETALA2 and microRNA172 determines the density of grains on the barley inflorescence. Proc Natl Acad Sci U S A. 110(41):16675–16680. http://dx.doi.org/10.1073/pnas.1311681110.

Huang X, Qian Q, Liu Z, Sun H, He S, Luo D, Xia G, Chu C, Li J, Fu X. 2009. Natural variation at the DEP1 locus enhances grain yield in rice. Nat Genet. 41(4):494–497. http://dx.doi.org/10.1038/ng.352.

Jain SK, Allard RW. 1960. POPULATION STUDIES IN PREDOMINANTLY SELF-POLLINATED SPECIES, I. EVIDENCE FOR HETEROZYGOTE ADVANTAGE IN A CLOSED POPULATION OF BARLEY. Proc Natl Acad Sci U S A. 46(10):1371–1377. https://www.ncbi.nlm.nih.gov/pubmed/16590760.

Junker A, Muraya MM, Weigelt-Fischer K, Arana-Ceballos F, Klukas C, Melchinger AE, Meyer RC, Riewe D, Altmann T. 2015. Optimizing experimental procedures for quantitative evaluation of crop plant performance in high throughput phenotyping systems. Front Plant Sci. 5:122101. https://www.frontiersin.org/journals/plant-science/articles/10.3389/fpls.2014.00770/pdf.

Klukas C, Chen D, Pape J-M. 2014. Integrated Analysis Platform: An open-source information system for high-throughput plant phenotyping. Plant Physiol. 165(2):506–518. http://dx.doi.org/10.1104/pp.113.233932.

Kuczyńska A, Surma M, Adamski T, Mikołajczak K, Krystkowiak K, Ogrodowicz P. 2013. Effects of the semi-dwarfing sdw1/denso gene in barley. J Appl Genet. 54(4):381–390. http://dx.doi.org/10.1007/s13353-013-0165-x.

Landis JB, Guercio AM, Brown KE, Fiscus CJ, Morrell PL, Koenig D. 2024 Jul 12. Natural selection drives emergent genetic homogeneity in a century-scale experiment with barley. Science. https://www.science.org/doi/10.1126/science.adl0038.

Lozano-Isla F. 2025 Feb 26. Tools and Statistical Procedures in Plant Science [R package inti version 0.6.7]. [accessed 2025 Jul 10]. https://CRAN.R-project.org/package=inti.

Mikołajczak K, Ogrodowicz P, Ćwiek-Kupczyńska H, Weigelt-Fischer K, Mothukuri SR, Junker A, Altmann T, Krystkowiak K, Adamski T, Surma M, et al. 2020. Image Phenotyping of Spring Barley (*Hordeum vulgare L.*) RIL Population Under Drought: Selection of Traits and Biological Interpretation. Front Plant Sci. 11:743. http://dx.doi.org/10.3389/fpls.2020.00743.

Muscolo A, Junker A, Klukas C, Weigelt-Fischer K, Riewe D, Altmann T. 2015. Phenotypic and metabolic responses to drought and salinity of four contrasting lentil accessions. J Exp Bot. 66(18):5467–5480. http://dx.doi.org/10.1093/jxb/erv208.

Navrátilová P, Toegelová H, Tulpová Z, Kuo Y-T, Stein N, Doležel J, Houben A, Šimková H, Mascher M. 2022. Prospects of telomere-to-telomere assembly in barley: Analysis of sequence gaps in the MorexV3 reference genome. Plant Biotechnol J. 20(7):1373–1386. http://dx.doi.org/10.1111/pbi.13816.

Neumann K, Zhao Y, Chu J, Keilwagen J, Reif JC, Kilian B, Graner A. 2017. Genetic architecture and temporal patterns of biomass accumulation in spring barley revealed by image analysis. BMC Plant Biol. 17(1):137. http://dx.doi.org/10.1186/s12870-017-1085-4.

Parent B, Shahinnia F, Maphosa L, Berger B, Rabie H, Chalmers K, Kovalchuk A, Langridge P, Fleury D. 2015. Combining field performance with controlled environment plant imaging to identify the genetic control of growth and transpiration underlying yield response to water-deficit stress in wheat. J Exp Bot. 66(18):5481–5492. https://academic.oup.com/jxb/article-abstract/66/18/5481/482520.

Pieruschka R, Schurr U. 2019. Plant phenotyping: Past, present, and future. Plant Phenomics. 2019(7507131):7507131. https://pmc.ncbi.nlm.nih.gov/articles/PMC7718630/.

Pommerrenig B, Junker A, Abreu I, Bieber A, Fuge J, Willner E, Bienert MD, Altmann T, Bienert GP. 2018. Identification of Rapeseed (Brassica napus) Cultivars With a High Tolerance to Boron-Deficient Conditions. Front Plant Sci. 9:1142. http://dx.doi.org/10.3389/fpls.2018.01142.

Purcell S, Neale B, Todd-Brown K, Thomas L, Ferreira MAR, Bender D, Maller J, Sklar P, de Bakker PIW, Daly MJ, et al. 2007. PLINK: a tool set for whole-genome association and population-based linkage analyses. Am J Hum Genet. 81(3):559–575. http://dx.doi.org/10.1086/519795.

Rajkumara S. 2008. Lodging in cereals - a review. Agric Rev. 29(1):55–60. [accessed 2026 Feb 18]. https://www.researchgate.net/publication/267204760_Lodging_in_cereals_-_a_review.

R Core Team. 2023. R: A Language and Environment for Statistical Computing. https://www.R-project.org.

Shaaf S, Bretani G, Biswas A, Fontana IM, Rossini L. 2019. Genetics of barley tiller and leaf development. J Integr Plant Biol. 61(3):226–256. http://dx.doi.org/10.1111/jipb.12757.

Sinclair TR, Sheehy JE. 1999. Erect leaves and photosynthesis in rice. Science. 283(5407):1455–1455. http://dx.doi.org/10.1126/science.283.5407.1455c.

Skov Kristensen P, Dockter C, Lundqvist U, Lu Q, Gregersen PL, Thordal-Christensen H, Hansson M. 2016. Genetic mapping of the barley lodging resistance locusErectoides-k. Plant Breed. 135(4):420–428. http://dx.doi.org/10.1111/pbr.12377.

Suneson CA. 1956. An Evolutionary Plant Breeding Method1. Agronomy Journal. 48(4):188–191. https://onlinelibrary.wiley.com/doi/abs/10.2134/agronj1956.00021962004800040012x.

Tanaka W, Pautler M, Jackson D, Hirano H-Y. 2013. Grass meristems II: inflorescence architecture, flower development and meristem fate. Plant Cell Physiol. 54(3):313–324. http://dx.doi.org/10.1093/pcp/pct016.

Tisné S, Serrand Y, Bach L, Gilbault E, Ben Ameur R, Balasse H, Voisin R, Bouchez D, Durand-Tardif M, Guerche P, et al. 2013. Phenoscope: an automated large-scale phenotyping platform offering high spatial homogeneity. Plant J. 74(3):534–544. http://dx.doi.org/10.1111/tpj.12131.

Tschiersch H, Junker A, Meyer RC, Altmann T. 2017. Establishment of integrated protocols for automated high throughput kinetic chlorophyll fluorescence analyses. Plant Methods. 13(1):1–16. https://plantmethods.biomedcentral.com/articles/10.1186/s13007-017-0204-4.

Tungland L, Chapko LB, Wiersma JV, Rasmusson DC. 1987. Effect of erect leaf angle on grain yield in barley1. Crop Sci. 27(1):37–40. http://dx.doi.org/10.2135/cropsci1987.0011183X002700010009x.

Yang W, Guo Z, Huang C, Wang K, Jiang N, Feng H, Chen G, Liu Q, Xiong L. 2015. Genome-wide association study of rice (Oryza sativa L.) leaf traits with a high-throughput leaf scorer. J Exp Bot. 66(18):5605–5615. http://dx.doi.org/10.1093/jxb/erv100.

Youssef HM, Mascher M, Ayoub MA, Stein N, Kilian B, Schnurbusch T. 2017. Natural diversity of inflorescence architecture traces cryptic domestication genes in barley (*Hordeum vulgare L.*). Genet Resour Crop Evol. 64(5):843–853. http://dx.doi.org/10.1007/s10722-017-0504-6.

Zheng Z, Hu H, Gao S, Zhou H, Luo W, Kage U, Liu C, Jia J. 2022. Leaf thickness of barley: genetic dissection, candidate genes prediction and its relationship with yield-related traits. Züchter Genet Breed Res. 135(6):1843–1854. http://dx.doi.org/10.1007/s00122-022-04076-1.

Zhou X, Stephens M. 2012. Genome-wide efficient mixed-model analysis for association studies. Nat Genet. 44(7):821–824. http://dx.doi.org/10.1038/ng.2310

Figures & Tables

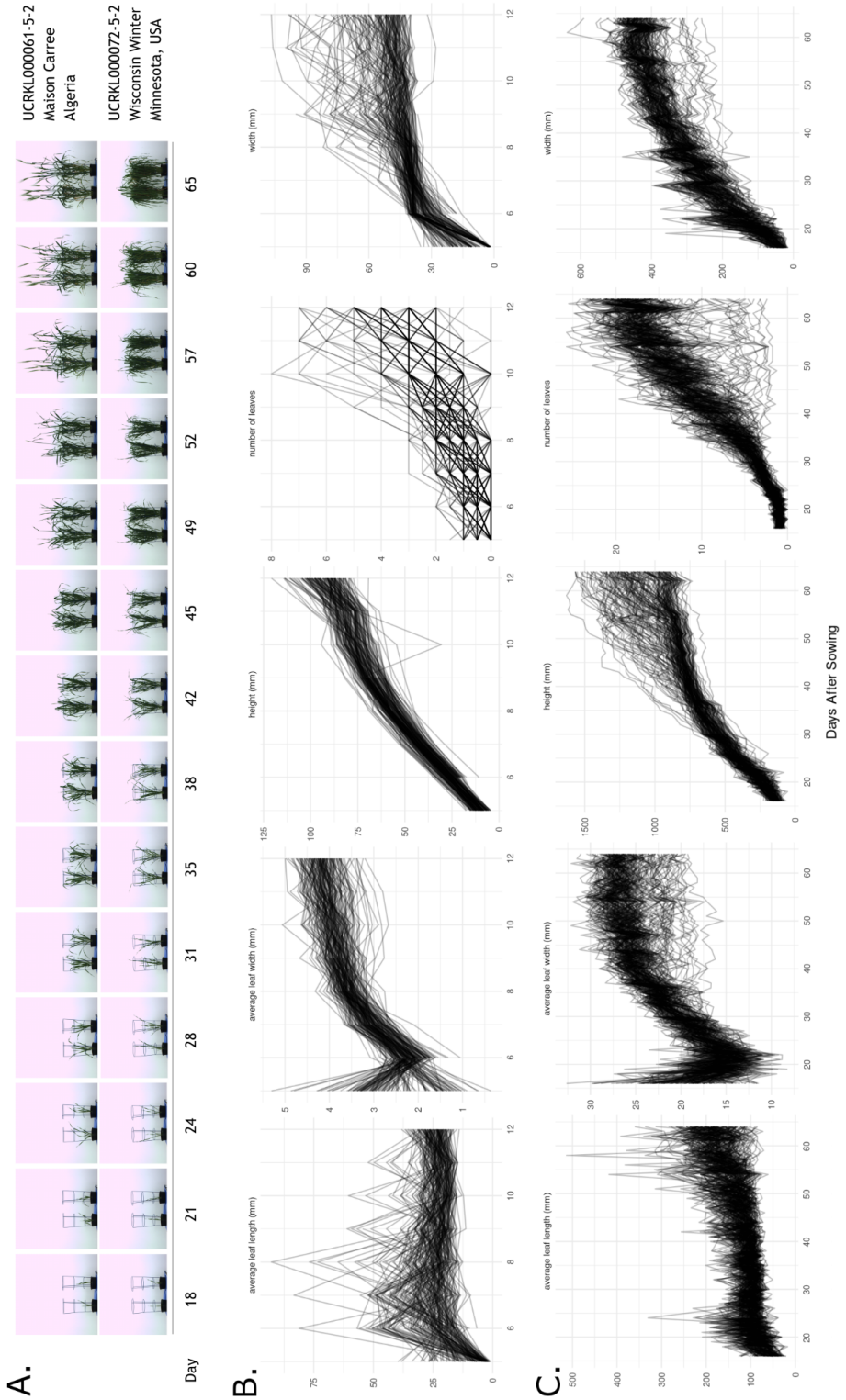

Figure 2.1 - Documenting the development of diverse barley backgrounds

A. Selection of daily side-view images for two parental lines adapted to different environments. **B-C.** Line plots of each genotype's recorded growth for the analyzed physical traits during seedling (**B**) and adult (**C**) stages.

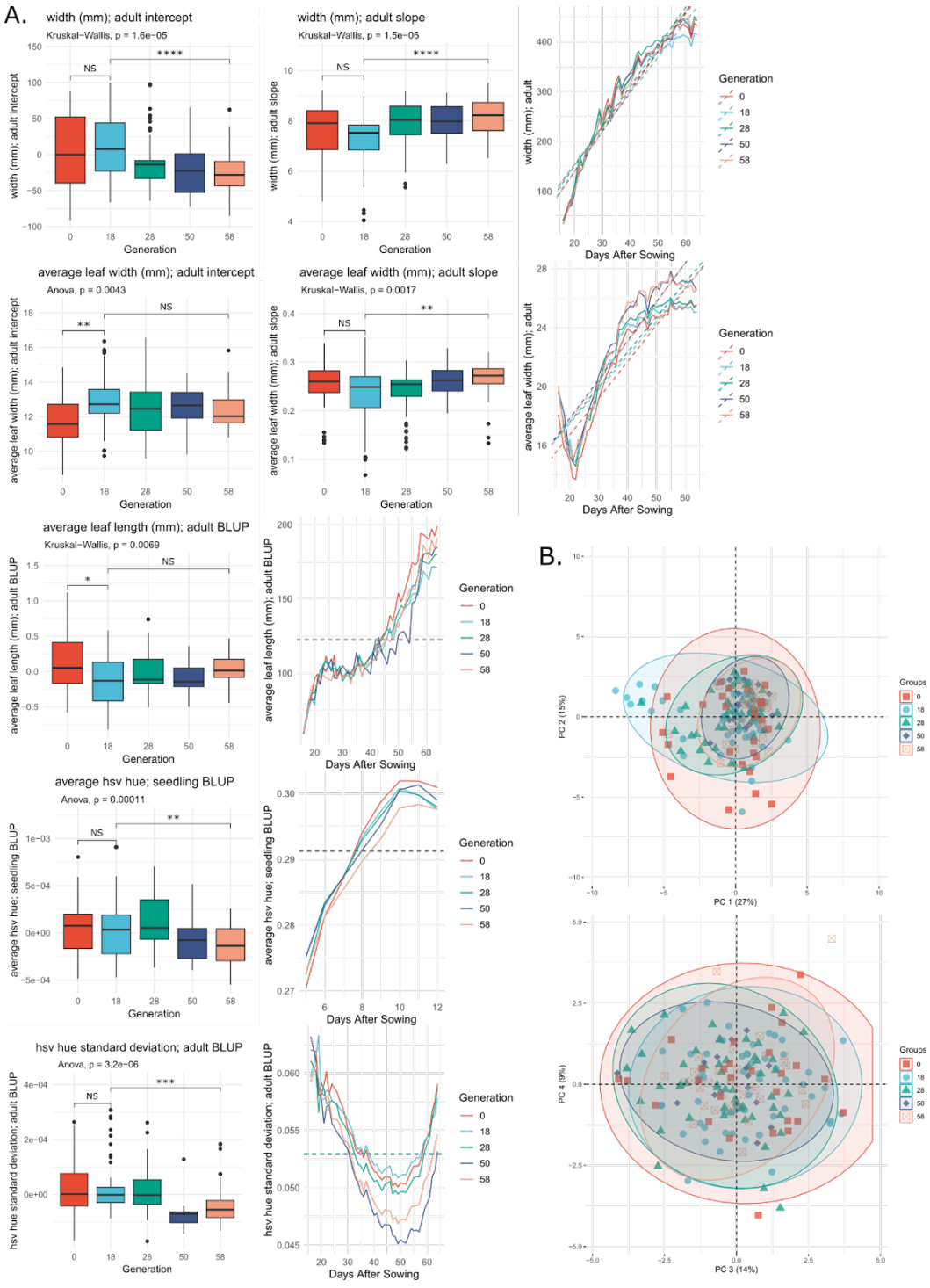
A.
width (mm); adult intercept
Kruskal–Wallis, p = 1.6e−05
NS
****
width (mm); adult intercept
Generation
width (mm); adult slope
Kruskal–Wallis, p = 1.5e−06
NS
****
width (mm); adult slope
Generation
width (mm); adult
Days After Sowing
Generation
0
18
28
50
58
average leaf width (mm); adult intercept
Anova, p = 0.0043
**
NS
average leaf width (mm); adult intercept
Generation
average leaf width (mm); adult slope
Kruskal–Wallis, p = 0.0017
NS
**
average leaf width (mm); adult slope
Generation
average leaf width (mm); adult
Days After Sowing
Generation
0
18
28
50
58
average leaf length (mm); adult BLUP
Kruskal–Wallis, p = 0.0069
*
NS
average leaf length (mm); adult BLUP
Generation
average leaf length (mm); adult BLUP
Days After Sowing
Generation
0
18
28
50
58
average hsv hue; seedling BLUP
Anova, p = 0.00011
NS
**
average hsv hue; seedling BLUP
Generation
average hsv hue; seedling BLUP
Days After Sowing
Generation
0
18
28
50
58
hsv hue standard deviation; adult BLUP
Anova, p = 3.2e−06
NS
***
hsv hue standard deviation; adult BLUP
Generation
hsv hue standard deviation; adult BLUP
Days After Sowing
Generation
0
18
28
50
58
B.
PC 2 (15%)
PC 1 (27%)
Groups
0
18
28
50
58
PC 4 (6%)
PC 3 (14%)
Groups
0
18
28
50
58

Figure 2.2 - The trait developments that distinguish generations

A. Selection of daily side-view images for two parental lines adapted to different environments. **B-C.** Line plots of each genotype's recorded growth for the analyzed physical traits during seedling (**B**) and adult (**C**) stages.

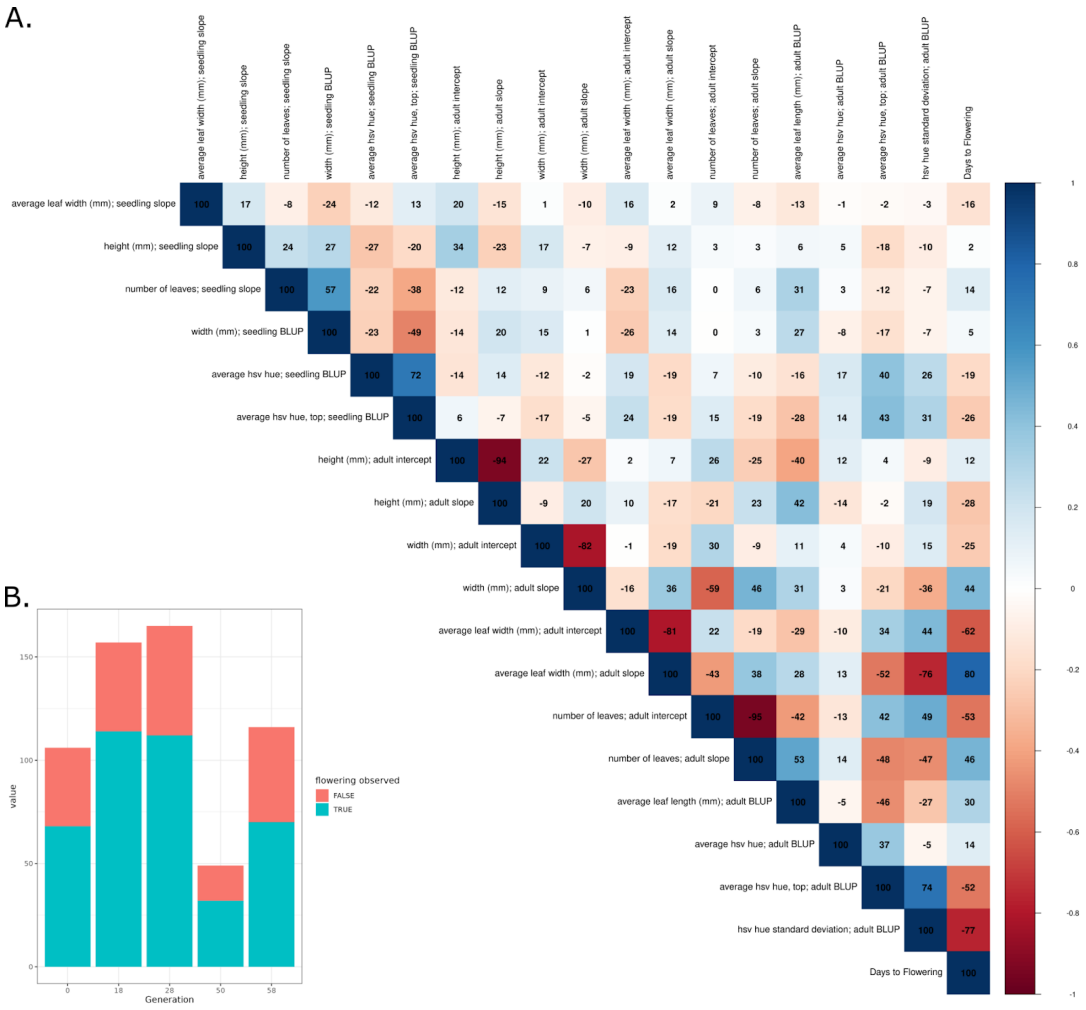

Figure 2.3 - Modeled trait relationships & flowering time

A. Heatmap of Spearman's correlation coefficients calculated for each trait pair. A more saturated square color indicates a higher positive (blue) or negative (red) correlation value. The correlation coefficient for each comparison is printed in each box. **B.** Stacked bar plot for flowering time observations per generation. Red bars indicate the number of individuals in each generation for which flowering was not observed, and blue bars represent the number of plants where flowering was observed.

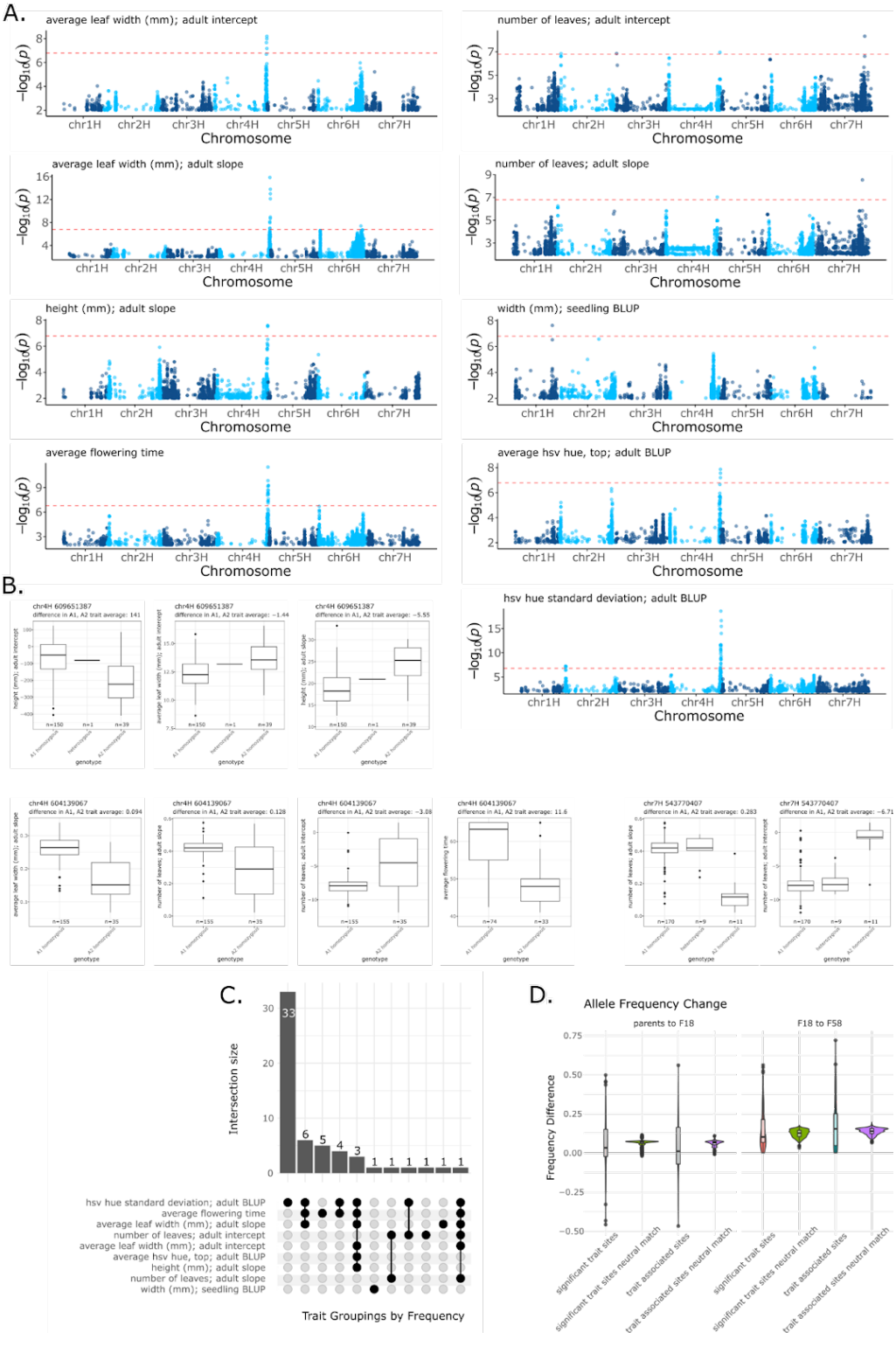
A.
average leaf width (mm); adult intercept
number of leaves; adult intercept
average leaf width (mm); adult slope
number of leaves; adult slope
height (mm); adult slope
width (mm); seedling BLUP
average flowering time
average hsv hue, top; adult BLUP
hsv hue standard deviation; adult BLUP
−log10(p)
Chromosome
chr1H chr2H chr3H chr4H chr5H chr6H chr7H
B.
C.
Intersection size
Trait Groupings by Frequency
hsv hue standard deviation; adult BLUP
average flowering time
average leaf width (mm); adult slope
number of leaves; adult intercept
average leaf width (mm); adult intercept
average hsv hue, top; adult BLUP
height (mm); adult slope
number of leaves; adult slope
width (mm); seedling BLUP
D.
Allele Frequency Change
parents to F18
F18 to F58
Frequency Difference
significant trait sites
significant trait sites neutral match
trait associated sites
trait associated sites neutral match

Figure 2.4 - Selection on the common genomic bases of measured developmental phenotypes

A. Manhattan plots of sites' association with each trait. Each point represents one tested site's -log10 scaled p-value. Red dashed lines represent the significance threshold at $p \leq 0.05$ with Bonferroni correction. Chromosomes are represented in alternating colors. **B.** Box plots of trait values for the observed genotypes (reference allele homozygote, alternate allele homozygote, and heterozygote if available) at selected significant GWAS sites. The bottom, middle, and top horizontal bars of each box represent the 1st quantile, median, and 3rd quantile values respectively. The vertical line indicates the group's range excluding outlier values represented by single points above and below. The difference in average trait value between homozygotes (A1 - A2) is printed at the top of each plot. **C.** Upset plot showing the number of suggestive sites identified in the GWAS that associate with specific traits or groups of traits. **D.** Violin plot showing distributions of allele frequency changes over generations for sites identified with GWAS analysis. The four groups are sites associated with traits which significantly changed averages over generations, sites associated with traits which did not significantly change over generations, and sites with starting allele frequencies matching each of those groups. The number of neutral sites examined was matched to the number of the trait-associated counterpart group. Allele frequency changes are measured between parents and progeny generation 18 (left) and between progeny generation 18 and 58 (right). Boxplots are overlaid on the violin plots where the bottom, middle, and top horizontal lines of each box represent the 1st quantile, median, and 3rd quantile values respectively. The vertical line indicates the group's range excluding outlier values represented by single points above and below.

Table 2.1 - ANOVA or Kruskal-Wallis and post hoc test results

ANOVA p-value	trait	equal variance	category	post-hoc parents to F_{18}	post-hoc F_{18} to F_{58}
3.19E-06	hue stddev BLUP adult	TRUE	color	9.16E-01	4.71E-04
1.07E-04	hue mean BLUP seedling	TRUE	color	9.92E-01	8.05E-03
4.26E-03	leaf width mean fluor (mm) intercept adult	TRUE	architecture	1.66E-03	2.49E-01
4.26E-03	leaftip count leaftips slope seedling	TRUE	architecture	1.68E-01	3.48E-01
9.12E-04	leaf width mean fluor (mm) slope seedling	FALSE	architecture	1.00E+00	1.82E-01
1.75E-02	height (mm) slope seedling	FALSE	architecture	4.87E-01	1.00E+00
1.61E-04	hue mean top BLUP seedling	FALSE	color	8.66E-01	1.00E+00
1.60E-05	width (mm) intercept adult	FALSE	architecture	9.65E-01	3.75E-05
1.48E-06	width (mm) slope adult	FALSE	architecture	3.33E-01	1.22E-05
1.67E-03	leaf width mean fluor (mm) slope adult	FALSE	architecture	5.37E-01	1.68E-03
2.08E-02	leaftip count leaftips intercept adult	FALSE	architecture	9.35E-01	1.00E+00
2.79E-02	leaftip count leaftips slope adult	FALSE	architecture	6.36E-01	8.70E-01
6.88E-03	leaf length mean fluor (mm) BLUP adult	FALSE	architecture	2.07E-02	5.91E-02
4.56E-02	hue mean top BLUP adult	FALSE	color	1.00E+00	1.17E-01

Table 2.2 - Haplotype-adjusted trait averages over generations

Generation	0	F_{18}	F_{28}	F_{50}	F_{58}
leaf width mean fluor (mm) intercept seedling	0.82	0.82	0.82	0.82	0.82
leaf width mean fluor (mm) slope seedling	0.30	0.31	0.30	0.31	0.31
height (mm) intercept seedling	-43.6	-43.6	-43.6	-43.6	-43.6
height (mm) slope seedling	11.8	12.0	11.8	12.0	12.0
leaftip count leaftips intercept seedling	-2.41	-2.41	-2.41	-2.41	-2.41
leaftip count leaftips slope seedling	0.49	0.47	0.46	0.46	0.48
leaf length mean fluor (mm) BLUP seedling	0.00	0.00	0.00	0.00	0.00
width (mm) BLUP seedling	0.15	0.02	-0.12	-0.03	-0.04
hue stddev BLUP seedling	0.00	0.00	0.00	0.00	0.00
hue mean BLUP seedling	0.00	0.00	0.00	0.00	0.00
hue mean top BLUP seedling	0.00	0.00	0.00	0.00	0.00
height (mm) intercept adult	-136.8	-77.4	-110.7	-94.3	-93.1
height (mm) slope adult	20.8	19.9	20.7	19.9	20.0
width (mm) intercept adult	1.21	9.00	-11.2	-22.3	-24.5
width (mm) slope adult	7.59	7.10	7.92	8.07	8.14
leaf width mean fluor (mm) intercept adult	11.8	12.9	12.6	12.5	12.4
leaf width mean fluor (mm) slope adult	0.25	0.23	0.24	0.26	0.26
leaftip count leaftips intercept adult	-6.93	-6.77	-7.99	-7.86	-7.51
leaftip count leaftips slope adult	0.38	0.37	0.42	0.41	0.40
leaf length mean fluor (mm) BLUP adult	0.15	-0.13	-0.01	-0.10	0.01
hue mean BLUP adult	-1.73E-5	7.86E-7	1.72E-5	2.04E-5	-8.79E-7
hue mean top BLUP adult	-6.78E-6	5.30E-5	5.29E-5	-2.73E-5	-4.54E-5
hue stddev BLUP adult	2.08E-5	3.80E-5	1.24E-5	-7.13E-5	-3.45E-5

Table 2.3 - Trait variance and Levene test results

trait	Generation 0 variance	Generation 18 variance	Generation 58 variance	Parents to F_{18} p-value	F_{18} to F_{58} p-value
leaf width mean fluor (mm) intercept seedling	0	0	0	NA	NA
leaf width mean fluor (mm) slope seedling	3.54E-06	2.17E-06	8.72E-07	0.368	0.013
height (mm) intercept seedling	0	0	0	NA	NA
height (mm) slope seedling	0.112	0.134	0.035	0.338	4.64E-04
leaftip count leaftips intercept seedling	0	0	0	NA	NA
leaftip count leaftips slope seedling	0.003	0.002	0.001	0.184	0.272
leaf length mean fluor (mm) BLUP seedling	0	0	0	NA	NA
width (mm) BLUP seedling	0.529	0.302	0.083	0.055	0.105
hue stddev BLUP seedling	0	0	0	NA	NA
hue mean BLUP seedling	8.09E-08	1.10E-07	5.25E-08	0.698	0.238
hue mean top BLUP seedling	2.01E-06	4.35E-07	3.06E-07	0.028	0.253
height (mm) intercept adult	19,249	11,538	14,685	0.126	0.488
height (mm) slope adult	31	14	17	0.004	0.338
width (mm) intercept adult	2,729	1,334	950	0.011	0.010
width (mm) slope adult	1.22	1.68	0.516	0.658	0.012
leaf width mean fluor (mm) intercept adult	1.90	2.05	1.18	0.899	0.097
leaf width mean fluor (mm) slope adult	3.20E-03	4.58E-03	1.71E-03	0.462	0.019
leaftip count leaftips intercept adult	6.74	12.1	2.29	0.513	0.003
leaftip count leaftips slope adult	0.01	0.02	0.00	0.439	0.003
leaf length mean fluor (mm) BLUP adult	0.20	0.09	0.04	0.076	1.61E-04
hue mean BLUP adult	4.54E-09	8.50E-09	3.99E-09	0.053	0.012
hue mean top BLUP adult	5.87E-08	4.86E-08	2.87E-08	0.787	0.005
hue stddev BLUP adult	1.22E-08	1.31E-08	6.08E-09	0.567	0.163

Table 2.4 - Genetic and phenotypic variance and broad-sense heritability

trait	data basis	phenotypic variance	genetic variance	broad-sense heritability
leaf width mean fluor (mm) slope seedling	overall	1.96E-06	7.79E-07	0.40
leaf width mean fluor (mm) slope seedling	parents	2.77E-06	0	0.00
leaf width mean fluor (mm) slope seedling	F_{18}	2.17E-06	9.85E-07	0.45
height (mm) slope seedling	overall	0.07	0.04	0.52
height (mm) slope seedling	parents	0.09	0.03	0.34
height (mm) slope seedling	F_{18}	0.12	0.08	0.69
leaftip count leaftips slope seedling	overall	0.00	0.00	0.50
leaftip count leaftips slope seedling	parents	0.00	0.00	0.49
leaftip count leaftips slope seedling	F_{18}	0.00	0.00	0.71
width (mm) BLUP seedling	overall	0.23	0.12	0.51
width (mm) BLUP seedling	parents	0.47	0.37	0.78
width (mm) BLUP seedling	F_{18}	0.32	0.21	0.65
hue mean BLUP seedling	overall	7.23E-08	5.84E-08	0.81
hue mean BLUP seedling	parents	6.98E-08	5.52E-08	0.79
hue mean BLUP seedling	F_{18}	9.44E-08	7.93E-08	0.84
hue mean top BLUP seedling	overall	5.86E-07	2.98E-07	0.51
hue mean top BLUP seedling	parents	2.00E-06	7.14E-07	0.36
hue mean top BLUP seedling	F_{18}	4.18E-07	3.21E-07	0.77
height (mm) intercept adult	overall	15,783	13,497	0.86
height (mm) intercept adult	parents	19,646	17,519	0.89
height (mm) intercept adult	F_{18}	13,868	11,351	0.82
height (mm) slope adult	overall	19.6	17.7	0.90
height (mm) slope adult	parents	31.1	29.2	0.94
height (mm) slope adult	F_{18}	16.8	14.4	0.86
width (mm) intercept adult	overall	1,769	1,226	0.69
width (mm) intercept adult	parents	2,818	2,098	0.74
width (mm) intercept adult	F_{18}	1,462	984	0.67
width (mm) slope adult	overall	1.20	0.95	0.79

width (mm) slope adult	parents	1.28	0.93	0.72
width (mm) slope adult	F_{18}	1.53	1.26	0.83
leaf width mean fluor (mm) intercept adult	overall	2.13	1.42	0.66
leaf width mean fluor (mm) intercept adult	parents	2.12	1.29	0.61
leaf width mean fluor (mm) intercept adult	F_{18}	2.36	1.71	0.72
leaf width mean fluor (mm) slope adult	overall	0.00	0.00	0.89
leaf width mean fluor (mm) slope adult	parents	0.00	0.00	0.90
leaf width mean fluor (mm) slope adult	F_{18}	0.00	0.00	0.92
leaftip count leaftips intercept adult	overall	5.66	5.11	0.90
leaftip count leaftips intercept adult	parents	6.83	6.27	0.92
leaftip count leaftips intercept adult	F_{18}	9.39	8.70	0.93
leaftip count leaftips slope adult	overall	0.01	0.01	0.91
leaftip count leaftips slope adult	parents	0.01	0.01	0.91
leaftip count leaftips slope adult	F_{18}	0.02	0.02	0.94
leaf length mean fluor (mm) BLUP adult	overall	0.10	0.08	0.77
leaf length mean fluor (mm) BLUP adult	parents	0.20	0.17	0.85
leaf length mean fluor (mm) BLUP adult	F_{18}	0.09	0.07	0.77
hue mean BLUP adult	overall	5.06E-09	3.80E-09	0.75
hue mean BLUP adult	parents	4.52E-09	3.85E-09	0.85
hue mean BLUP adult	F_{18}	5.73E-09	4.77E-09	0.83
hue mean top BLUP adult	overall	3.97E-08	3.71E-08	0.93
hue mean top BLUP adult	parents	5.87E-08	5.60E-08	0.95
hue mean top BLUP adult	F_{18}	4.83E-08	4.48E-08	0.93
hue stddev BLUP adult	overall	9.12E-09	8.67E-09	0.95
hue stddev BLUP adult	parents	1.22E-08	1.17E-08	0.96
hue stddev BLUP adult	F_{18}	1.07E-08	1.03E-08	0.96
Flowering (Days after sowing)	overall	63.5	59.9	0.94
Flowering (Days after sowing)	parents	65.8	64.3	0.98
Flowering (Days after sowing)	F_{18}	73.4	69.1	0.94

Table 2.5 - Breeders equation results

Generation	trait	response	H2	selection
Parents to F_{18}	leaf width mean fluor mm intercept seedling	0.00000	NA	NA
Parents to F_{18}	leaf width mean fluor mm slope seedling	0.00002	0.00000	Inf
Parents to F_{18}	height mm intercept seedling	0.00000	NA	NA
Parents to F_{18}	height mm slope seedling	0.00671	0.34267	0.01957
Parents to F_{18}	leaftip count leaftips intercept seedling	0.00000	NA	NA
Parents to F_{18}	leaftip count leaftips slope seedling	-0.00111	0.49301	-0.00225
Parents to F_{18}	leaf length mean fluor mm BLUP seedling	0.00000	NA	NA
Parents to F_{18}	width mm BLUP seedling	-0.00710	0.78404	-0.00905
Parents to F_{18}	hue stddev BLUP seedling	0.00000	NA	NA
Parents to F_{18}	hue mean BLUP seedling	0.00000	0.79137	0.00000
Parents to F_{18}	hue mean top BLUP seedling	0.00001	0.35665	0.00002
Parents to F_{18}	height mm intercept adult	3.29550	0.89174	3.69558
Parents to F_{18}	height mm slope adult	-0.04510	0.93877	-0.04804
Parents to F_{18}	width mm intercept adult	0.43301	0.74460	0.58154
Parents to F_{18}	width mm slope adult	-0.02716	0.72452	-0.03748
Parents to F_{18}	leaf width mean fluor mm intercept adult	0.06322	0.60519	0.10446
Parents to F_{18}	leaf width mean fluor mm slope adult	-0.00114	0.90256	-0.00126
Parents to F_{18}	leaftip count leaftips intercept adult	0.00930	0.91769	0.01014
Parents to F_{18}	leaftip count leaftips slope adult	-0.00047	0.91363	-0.00051
Parents to F_{18}	leaf length mean fluor mm BLUP adult	-0.01550	0.85259	-0.01818
Parents to F_{18}	hue mean BLUP adult	0.00000	0.85136	0.00000
Parents to F_{18}	hue mean top BLUP adult	0.00000	0.95417	0.00000
Parents to F_{18}	hue stddev BLUP adult	0.00000	0.95854	0.00000
Parents to F_{18} sd	leaf width mean fluor mm intercept seedling	NA	NA	NA
Parents to F_{18} sd	leaf width mean fluor mm slope seedling	0.00998	0.00000	Inf

Parents to F_{18} sd	height mm intercept seedling	NA	NA	NA
Parents to F_{18} sd	height mm slope seedling	0.02146	0.34267	0.06264
Parents to F_{18} sd	leaftip count leaftips intercept seedling	NA	NA	NA
Parents to F_{18} sd	leaftip count leaftips slope seedling	-0.02676	0.49301	-0.05428
Parents to F_{18} sd	leaf length mean fluor mm BLUP seedling	NA	NA	NA
Parents to F_{18} sd	width mm BLUP seedling	-0.01454	0.78404	-0.01855
Parents to F_{18} sd	hue stddev BLUP seedling	NA	NA	NA
Parents to F_{18} sd	hue mean BLUP seedling	-0.00518	0.79137	-0.00655
Parents to F_{18} sd	hue mean top BLUP seedling	0.00989	0.35665	0.02774
Parents to F_{18} sd	height mm intercept adult	0.02747	0.89174	0.03081
Parents to F_{18} sd	height mm slope adult	-0.01084	0.93877	-0.01155
Parents to F_{18} sd	width mm intercept adult	0.01125	0.74460	0.01511
Parents to F_{18} sd	width mm slope adult	-0.02462	0.72452	-0.03398
Parents to F_{18} sd	leaf width mean fluor mm intercept adult	0.04491	0.60519	0.07422
Parents to F_{18} sd	leaf width mean fluor mm slope adult	-0.02046	0.90256	-0.02267
Parents to F_{18} sd	leaftip count leaftips intercept adult	0.00364	0.91769	0.00397
Parents to F_{18} sd	leaftip count leaftips slope adult	-0.00438	0.91363	-0.00479
Parents to F_{18} sd	leaf length mean fluor mm BLUP adult	-0.04973	0.85259	-0.05833
Parents to F_{18} sd	hue mean BLUP adult	0.01350	0.85136	0.01586
Parents to F_{18} sd	hue mean top BLUP adult	0.01635	0.95417	0.01714
Parents to F_{18} sd	hue stddev BLUP adult	0.00967	0.95854	0.01009
F_{18} to F_{58}	leaf width mean fluor mm intercept seedling	0.00000	NA	NA
F_{18} to F_{58}	leaf width mean fluor mm slope seedling	0.00001	0.45493	0.00003
F_{18} to F_{58}	height mm intercept seedling	0.00000	NA	NA
F_{18} to F_{58}	height mm slope seedling	0.00103	0.68758	0.00150
F_{18} to F_{58}	leaftip count leaftips intercept seedling	0.00000	NA	NA
F_{18} to F_{58}	leaftip count leaftips slope seedling	0.00036	0.70507	0.00051
F_{18} to F_{58}	leaf length mean fluor mm BLUP seedling	0.00000	NA	NA

F_{18} to F_{58}	width mm BLUP seedling	-0.00166	0.65490	-0.00254
F_{18} to F_{58}	hue stddev BLUP seedling	0.00000	NA	NA
F_{18} to F_{58}	hue mean BLUP seedling	0.00000	0.84088	-0.00001
F_{18} to F_{58}	hue mean top BLUP seedling	0.00000	0.76855	0.00000
F_{18} to F_{58}	height mm intercept adult	-0.39245	0.81851	-0.47947
F_{18} to F_{58}	height mm slope adult	0.00199	0.85781	0.00232
F_{18} to F_{58}	width mm intercept adult	-0.83832	0.67315	-1.24536
F_{18} to F_{58}	width mm slope adult	0.02583	0.82829	0.03118
F_{18} to F_{58}	leaf width mean fluor mm intercept adult	-0.01321	0.72406	-0.01824
F_{18} to F_{58}	leaf width mean fluor mm slope adult	0.00091	0.91840	0.00100
F_{18} to F_{58}	leaftip count leaftips intercept adult	-0.01864	0.92577	-0.02014
F_{18} to F_{58}	leaftip count leaftips slope adult	0.00073	0.93608	0.00078
F_{18} to F_{58}	leaf length mean fluor mm BLUP adult	0.00339	0.77057	0.00440
F_{18} to F_{58}	hue mean BLUP adult	0.00000	0.83113	0.00000
F_{18} to F_{58}	hue mean top BLUP adult	0.00000	0.92864	0.00000
F_{18} to F_{58}	hue stddev BLUP adult	0.00000	0.96135	0.00000
F_{18} to F_{58} sd	leaf width mean fluor mm intercept seedling	NA	NA	NA
F_{18} to F_{58} sd	leaf width mean fluor mm slope seedling	0.00916	0.45493	0.02014
F_{18} to F_{58} sd	height mm intercept seedling	NA	NA	NA
F_{18} to F_{58} sd	height mm slope seedling	0.00331	0.68758	0.00481
F_{18} to F_{58} sd	leaftip count leaftips intercept seedling	NA	NA	NA
F_{18} to F_{58} sd	leaftip count leaftips slope seedling	0.00869	0.70507	0.01233
F_{18} to F_{58} sd	leaf length mean fluor mm BLUP seedling	NA	NA	NA
F_{18} to F_{58} sd	width mm BLUP seedling	-0.00341	0.65490	-0.00520
F_{18} to F_{58} sd	hue stddev BLUP seedling	NA	NA	NA
F_{18} to F_{58} sd	hue mean BLUP seedling	-0.01551	0.84088	-0.01844
F_{18} to F_{58} sd	hue mean top BLUP seedling	-0.00397	0.76855	-0.00517
F_{18} to F_{58} sd	height mm intercept adult	-0.00327	0.81851	-0.00400
F_{18} to F_{58} sd	height mm slope adult	0.00048	0.85781	0.00056

F_{18} to F_{58} sd	width mm intercept adult	-0.02178	0.67315	-0.03236
F_{18} to F_{58} sd	width mm slope adult	0.02341	0.82829	0.02827
F_{18} to F_{58} sd	leaf width mean fluor mm intercept adult	-0.00938	0.72406	-0.01296
F_{18} to F_{58} sd	leaf width mean fluor mm slope adult	0.01648	0.91840	0.01794
F_{18} to F_{58} sd	leaftip count leaftips intercept adult	-0.00729	0.92577	-0.00788
F_{18} to F_{58} sd	leaftip count leaftips slope adult	0.00681	0.93608	0.00728
F_{18} to F_{58} sd	leaf length mean fluor mm BLUP adult	0.01088	0.77057	0.01412
F_{18} to F_{58} sd	hue mean BLUP adult	-0.00056	0.83113	-0.00067
F_{18} to F_{58} sd	hue mean top BLUP adult	-0.01211	0.92864	-0.01304
F_{18} to F_{58} sd	hue stddev BLUP adult	-0.01838	0.96135	-0.01912

Chapter 3 - Evolutionary rescue by ultra-rare genotypes a quarter century after environmental shift

Abstract

Plants are dependent on their local environment for survival, and the rapid climate shifts arising due to climate change make it imperative to understand how plant populations can survive such environmental changes. A population's standing genetic diversity plays a major role in facilitating adaptation, especially over a short time span and when gene flow is not beneficial or available. However, it is challenging to monitor how diversity levels change in response to real-world selective pressures over a large timespan. This work uses a unique long-term evolution experiment in barley to clarify how segregating genetic variants are maintained and removed in a large population over nearly 30 years in response to extreme environmental change. The population was grown in parallel in Davis, California and Bozeman, Montana after pre-adapting to the environment in Davis for more than 20 generations. Pooled-population and individual genome sequencing at multiple time points shows that extremely rare genetic variants re-emerge after the population's transfer. Furthermore, this study finds that the same genome sites are associated with fitness benefit and detriment in an environment-dependent manner (antagonistic pleiotropy). This research provides unique insight into how a real-world plant population responds to radical environmental change and the importance of even low levels of standing genetic diversity on long-term fitness.

Introduction

A population faces extinction when the impact of environmental change outpaces its rate of adaptation (Gomulkiewicz and Holt 1995). Rapid adaptation depends on the availability of genetic variants that confer increased fitness under new conditions (Barrett and Schluter 2008). The presence and frequency of such variants are shaped by evolutionary history and by the fitness effects of alleles across environments (Charlesworth 2009). Episodes of strong selection or periods of reduced population size can erode genetic diversity through drift and both direct and linked selection (Osmond and Coop 2020). It is essential that we understand the genetic determinants of robust adaptive response to predict how populations will respond to this era of rapid environmental changes.

Predominant self-fertilization, as found in many plants and crops, can facilitate rapid adaptation by promoting the co-segregation of favorable alleles and the rapid increase of high-fitness multilocus haplotypes (Stebbins 1957). In outcrossing populations, recombination tends to break apart such combinations, slowing their response to selection. However, the same process that accelerates adaptation in selfing populations can reduce genetic diversity (Pollak 1987), thereby limiting future adaptation through standing variation (Glémin et al. 2006; Charlesworth and Charlesworth 1995). Consistent with this expectation, self-fertilizing species typically harbor low levels of within-population diversity (Barrett et al. 2014), and experimental studies have documented rapid losses of variation during adaptation (Noël et al. 2017; Landis et al. 2024). These observations raise a central question: how do self-fertilizing populations

adapt repeatedly to environmental change when genetic diversity is expected to be progressively depleted?

Here, we address this question by directly observing evolution after multiple bouts of selection in the barley Composite Cross II (CCII) long-term evolution experiment (Harlan and Martini 1929). Barley (*Hordeum vulgare* ssp. *vulgare*) is a predominantly self-fertilizing crop that has experienced repeated environmental transitions since domestication approximately 10,000 years ago (Badr et al. 2000). After emerging from the Fertile Crescent, barley spread into many environments as human populations migrated and exchanged seed. Historical barley cultivars were genetically heterogeneous, suggesting that adaptation to local environments may have relied on standing genetic variation (Kahler and Allard 1981). CCII was founded in 1929 using the recombinant progeny of 28 barley parents chosen to represent global phenotypic and geographic diversity (Harlan and Martini 1929) Figure 1). Over 15,000 recombinant genotypes were generated in an all by all intercross design between the parents (half diallel) to produce F_1 progeny. F_1 plants were selfed to generate F_2 families that were combined in equal proportions to found the experiment. The population was fall planted in Davis, CA, USA, grown with minimal human intervention and harvested in the spring. Each year the previous harvest was used to found a new generation allowing it to evolve to the Davis, CA environmental conditions for more than 50 generations.

Previous studies have found that, in Davis, adaptive evolution restructured genetic and phenotypic diversity in CCII genome-wide (Harlan et al. 1940; Bal et al. 1959; Allard 1996). Selection targeted genes involved in reproductive biology, favoring

alleles that are common in Mediterranean environments, and by generation F_{18D} several multilocus haplotypes have risen to intermediate frequencies in the population (Landis et al. 2024). By generation F_{50}, over half of the population is derived from a single ancestor that was the progeny of two Mediterranean parents that has driven out most other variation.

At generation F_{24}, 15,000 seed from the initial Davis site were used to found a parallel CCII competition experiment in Bozeman, MT, USA (Figure 1) that, in contrast to the fall planted Davis experiment, was spring planted (Allard 1996; Hockett et al. 1983). The Bozeman CCII was propagated for an additional 26 generations using the same methodology as that applied in Davis with minor modifications. The shift from winter growth in Mediterranean climate to spring growth in a Continental climate parallels the historic adaptation of barley as it was dispersed across Africa, Europe, and East Asia. In this study we characterize how the transition to Bozeman influenced the genetics of the CCII and we explore the genomic basis of sequential adaptation across multiple environments.

Methods

CCII germplasm and growth conditions

The growth and sequencing of the CCII Bozeman pooled populations was conducted as previously described for the Davis CCII pools, but libraries were sequenced on a Novaseq 6000 (Landis et al. 2024). The parental sequencing was described in the same study.

48 individual CCII progeny from generations $F_{24D,3B}$ and $F_{24D,26B}$ were placed on wet paper towels on petrie plates and germinated in the dark for 4 days until transplanting into pots. The plants were then grown in long day conditions 14 hours of light, 10 hours of darkness until a leaf could be harvested into a 96-well plate for genomic DNA extraction using the CTAB method. DNA was quantified by Quant-It PicoGreen assay (Thermo Fisher Scientific, P11496) and libraries prepared according to the KpnI reduced-representation protocol described in Rowan et al. 2017. The library was sequenced on an Illumina Hiseq4000 as single end 150bp reads.

For the whole genome sequencing dataset, the resulting DNA was used as input for the Illumina Nextera DNA Flex Library Prep kit and was sequenced across two lanes of an Illumina NovaSeq instrument using paired end 150bp setting. For the genotype by sequencing dataset, samples were processed as in (Landis et al. 2024).

Variant discovery in the CCII parents and allele counts in progeny pools

We re-analyzed the CCII parental data using the updated Barley Morex v3 reference genome (Mascher et al. 2021) by mapping reads using bwa mem (v.0.7.19) (Li and Durbin 2009) and sorting and indexing the resulting bam files with samtools (v.1.22.1) (Li et al. 2009). The resulting bam files were processed using the Genome Analysis Toolkit (v.4.6.2.0) (Van der Auwera et al. 2013) with the markduplicates tool, haplotypecaller and combineGVCFs tools, and ultimately variant calling using the GenotypeVCF tool. The raw VCF file was filtered using bcftools view (v.1.22) (Danecek et al. 2021) with the parameters ‘N_ALT=1 & N_MISSING<2 & MIN(FORMAT/DP)>1 & COUNT(GT="het")<3

& INFO/DP<400 & QUAL>30 & TYPE="snp"' followed by an additional filtering step 'FMT/GT="AA" & FMT/GQ>5'.

Characterization of allele frequencies in CCII pools

The alignment of pooled sequences was conducted in the same manner as for the parental samples. The biallelic SNPs identified using the parental sequences were then scored in each pool by first generating a pileup file using the bcftools mpileup tool (v.1.22) (Danecek et al. 2021) using the -R parameter to specify the parental vcf and the -a parameter to output "FORMAT/AD". The output of mpileup was passed to the bcftools query tool with the parameters -f '%CHROM,%POS,%REF,%ALT,[%AD]\n' to print allelic counts at each covered site in the pool. Prior to combining the counts from different pools, the script process_mpile.py was used to add missing sites with count data "NA NA" to each count file at uncovered sites in that specific pool.

The custom Rscript sum_counts.R was then used to combine count data for pools sequenced across multiple lanes and count data were merged for all pools and the parental allele counts were merged into a single file and were filtered to remove sites with no coverage in any pool.

Genotypic characterization of individual CCII progeny

Raw individual genotypes for the CCII parents, 219 F_{18D}, 219 F_{28D}, 217 F_{50D}, and 216 F_{58D} were generated from previously generated genotyping by sequencing data using the same methodology (Landis et al. 2024) but substituting the newer Morex v3 barley reference genome (Mascher et al. 2021) for the older Morex v2 reference (Monat et al.

2019). Sequencing data for 49 $F_{24D,3B}$ and 43 $F_{24D,26B}$ samples generated using the same approach were added to the CCII Davis dataset for this publication. In brief, the CCII parent and progeny sequences were aligned to the Morex v3 barley reference genome using the aligned using the bwa mem (v.0.7.19) aligner (Li and Durbin 2009) and raw SNP calls were generated for the parents only using the bcftools mpileup (v.1.22) (Danecek et al. 2021) to call pipeline. The parental SNPs were filtered in bcftools view using 'TYPE="snp" & COUNT(GT="het")<4 & MIN(AD[*:0]+AD[*:1])>3 & DP>100 & DP<1000 & QUAL>500 & N_ALT=1' and the resulting sites were scored in each progeny bam using the site_caller2.py custom script and merged to generate a VCF file. Missing data in the final progeny VCF were imputed with beagle (v.4.1) using the parental genotype VCF as a reference.

Whole genome skim sequencing of Bozeman individuals

To increase the sample size of Bozeman genotypes, 96 $F_{24D,3B}$ and 96 $F_{24D,26B}$ individuals were genotyped using a low coverage whole genome sequencing strategy. Seedlings were germinated on plates and transferred to soil under 20h light/cycles and 22°C. Fresh leaf tissue was flash-frozen in liquid nitrogen and homogenized in 96-well plates using a Qiagen TissueLyser II for DNA extraction via a standard CTAB protocol. Genomic libraries were prepared using the Illumina DNA Prep Kit with half-reaction reagent adjustments. Paired-end 150 bp whole-genome sequencing was then conducted on a NovaSeq X 25B instrument at the UC Davis DNA Technologies Core. Reads were mapped to the Morex v3 reference genome (Mascher et al. 2021) using the strategy applied to the parental and pooled sequencing datasets. At each site identified in the

parental GBS dataset the overlapping nucleotides were scored to generate genotype calls using the site_caller.py script, merged into a single VCF file with missing data imputed as described for the GBS datasets above. The GBS and low coverage whole genome sequencing datasets were then combined using bcftools merge (Danecek et al. 2021).

Analysis of the genetic change and relationships amongst the CCII progeny across Bozeman and Davis sites using pooled sequencing data

Allele counts were inputted into R (v.4.5.0) and the Rstudio environment (v.2023.09.1-494) and sites were filtered for combined coverage extremes across all pooled sequencing datasets (bottom and top 0.01 quantile threshold). Reference allele frequency, minor allele frequency (polarized against the minor allele in the parents), and H_e and changes in each of these statistics over time were calculated at the site level and then averaged over all sites within each generation to explore global trajectories. To predict He and the fraction of parental segregating SNPs at F_{24D} we fit a linear regression for each diversity statistic using the observed Davis values (F_{2D}, F_{18D}, F_{28D}, and F_{58D}). Euclidean distances between each parent and the progeny allele frequencies, treating parent genotypes as frequencies 0, 0.5, and 1 for homozygous reference, heterozygous, and homozygous alternate, were used to conduct multidimensional scaling analysis.

Estimation of the frequency of rare parental progeny in pooled sequencing

We used the genome-wide frequency of private alleles for each parent to generate a lower bound estimate of the frequency (*f*) of the progeny of that parent at each CCII timepoint in the pooled sequencing dataset. The average coverage in our dataset fell

between 50-70x, which is too low to consistently detect rare recombinants in CCII. However, by combining data across all sites, rare private alleles from each parent can be detected. For each site, the probability of failing to recover the parent specific private allele (p_u) is:

$$P_u = (1 - f)^d$$

Where d is the depth of sequencing at the site and f is the frequency of the rare genotype in the pool. The probability of seeing the private allele at one site is:

$$P_u = 1 - (1 - f)^d$$

Substituting the observed proportion of sites where the private allele was detected (p_{obs}) and rearranging to solve for f we get:

$$f = 1 - (1 - p_{obs})^{1/d}$$

This estimator is most accurate for low frequencies. We estimated the frequency of progeny for each of the two-rowed parents.

Lineage frequency analysis and ancestry estimation

Genetic distances between the WGS and GBS Bozeman samples were calculated in plink (v.1.90b6.25) and clustered with hclust using the “average” method in R. Clusters were defined with cutree h = 0.02. Haplotype diversity and associated variance was calculated as in (Nei 1987). A single randomly chosen individual was selected to represent each cluster for ancestry analysis. Each cluster representative was compared to each of the 28 parents in 500 windows to identify segments of inheritance by descent

(IBD; distance < 0.02). Primary ancestry was assigned to the parent with the maximum IBD segments with the representative genotype. Secondary ancestry was assigned to the parent that had the maximum IBD segments, after removal of the IBD regions with the primary ancestor and so on.

Identifying the footprint of directional selection

Regions targeted by selection over the first 18 generations of evolution in Davis were identified in a previous study (Landis et al. 2024) and the coordinates of these regions were translated manually from the Barley Morex v2 reference genome (Monat et al. 2019) to the Morex v3 reference genome (Mascher et al. 2021) by blasting overlapping annotated genes.

To identify regions of the genome where allele frequencies changed more than would be expected neutrally in Bozeman, we calculated Earth Mover's Distance (EMD) (Rubner et al. 2002) in 500 SNP windows. Briefly, EMD describes the dissimilarity between two distributions, in this case allele frequency distributions within the same SNP window at two different generations. A high EMD value indicates that a relatively high amount of work would need to be done to convert one distribution into the other, and is often used in computer science for image retrieval and edge detection, for example (Rubner et al., 2000 and Ruzon and Tomasi, 2001) (Ruzon and Tomasi 2001; Rubner 2000). We calculated EMD using the `stats.wasserstein_distance` function in the scipy package in python (Version 1.11.1) (Virtanen et al. 2020).

To compare observed EMD distributions to what would be expected under neutral evolution, we simulated changes in allele frequencies in windows using a custom

simulation in python (Supplemental file 1). The simulation uses real CCII founder allele frequencies in windows, constructs a starting population using those frequencies, and then allows the population to change for a number of generations before calculating an EMD comparing two intermediate generations. At each generation individuals are chosen as parents and their genome is used as-is in the next generation. This is akin to 100% selfing in a population comprising fully homozygous individuals, which should be conservative with regard to identifying extreme allele frequency changes. Each iteration of the simulation uses a randomly drawn window from the real starting frequencies, and we ran the simulation for 150k iterations to generate a null distribution. Because it is difficult to know both the number of plants maintained in each generation of CCII and the resulting effective population size, we ran the simulation with both 1000 and 100 individuals to determine which null distribution best describes the real data.

Candidate genes were identified using overlaps with selected regions with genes with known function and manual analysis .

Results

Environmental shift reverses the evolutionary trajectory of CCII

To understand how the shift to a new environment affected evolution in CCII we characterized the frequency of genetic differences throughout the genome at several time points in both Bozeman, MT, USA and Davis, CA, USA (Figure 1B). First, we defined the founding diversity of CCII by re-characterizing genetic variation amongst the CCII parents (Landis et al. 2024). Using whole genome sequencing we identified

21,445,703 single nucleotide polymorphisms that segregated in the founding population of CCII. We then estimated the evolutionary trajectories of each genetic variant in pools of 1000 progeny in Davis, CA (F_{18D}, F_{28D}, and F_{58D}) and in Bozeman, MT (24 generations in Davis, followed by 3 or 26 in Bozeman, MT, $F_{24D,3B}$ and $F_{24D,26B}$).

In Davis, CCII lost genetic diversity at a rapid, constant rate (H_e and the fraction of founder variants segregating) and is near homogeneity by F_{58D} (Landis et al. 2024) (Figure 2A and B). The allele frequency spectrum of genetic variants polarized by the minor allele in the founders revealed a progressive removal of intermediate frequency alleles, mostly due to the fixation of the rarer of the two parent alleles genome-wide (Figure 2C). However, a portion of alleles that were initially rare have reached near fixation by F_{58D}. The existence of alleles that start at very low frequencies but rapidly rise to near fixation is consistent with the previous finding of strong directional selection operating on some loci in CCII in Davis (Landis et al. 2024; Saghai-Maroof et al. 1984).

The shift to Bozeman dramatically altered the evolutionary trajectory of CCII. Over the first three generations in Bozeman, the depletion of genetic diversity accelerated (Figure 2A and B) largely due to the loss of less common founding alleles (Figure 2C). Over the subsequent 23 generations, the loss of genetic diversity observed in Davis was completely reversed, and H_e ultimately returned to levels closer to that of the founders (Figure 2A and B). Unlike F_{50D} in Davis, the $F_{24D,26B}$ AFS is enriched for intermediate frequency alleles with fewer sites falling into either the lowest or highest frequency bins (Figure 2C).

Globally, the pre-shift frequency of an allele is predictive of its fate in Bozeman. SNPs found at low or intermediate frequencies in F_{18D} remain enriched at low or intermediate frequencies respectively in $F_{24D,26B}$ (Figure 2D). A minority of the 13,682,680 alleles segregating in Bozeman $F_{24D,26B}$ (10%) were below frequencies that we could detect in Davis samples. However, both rare and undetected alleles in F_{18D} show similar evolutionary trajectories (Figure 2D) indicating that the undetected alleles were present in F_{18D}, but not sampled in our sequencing data.

Together, these results demonstrate that the return in genetic diversity in Bozeman is due to a global movement towards intermediate allele frequencies in combination with the reappearance of alleles that were rare in Davis.

Allelic origin drives the return of genetic diversity in CCII

Previous work found that CCII in Davis adapted by favoring alleles from Mediterranean environments (Landis et al. 2024). We hypothesized that the return of genetic diversity in Bozeman was due to a shift in selection pressures favoring alleles adapted to Continental climates. We calculated distance matrices between all the parents and the progeny pools and fit a multidimensional scaling model to visualize the relationships over evolutionary time in two dimensions (Figure 3).

As expected, the Davis population evolved favoring alleles from Mediterranean barley and moves progressively toward these parents in the MDS plot over time. The Bozeman population initially remained on a similar evolutionary trajectory, but then reversed to become more similar to eurasian types. The $F_{24D,26B}$ sample is found at an intermediate position relative to the parents, similar to the predicted starting position of

the experiment, but without evidence of contribution from Asian parents that are found at higher positions along MDS 2.

The return of diversity from Eurasian barley was notable since these types were not common after the first decade of CCII evolution at Davis. To understand the process by which eurasian alleles re-emerged, we genotyped 871 individuals from the Davis CCII and 145 and 139 individuals from $F_{24D,3B}$ and $F_{24D,26B}$ respectively at 425,098 genetic markers segregating in the CCII parents. Previous work found that many near identical samples could be found in CCII, especially in the later generations where a large number of individuals could be collapsed into genetic clusters derived from a single CCII recombinant (Landis et al. 2024). We also identified near identical samples in our Bozeman dataset (Figure 4A) leading us to cluster samples by genetic similarity across the entire experiment. Consistent with previous findings, clustering of CCII progeny revealed a large number of near identical individuals (Figure 4B) with only 288 unique lineages segregating amongst the sample of 1155 individuals spanning the entire experiment.

We identified 238 discrete lineages in the 871 genotyped samples from Davis and 60 lineages in the 284 genotyped samples from Bozeman (Figure 4B). Haplotype diversity showed a similar pattern to the pool sequencing diversity; increased loss of haplotype variation was observed after the shift to Bozeman, but haplotype diversity did not fall in Bozeman at the same rate as observed in Davis (Figure 4C). Though haplotype diversity was relatively stable in Bozeman, the composition of the population changed substantially over time relative to the founding diversity present in Davis. In

$F_{24D,3B}$, 51.8% of the samples were assigned to a lineage that we also identified in at least one of the Davis samples (F_{18D}, F_{28D}, F_{50D}, or F_{58D}). However, only 24.3% of the lineages that we observe in $F_{24D,3B}$ were found in Davis. Thus, common variation preceding the shift is more likely to be transmitted to the Bozeman site. These fractions dropped rapidly over the subsequent 23 generations in Bozeman. In $F_{24D,26B}$ 21.6% of individuals were clustered with a multilocus haplotype identified in Davis. 16.1% of observed lineages in $F_{24D,26B}$ were also sampled in Davis. Eight of the ten most common lineages three generations after the shift (accounting for 74.5% of lineages observed at that timepoint), decreased in frequency with the other two staying approximately the same (Figure 4D). Genotypes common directly after the shift are being replaced by $F_{24D,26B}$ with rapidly expanding lineages that were not sampled or at low frequency in $F_{24D,3B}$.

By F_{50D} the Davis population is dominated by a single ancestral lineage (Landis et al. 2024) (Lin^{1}). With this new dataset, we can differentiate two sublineages within Lin^{1} that appear to be segregants from a common parent (Lin^{1a} and Lin^{1b}, Figure 5A-B). Lin^{1a}, Lin^{1b}, and a third lineage, Lin^{2}, together compose 78% of CCII at F_{50D} and 68% at F_{58D}. Lin^{2} shows extensive similarity to Lin^{1} and may also represent a segregant from the same ancestor, but inherited a different haplotype on much of chromosome 5H (Figure 5B). Identification of regions of identity by descent between Lin^{1} and Lin^{2} and the CCII parents reveals that all three lineages share predominant ancestry with North African barley adapted to Mediterranean climates (Table 1). Atlas, the Californian derived ancestor, made the largest contribution to all three successful lineages, with smaller

contributions from the Algerian cultivar Maison Carree and the Egyptian traditional cultivar Minia. Though barley is an infrequent outcrosser (< 2%) (Jain and Allard 1960), ancestry from three different parents in these lineages confirms that rapid adaptation was facilitated by outcrossing events (Kahler et al. 1975).

In Bozeman, three lineages together compose just under half (41.7%) of the population by $F_{24D,26B}$. Lin^4 was the most common lineage directly after the shift to Bozeman and the second most common lineage at the end of the experiment (Figure 5A). Lin^4 is present in Davis samples, though at low frequencies (F_{18D} and F_{50D} less than 2%) and rose rapidly in Bozeman to compose 31.2% of the population. Like the successful lineages in Davis, Lin^1 and Lin^2, the genome of Lin^4 has extensive regional IBD with the North African parents Atlas and Maison Carre, but it does not share ancestry with Minia (Table 1). Lin^4 was less successful in the subsequent 23 years of evolution in Bozeman leading to $F_{24D.B26}$ dropping to 11.5% of the sampled individuals.

Lin^3 and Lin^5, the most common and third most common lineages in Bozeman $F_{24D,26B}$ were not found in our $F_{24D,3B}$ sample or in any Davis sample (Figure 5A). Barley inflorescence architecture is dimorphic, with some varieties producing two rows of seed (two-rowed) and others producing six rows (six-rowed). In previous studies, two-rowed types were strongly selected against in Davis (Harlan et al. 1940). Both Lin^3 and Lin^5 had significant IBD with the two-rowed Turkish barley, White Smyrna (Table 1). Though White Smyrna geographically was sampled near the Mediterranean, it groups with Eurasian types in genetic analysis (Landis et al. 2024) and we will refer to it as such here. Lin^5 also shared ancestry with the eurasian, two-rowed parent Hannchen. The secondary and

tertiary ancestry in Lin^3 was from Everest and Lion, though these combined contributions were estimated to be less than 12% of the genome which may suggest a more complicated ancestry.

These data demonstrate that many of the most successful genotypes after the shift to Bozeman were derived from at least one two-rowed parent despite the observation that two-rowed types are maladaptive in the Davis CCII. We grew a random subset of our Bozeman individuals to flowering to confirm the reappearance of two-rowed types and found that 3.2% of $F_{24D,26B}$ (n=93) and 31% of $F_{24D,3B}$ (n=84) produced two-rowed inflorescences (Figure 5C). These included all the Lin^3 and Lin^5 samples grown to flowering (n=14 and n=7) respectively. The other two-rowed lineages from $F_{24D,26B}$ all had ancestry from White Smyrna and Hannchen, though the proportions varied by accession (Figure 5D). The three two-rowed individuals found in $F_{24D,3B}$ all belonged to the same multilocus haplotype with predominant ancestry from White Smyrna and the six-rowed parent Sandrel.

These observations explain the pattern of evolution observed using our pooled sequencing dataset: rare genotypes in Davis with ancestry from two-rowed, Eurasian parents have rapidly increased to intermediate frequencies at the Bozeman site. This process is in transition, with some progeny of Mediterranean parents still present, though decreasing, in $F_{24D,26B}$.

Ultra rare multilocus haplotypes in Davis CCII facilitated rapid adaptation in Bozeman

The reappearance of two-rowed barley in CCII bozeman is surprising given that we have not observed two-rowed barley in our sample of 219 F_{18}. However, the CCII was grown

at much larger population sizes of 5000-15,000 individuals per generation, and rare progeny of two-rowed and Eurasian parents may segregate at lower frequencies than our sampling is likely to detect. To determine whether the progeny of some two-rowed parents may segregate at low frequencies in F_{18D} we characterized the segregation of private SNPs unique to each parent in our pooled sequencing dataset.

The coverage at an individual SNP in our pooled sequencing is unlikely to sample very rare variants. However, the rate that private alleles are sampled across thousands of sites can be used to estimate the frequency of the progeny of a specific parent (Materials and Methods). We detected private alleles from all of the parents segregating in F_{18D}. For example, 7.82% of White Smyrna private alleles were segregating in F_{18D}. We used these values to estimate the frequency of progeny of two-rowed parents across the Davis experiment, and as expected, we find that progeny of two-rowed parents are rare (Figure 5D, $f < 0.01$). White Smyrna is one of the least represented parents at F_{18D}, though it increases somewhat in frequency at F_{28D} (Figure 5D, from f = 0.001 to 0.003). In a population of 15,000 individuals we estimate that at F_{18D} there were a few hundred progeny of two-rowed parents and around 15 progeny of White Smyrna specifically. Importantly, the evidence for two-rowed ancestry trends downward in Davis over time.

These results indicate that the rise of extremely rare variation from two-row/eurasian types was key to the return of genetic variation in CCII in Bozeman. Because the rise of these initially rare multilocus genotypes has not yet wiped out all of the previously adapted Mediterranean types by F_{24D26B}, the population remains in the transitional state of high genetic diversity, presumably on its way toward homogeneity for

eurasian type alleles. The degree of genotype replacement that we observe in Bozeman can not be explained by drift alone given the large population sizes used in the CCII.

Allelic trade-offs during adaptation across diverging environments

The rapid replacement of Mediterranean with Continental ancestry in Bozeman is strong evidence for local adaptation in the CCII parents. This leads us to a key question in understanding the genetic basis of environmental adaptation: do adaptive alleles in one environment typically have negative effects in the other environment (antagonistic pleiotropy), or are they adaptive in one environment and neutral in the other (conditional neutrality)? The answer to this question is directly related to the ability of populations to harbor alleles that can facilitate adaptation to new environments (Yeaman 2022). While the relative importance antagonistic pleiotropy and conditional neutrality have been directly studied through QTL studies in a limited number of species (Anderson et al. 2013; Ågrena et al. 2013; Oakley et al. 2023; Lowry et al. 2019; Hall et al. 2010; Troth et al. 2018), the long-term nature of the CCII experiments allows us to investigate the potential consequences of evolution under these two regimes.

To answer this question, we compared the direction of allele frequency change across the genome over the first 18 generations of evolution in Davis and the 26 generations after the shift to Bozeman. We found a strong anticorrelation in the direction of allele frequency change throughout the genome as adaptation occurred to contrasting environments (Figure 6A, $r = -0.72$; $p < 2e\text{-}16$).

A previous study identified 52 regions of the genome (5.04%) that showed unusually strong patterns of directional selection over the first 18 generations of

evolution of CCII in Davis (loss of genetic diversity and change in allele frequency) (Landis et al. 2024). We complemented this set of regions with regions targeted by directional selection in Bozeman after the shift by comparing allele frequency distributions between F_{24B3} and F_{24B26} (2.25% of the genome, see Materials and Methods). SNPs that fell into these regions showed an even stronger pattern of anticorrelation as compared to the genome-wide pattern consistent with antagonistic pleiotropy operating on at least some of these strongly selected regions (Figure 6B).

The Bozeman and Davis populations show a striking overlap in their selected genomic regions: 70.7% of Davis-selected and 21.0% of Bozeman-selected regions overlap ($p < 0.001$), suggesting shared targets of selection. All of the overlapping regions have strong negative correlations in change of allele frequency at the two sites ($r <= -0.842$) indicating that selection is driving allele frequencies in the opposite direction at the two sites. We label these regions as candidate targets of antagonistic pleiotropy (AP targets).

AP targets were clustered on chromosome 2H and 5H near previously described structural variants (Jayakodi et al. 2020; Jayakodi et al. 2024; Wonneberger et al. 2023). Of the candidate genes that were highlighted as potential targets of selection in Davis (Landis et al. 2024), *HvCENTRORADIALIS* (*HvCEN*) was targeted by selection at both sites. *HvCEN* is a key regulator of barley flowering time, and mutations in HvCEN facilitate barley fitness across Mediterranean and Continental climates (Comadran et al. 2012; Russell et al. 2016). In Davis, the early flowering, Mediterranean allele was favored while in Bozeman the late flowering allele from White Smyrna was favored. *Vrs1*,

the gene which delineates spike row number diversity in barley (Komatsuda et al. 2007), is downstream from one of our selected regions, but does not directly overlap.

Discussion

Our analysis of the shift of CCII from the winter planted, Mediterranean climate of Davis to the spring planted, Continental climate of Bozeman reveals several important patterns. First, the massive impact of local adaptation in Bozeman parallels previous observations of the CCII in Davis (Landis et al. 2024). Adaptation to both environments involved a major, rapid restructuring of genetic diversity that strongly favored alleles drawn from similar conditions to the experimental site. It is not surprising that barley contains genetic diversity that contributes to local adaptation; this was recognized by the founders of the CCII nearly a century ago (Harlan and Martini 1929). However, the pace and magnitude of the effect of selection is remarkable. The ongoing complete genomic exchange in Bozeman and the recapitulation of the global pattern of genetic divergence in Barley over just a few decades is not likely to be due to random chance.

Second, a small number of successful lineages have risen to high frequencies in the population at both sites. In Davis, this eventually leads to three quarters of the population being composed of genotypes that likely shared a single common ancestor in the earlier generations of the CCII. At Bozeman, successful lineages do not share the same degree of similarity, though they do share some of the same parents. Studies of self fertilizing species in both animals and plants have found low within population genetic diversity and local dominance of relatively few multilocus haplotypes (Hughes

and Simons 2015; Montesinos et al. 2009; Siol et al. 2008; Barrière and Félix 2007; Bomblies et al. 2010). Low genetic diversity in self-fertilizing species is often attributed to neutral processes (Jullien et al. 2019). At least in the CCII, a few successful multilocus haplotypes can emerge from a very diverse founder population predominantly due to selection. The low effective rate of recombination in Barley, resulting from its self fertilizing mating system, amplifies the loss of genetic diversity resulting from directional selection. Perhaps the local homogeneity of self-fertilizing populations is influenced by selection more than previously suggested.

While linked selection may play an important role in amplifying the wholesale replacement of lineages across environments, it is clear that alleles selected strongly in one environment are disadvantageous at the other environment. This contrasts with previous findings that the majority of fitness associated QTL in experimental populations showed evidence for conditional neutrality (Anderson et al. 2013; Ågrena et al. 2013; Oakley et al. 2023; Lowry et al. 2019; Hall et al. 2010; Troth et al. 2018). This discrepancy might result from the effect size or seasonal stability of the two classes of variants; if antagonistic pleiotropy is more common at loci with consistent, large effects then it may have a larger impact over multiple generations.

Fourth, even though the progeny of two-rowed, Eurasian were not fit in Davis, they reappear after just three generations of adaptation to Bozeman, and are found at intermediate frequencies just 26 generations after the shift in environments. The sudden reappearance of types that are thought to have low fitness in Davis could have several explanations. Migration of previously extinct types, either through outcrossing with other

barley or through direct seed contamination is one possible explanation. It is not likely that large scale intercrossing or bulk contamination occurred given the precautions taken against such an event. It is possible that rare events give rise to segregation of fit individuals that were previously extinct, but this does not affect many of the conclusions of the work. Under this model, adaptive evolution still depends on ultra-rare genotypes, the only change is whether the non-adaptive types persisted in the Davis population. Importantly, we find evidence that unfit types still segregate at low frequencies in Davis. This result indicates that very rare maladapted types persist in the CCII. It is not clear how they are maintained, but perhaps fluctuating environmental conditions from year to year alter the fitness of these types enough for them to persist.

In the CCII, enough rare types persist in the population after 18 generations of adaptation to seed variance for a new environment. The segregation of a small number of such types may also seed adaptation as early varieties were transported to new sites or when a wild self-fertilizing species is introduced to a new locale. It remains unclear how long these rare types can be maintained in a population. Maintenance of rare types could be critical for the longer term survival of many plant species in a changing world.

References

Ågrena J, Oakley CG, McKay JK, Lovell JT, Schemske DW. 2013. Genetic mapping of adaptation reveals fitness tradeoffs in Arabidopsis thaliana. Proc Natl Acad Sci U S A. 110(52):21077–21082.

Allard RW. 1996. Genetic basis of the evolution of adaptedness in plants. Euphytica. 92(1):1–11.

Anderson JT, Lee C-R, Rushworth CA, Colautti RI, Mitchell-Olds T. 2013. Genetic trade-offs and conditional neutrality contribute to local adaptation. Mol Ecol. 22(3):699–708.

Badr A, Müller K, Schäfer-Pregl R, El Rabey H, Effgen S, Ibrahim HH, Pozzi C, Rohde W, Salamini F. 2000. On the origin and domestication history of Barley (*Hordeum vulgare*). Mol Biol Evol. 17(4):499–510.

Bal BS, Suneson CA, Ramage RT. 1959. Genetic shift during 30 generations of natural selection in barley. Agron J. 51(9):555–557.

Barrett RDH, Schluter D. 2008. Adaptation from standing genetic variation. Trends Ecol Evol. 23(1):38–44.

Barrett SCH, Arunkumar R, Wright SI. 2014. The demography and population genomics of evolutionary transitions to self-fertilization in plants. Philos Trans R Soc Lond B Biol Sci. 369(1648).

Barrière A, Félix M-A. 2007. Temporal dynamics and linkage disequilibrium in natural Caenorhabditis elegans populations. Genetics. 176(2):999–1011.

Bomblies K, Yant L, Laitinen RA, Kim S-T, Hollister JD, Warthmann N, Fitz J, Weigel D. 2010. Local-scale patterns of genetic variability, outcrossing, and spatial structure in natural stands of Arabidopsis thaliana. PLoS Genet. 6(3):e1000890.

Charlesworth B. 2009. Fundamental concepts in genetics: effective population size and patterns of molecular evolution and variation. Nat Rev Genet. 10(3):195–205.

Charlesworth D, Charlesworth B. 1995. QUANTITATIVE GENETICS IN PLANTS: THE EFFECT OF THE BREEDING SYSTEM ON GENETIC VARIABILITY. Evolution. 49(5):911–920.

Comadran J, Kilian B, Russell J, Ramsay L, Stein N, Ganal M, Shaw P, Bayer M, Thomas W, Marshall D, et al. 2012. Natural variation in a homolog of Antirrhinum CENTRORADIALIS contributed to spring growth habit and environmental adaptation in cultivated barley. Nat Genet. 44(12):1388–1392.

Danecek P, Bonfield JK, Liddle J, Marshall J, Ohan V, Pollard MO, Whitwham A, Keane T, McCarthy SA, Davies RM, et al. 2021. Twelve years of SAMtools and BCFtools. Gigascience. 10(2). doi:10.1093/gigascience/giab008. http://dx.doi.org/10.1093/gigascience/giab008.

Glémin S, Bazin E, Charlesworth D. 2006. Impact of mating systems on patterns of sequence polymorphism in flowering plants. Proc Biol Sci. 273(1604):3011–3019.

Gomulkiewicz R, Holt RD. 1995. WHEN DOES EVOLUTION BY NATURAL SELECTION PREVENT EXTINCTION? Evolution. 49(1):201–207.

Hall MC, Lowry DB, Willis JH. 2010. Is local adaptation in Mimulus guttatus caused by trade-offs at individual loci?: TRADE-OFFS CAN CONTRIBUTE TO ADAPTATION IN MIMULUS. Mol Ecol. 19(13):2739–2753.

Harlan HV, Martini ML. 1929. A Composite Hybrid Mixture. Agron J. 21(4):487.

Harlan HV, Martini ML, Stevens H, Others. 1940. A study of methods in barley breeding. Technical Bulletin United States Department of Agriculture.(720). http://www.cabdirect.org/abstracts/19401601037.html.

Hockett EA, Eslick RF, Qualset CO, Dubbs AL, Stewart VR. 1983. Effects of Natural Selection in Advanced Generations of Barley Composite Cross II1. Crop Sci. 23(4). https://www.researchgate.net/publication/250113113_Effects_of_Natural_Selection_in_Advanced_Generations_of_Barley_Composite_Cross_II1.

Hughes PW, Simons AM. 2015. Microsatellite evidence for obligate autogamy, but abundant genetic variation in the herbaceous monocarp Lobelia inflata (Campanulaceae). J Evol Biol. 28(11):2068–2077.

Jain SK, Allard RW. 1960. POPULATION STUDIES IN PREDOMINANTLY SELF-POLLINATED SPECIES, I. EVIDENCE FOR HETEROZYGOTE ADVANTAGE IN A CLOSED POPULATION OF BARLEY. Proc Natl Acad Sci U S A. 46(10):1371–1377.

Jayakodi M, Lu Q, Pidon H, Rabanus-Wallace MT, Bayer M, Lux T, Guo Y, Jaegle B, Badea A, Bekele W, et al. 2024. Structural variation in the pangenome of wild and domesticated barley. Nature. 636(8043):654–662.

Jayakodi M, Padmarasu S, Haberer G, Bonthala VS, Gundlach H, Monat C, Lux T, Kamal N, Lang D, Himmelbach A, et al. 2020. The barley pan-genome reveals the hidden legacy of mutation breeding. Nature. 588(7837):284–289.

Jullien M, Navascués M, Ronfort J, Loridon K, Gay L. 2019. Structure of multilocus genetic diversity in predominantly selfing populations. Heredity (Edinb). 123(2):176–191.

Kahler AL, Allard RW. 1981. Worldwide patterns of genetic variation among four esterase loci in Barley (*Hordeum vulgare L.*). Theor Appl Genet. 59(2):101–111.

Kahler AL, Clegg MT, Allard RW. 1975. Evolutionary Changes in the Mating System of an Experimental Population of Barley (*Hordeum vulgare L.*). Proc Natl Acad Sci U S A. 72(3):943–946.

Komatsuda T, Pourkheirandish M, He C, Azhaguvel P, Kanamori H, Perovic D, Stein N, Graner A, Wicker T, Tagiri A, et al. 2007. Six-rowed barley originated from a mutation in a homeodomain-leucine zipper I-class homeobox gene. Proc Natl Acad Sci U S A. 104(4):1424–1429.

Landis JB, Guercio AM, Brown KE, Fiscus CJ, Morrell PL, Koenig D. 2024. Natural selection drives emergent genetic homogeneity in a century-scale experiment with barley. Science. 385(6705):eadl0038.

Li H, Durbin R. 2009. Fast and accurate short read alignment with Burrows-Wheeler transform. Bioinformatics. 25(14):1754–1760.

Li H, Handsaker B, Wysoker A, Fennell T, Ruan J, Homer N, Marth G, Abecasis G, Durbin R, 1000 Genome Project Data Processing Subgroup. 2009. The Sequence Alignment/Map format and SAMtools. Bioinformatics. 25(16):2078–2079.

Lowry DB, Lovell JT, Zhang L, Bonnette J, Fay PA, Mitchell RB, Lloyd-Reilley J, Boe AR, Wu Y, Rouquette FM Jr, et al. 2019. QTL × environment interactions underlie adaptive divergence in switchgrass across a large latitudinal gradient. Proc Natl Acad Sci U S A. 116(26):12933–12941.

Mascher M, Wicker T, Jenkins J, Plott C, Lux T, Koh CS, Ens J, Gundlach H, Boston LB, Tulpová Z, et al. 2021. Long-read sequence assembly: a technical evaluation in barley. Plant Cell. 33(6):1888–1906.

Monat C, Padmarasu S, Lux T, Wicker T, Gundlach H, Himmelbach A, Ens J, Li C, Muehlbauer GJ, Schulman AH, et al. 2019. TRITEX: chromosome-scale sequence assembly of Triticeae genomes with open-source tools. Genome Biol. 20(1):284.

Montesinos A, Tonsor SJ, Alonso-Blanco C, Picó FX. 2009. Demographic and genetic patterns of variation among populations of Arabidopsis thaliana from contrasting native environments. PLoS One. 4(9):e7213.

Nei M. 1987. Molecular evolutionary genetics. https://books.google.com/books?hl=en&lr=&id=UhRSsLkjxDgC&oi=fnd&pg=PP11&dq=1987+nei&ots=QvdsPfFRlz&sig=MkYnl02TwdivYjvcSZVU0_KkBMc.

Noël E, Jarne P, Glémin S, MacKenzie A, Segard A, Sarda V, David P. 2017. Experimental evidence for the negative effects of self-fertilization on the adaptive potential of populations. Curr Biol. 27(2):237–242.

Oakley CG, Schemske DW, McKay JK, Ågren J. 2023 Jun 14. Ecological genetics of local adaptation in Arabidopsis: An 8-year field experiment. Mol Ecol. http://dx.doi.org/10.1111/mec.17045.

Osmond MM, Coop G. 2020. Genetic signatures of evolutionary rescue by a selective sweep. Genetics. 215(3):813–829.

Pollak E. 1987. On the theory of partially inbreeding finite populations. I. Partial selfing. Genetics. 117(2):353–360.

Rubner Y. 2000. The Earth Mover's Distance as a Metric for Image Retrieval. Int J Comput Vis. 40(2):99–121.

Rubner Y, Tomasi C, Guibas LJ. 2002. A metric for distributions with applications to image databases. In: Sixth International Conference on Computer Vision (IEEE Cat. No.98CH36271). Narosa Publishing House. p. 59–66.

Russell J, Mascher M, Dawson IK, Kyriakidis S, Calixto C, Freund F, Bayer M, Milne I, Marshall-Griffiths T, Heinen S, et al. 2016. Exome sequencing of geographically diverse barley landraces and wild relatives gives insights into environmental adaptation. Nat Genet. 48(9):1024–1030.

Ruzon MA, Tomasi C. 2001. Edge, junction, and corner detection using color distributions. IEEE Trans Pattern Anal Mach Intell. 23(11):1281–1295.

Saghai-Maroof MA, Soliman KM, Jorgensen RA, Allard RWL. 1984. Ribosomal DNA spacer-length polymorphisms in barley: Mendelian inheritance, chromosomal location, and population dynamics. Proceedings of the National Academy of Sciences. 81(24):8014–8018.

Siol M, Prosperi JM, Bonnin I, Ronfort J. 2008. How multilocus genotypic pattern helps to understand the history of selfing populations: a case study in Medicago truncatula. Heredity (Edinb). 100(5):517–525.

Stebbins GL. 1957. Self Fertilization and Population Variability in the Higher Plants. Am Nat. 91(861):337–354.

Troth A, Puzey JR, Kim RS, Willis JH, Kelly JK. 2018. Selective trade-offs maintain alleles underpinning complex trait variation in plants. Science. 361(6401):475–478.

Van der Auwera GA, Carneiro MO, Hartl C, Poplin R, Del Angel G, Levy-Moonshine A, Jordan T, Shakir K, Roazen D, Thibault J, et al. 2013. From FastQ data to high confidence variant calls: the Genome Analysis Toolkit best practices pipeline. Curr Protoc Bioinformatics. 43:11.10.1–33.

Virtanen P, Gommers R, Oliphant TE, Haberland M, Reddy T, Cournapeau D, Burovski E, Peterson P, Weckesser W, Bright J, et al. 2020. SciPy 1.0: fundamental algorithms for scientific computing in Python. Nat Methods. 17(3):261–272.

Wonneberger R, Schreiber M, Haaning A, Muehlbauer GJ, Waugh R, Stein N. 2023. Major chromosome 5H haplotype switch structures the European two-rowed spring barley germplasm of the past 190 years. Theor Appl Genet. 136(8):174.

Yeaman S. 2022. Evolution of polygenic traits under global vs local adaptation. Genetics. 220(1):iyab134.

Figures & Tables

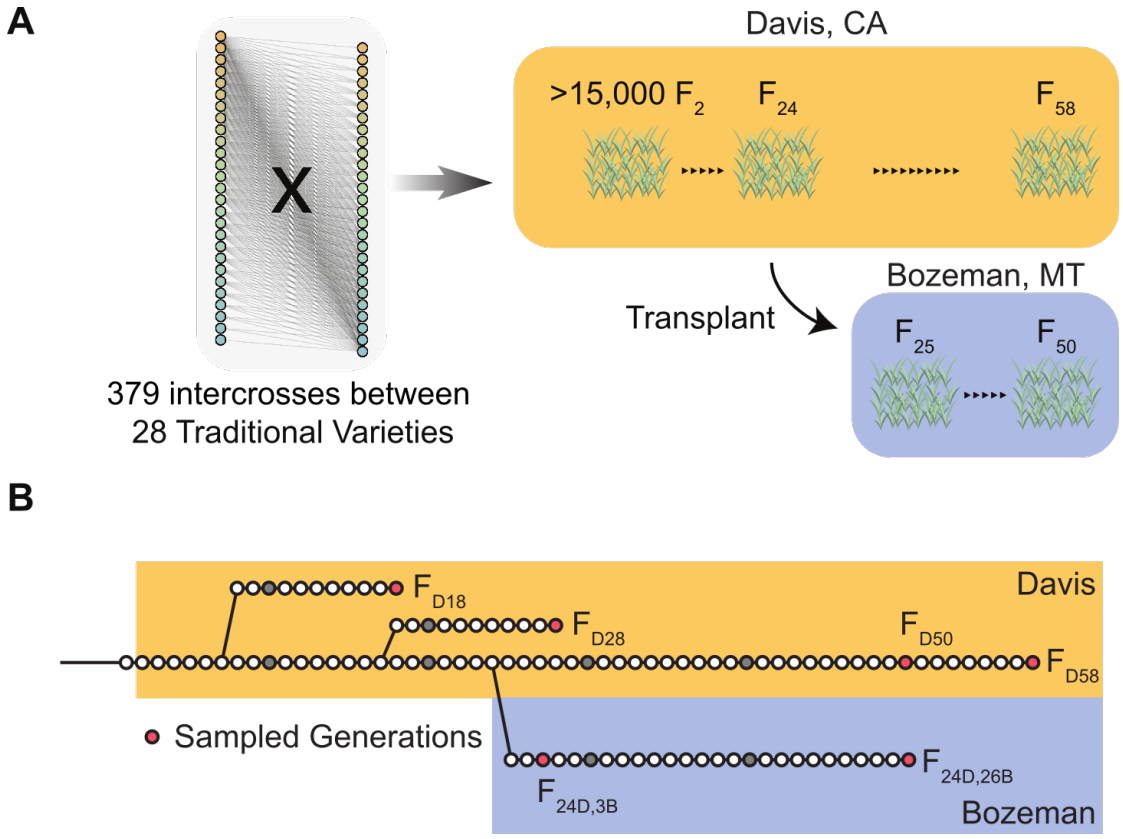

Figure 3.1 - The design of the Composite Cross II multisite experiment

A. The composite cross II began with intercrosses of 28 barley accessions collected to represent global barley diversity. After the resulting F_1 progeny were selfed, a large composite population was formed from 15,000 F_2. The population was grown at Davis, CA, USA through generation F_{24} and a subsample of over 5,000 seed were used to found the Bozeman, MT, USA experiment. Later generations of CCII were propagated using a population of 5,000 individuals. **B.** Sampling scheme for the CCII generations surveyed in this study. Earlier generations were maintained as live seed by less frequent propagation at each site. The timing of events inferred from historical notation.

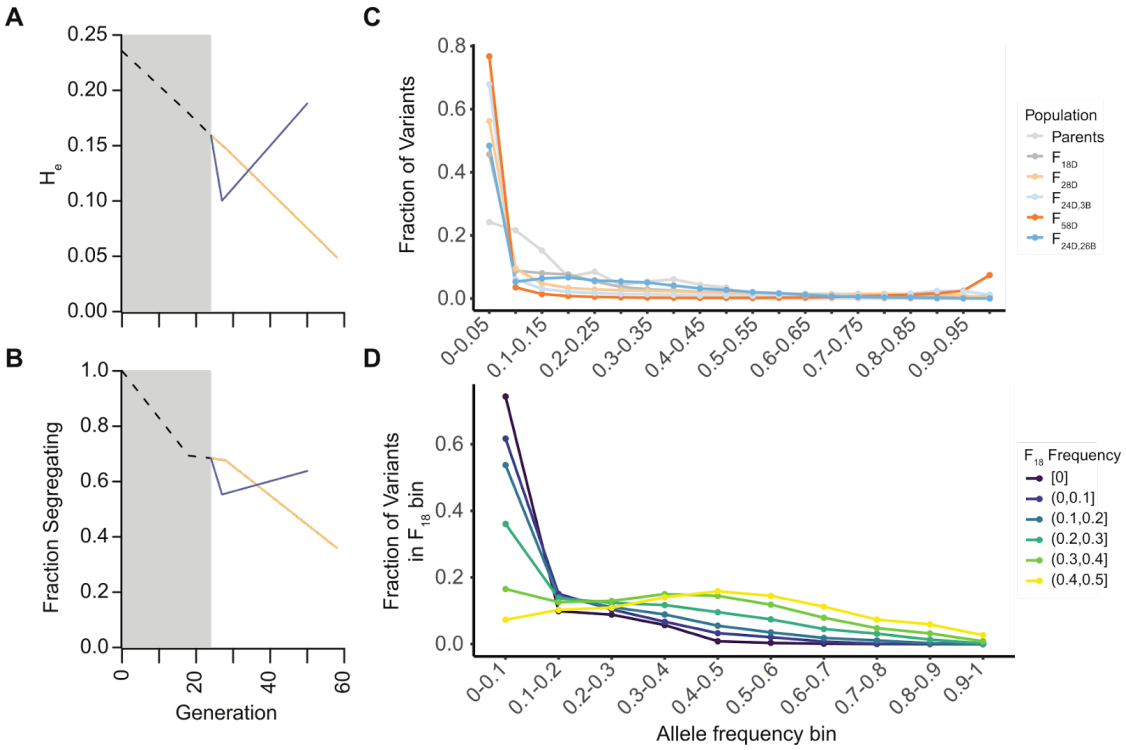

Figure 3.2 - Environmental shift redirects the evolutionary trajectory of the CCII

A. Expected heterozygosity (H_e) and **B.** fraction of founder variants segregating across CCII before and after environmental shift. The grey box indicates pre-shift values, and post shift values are shown for CCII Davis (orange) and CCII Bozeman (darkblue). **C.** The allele frequency spectrum across all sites and in all pools. The allele frequency spectrum is polarized to the minor allele at the start of the experiment. The Bozeman late sample shows an enrichment for intermediate frequency alleles relative to the late generation Davis samples. **D.** The frequency spectrum in $F_{24D,26B}$ separated by starting frequency bins in F_{18D}.

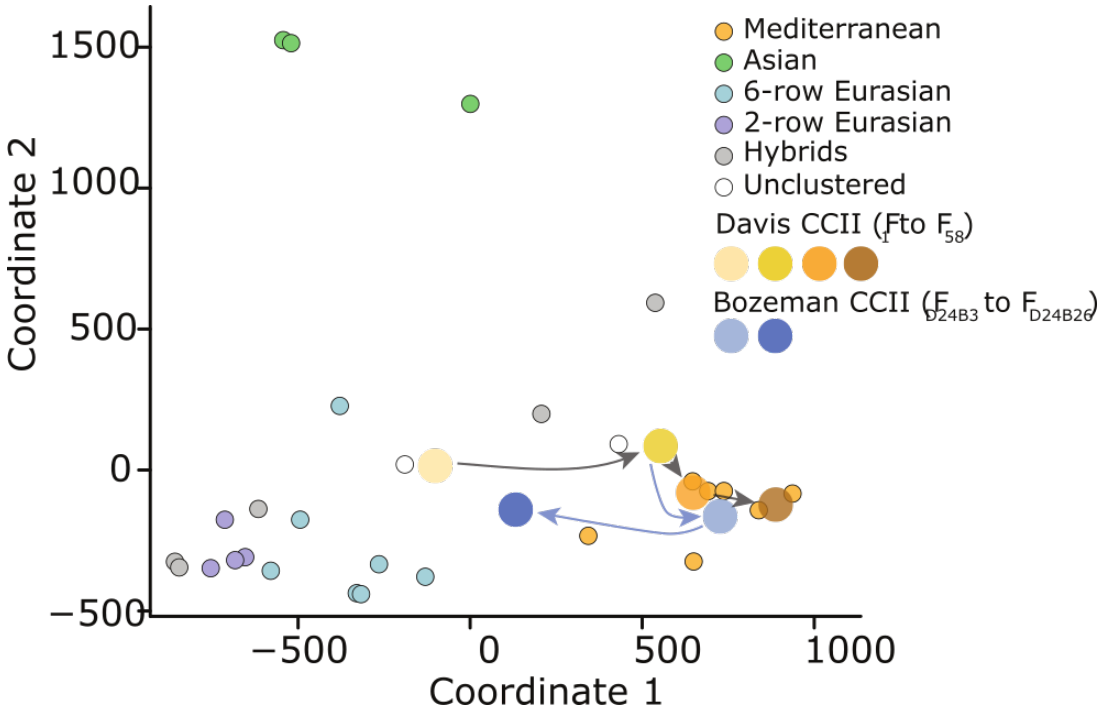

Figure 3.3 - The re-emergence of Eurasian genetic diversity in CCII Bozeman

Multidimensional scaling (MDS) analysis of genetic diversity amongst the CCII parents and the pooled sequencing samples from Davis and Bozeman.

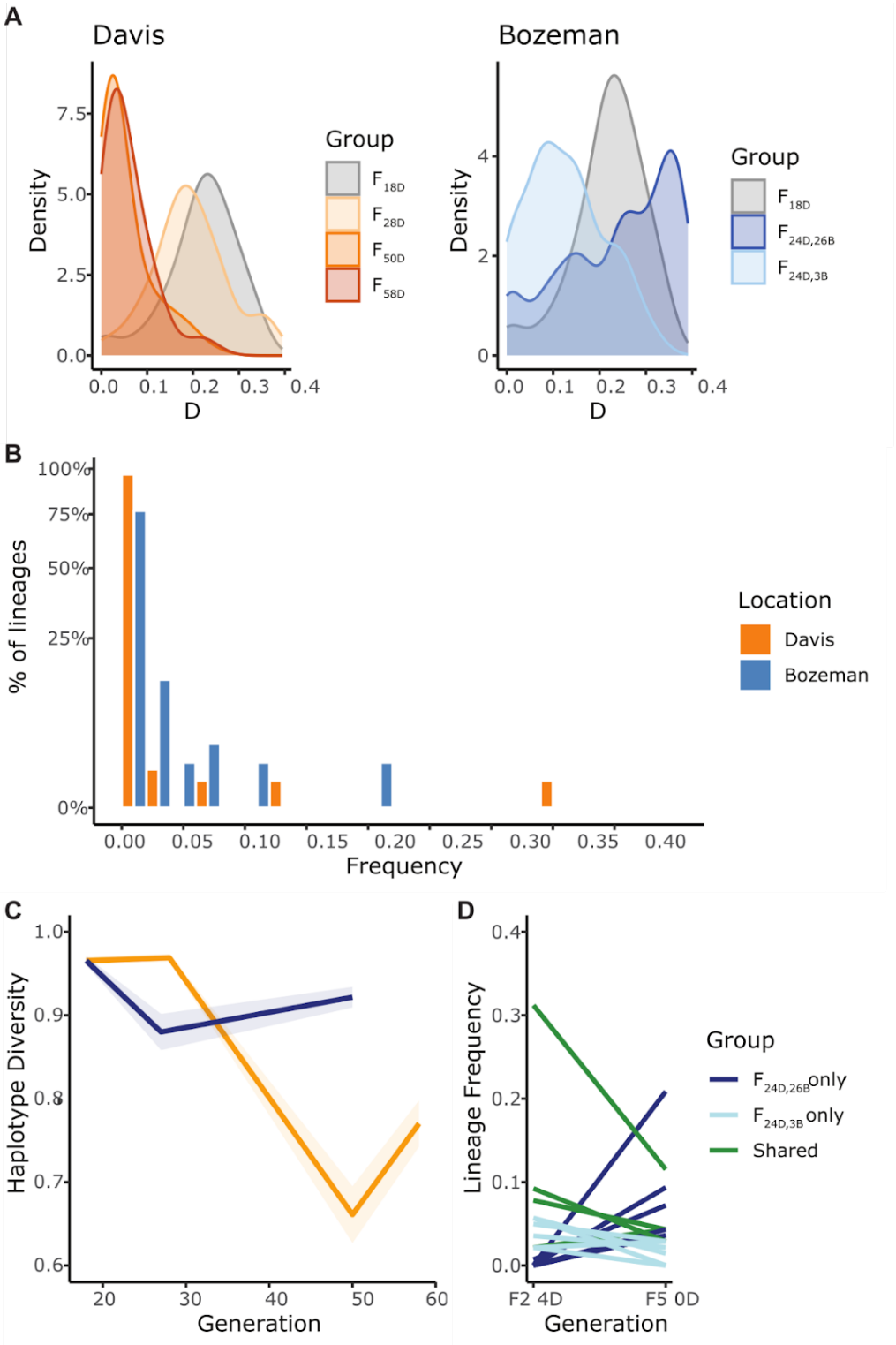
A
Davis
Density
D
Group
F_{18D}
F_{28D}
F_{50D}
F_{58D}
Bozeman
Density
D
Group
F_{18D}
$F_{24D,26B}$
$F_{24D,3B}$
B
% of lineages
Frequency
Location
Davis
Bozeman
C
Haplotype Diversity
Generation
D
Lineage Frequency
Generation
Group
$F_{24D,26B}$only
$F_{24D,3B}$only
Shared

Figure 3.4 - Rare haplotypes drive the return of genetic diversity in CCII Bozeman

A. The distribution of genome-wide genetic distances between individuals at each site and time point. **B.** The frequency distribution of lineages in Bozeman and Davis. **C.** Haplotype diversity calculated from the frequencies of lineages at each time point and site. **D.** The change in frequency of the 10 most common lineages at each Bozeman timepoint. Lineages found amongst the top 10 at both time points are highlighted in green.

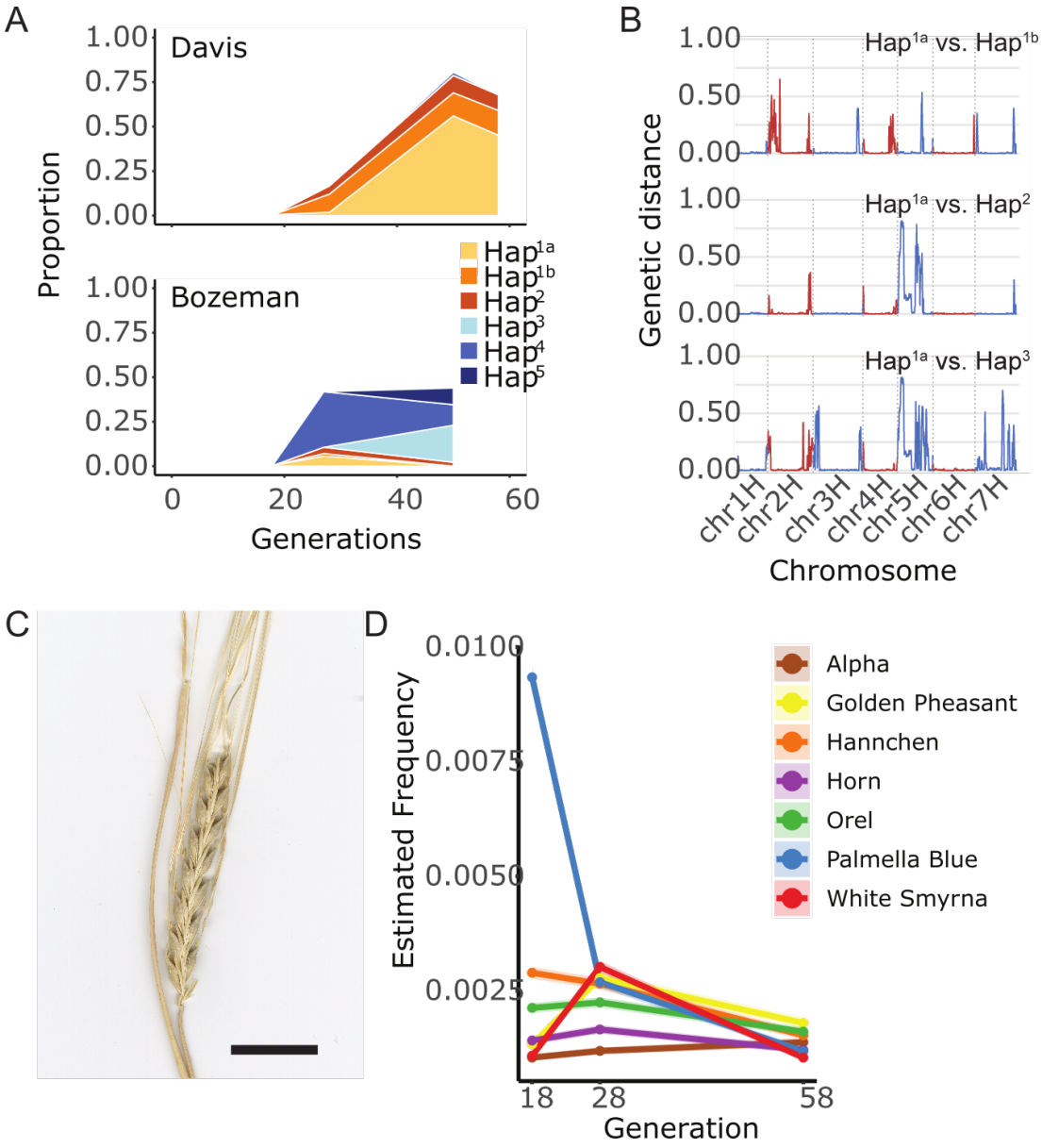

Figure 3.5 - The emergence of dominant lineages during adaptation.

A. The frequencies of the top 3 most common lineages at the last sampled time point at both sites. **B.** Comparison of the genomes of the most common lineages in Davis in 1000 SNP windows. **C.** Two rowed segregant in Bozeman. Scale bar is 2 cm. **D.** Estimated frequencies (f) of the progeny of each of the two-rowed parents.

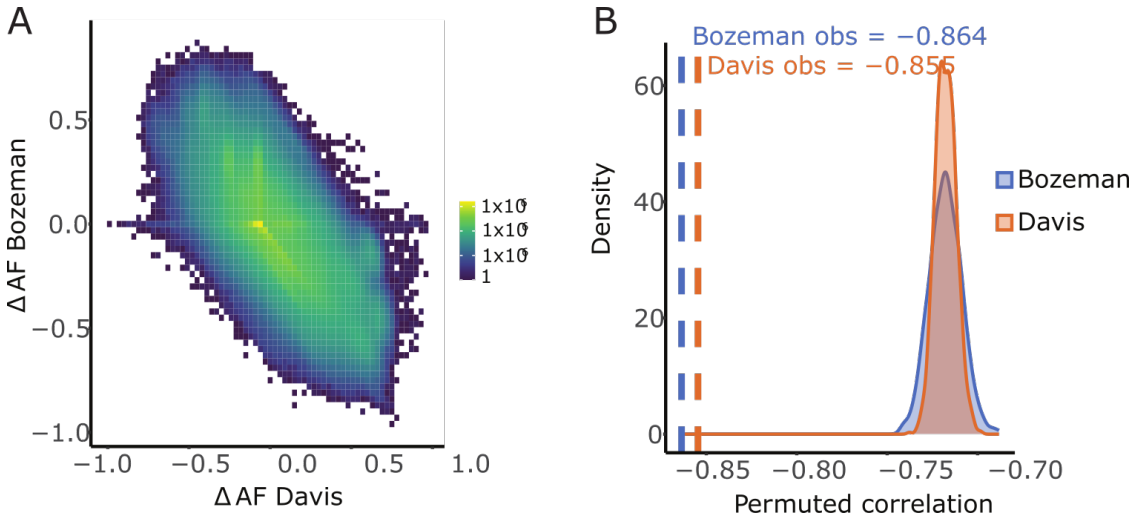

Figure 3.6 - Evidence for antagonistic pleiotropy at strongly selected loci across environments

A. Genome-wide changes in allele frequencies in Davis (F_{2D} - F_{18D}) and Bozeman (F_{18D}-$F_{24D,26}$). **B.** Correlation in allele frequency change in selected regions compared to 1000 random permutations.

Table 3.1 - Top three ancestries assigned by IBD analysis of discussed lineages in CCII

Lineage	Primary	Secondary	Tertiary
Lin1a	Atlas	Maison Carree	Minia
	0.62	0.17	0.08
Lin1b	Atlas	Minia	Maison Carree
	0.62	0.16	0.11
Lin2	Atlas	Minia	Maison Carree
	0.66	0.15	0.08
Lin3	White Smyrna	Everest	Lion
	0.60	0.07	0.04
Lin4	Atlas	Maison Carree	Club Mariout
	0.71	0.11	0.03
Lin5	White Smyrna	Hannchen	Horn
	0.72	0.26	0.00
Lin251	White Smyrna	Sandrel	Palmella Blue
	0.66	0.31	0.00
Lin278	White_Smyrna	Hannchen	Horn
	0.86	0.11	0.00
Lin272	Hannchen	White_Smyrna	Orel
	0.70	0.15	0.06

Conclusion

This dissertation explores the evolutionary process with a unique evolution experiment of intercrossed barley conducted over the course of nearly a century. This resource provides an opportunity for studying environmental adaptation in a multicellular and crop species with well-documented history during adaptation to multiple environments. In Chapter 1, I conducted field trials with genetically diverse lines from generations throughout the population's history where I scored flowering time, fecundity, and 100-seed weight. The experiment shows a different perspective on the population's environmental adaptation from a previous greenhouse experiment. Changes in flowering time and their genetic basis are evident despite the lack of clear relationship between flowering time and fecundity in this case. On the other hand 100-seed weight shows consistent evolutionary drive toward higher mass. This chapter shows the potential for antagonistic pleiotropy especially for environmentally responsive traits like flowering time and the importance of multi-environment field trials for crop varieties.

In Chapter 2, I leveraged the power of daily photographs on an automatic phenotyping platform to better understand the variety of traits that support increased fitness and competition in the CC II's evolution. This experiment provides evidence for the benefit of wider plants and leaves over an individual's lifespan and reinforces earlier findings of strong contraction of genetic and phenotypic variance during the early phase of the experiment. I further found evidence for the strong genetic basis and underlying genome regions controlling trait variance and that selection appears to act non-neutrally on these regions.

In Chapter 3, I document how genetic diversity recovers in the Bozeman population due to the re-emergence of rare genetic variants from extremely low frequency in the Davis population. I show evidence for large allele frequency shifts genome-wide at many of the same genomic locations across environments which supports the idea of antagonistic pleiotropy at these key loci. This experiment provides interesting insight into how populations can balance short and long term evolution through the preservation of rare variants in large populations. It remains unclear whether incomplete selection or year-over-year climate variation contributes more to this phenomena.